STUDIES ON OXIDATIVE DECOMPOSITION OF BENZENE IN LIQUID PHASE USING TITANIUM DIOXIDE PHOTOCATALYST

A dissertation submitted to

THE GRADUATE SCHOOL OF ENGINEERING SCIENCE

OSAKA UNIVERSITY

in partial fulfillment of the requirements for the degree of

DOCTOR OF PHILOSOPHY IN SCIENCE

By

THUAN DUC BUI

September 2010

CONTENTS

Abstract

Photocatalysis based on the utilization of solar energy has been considered to be green chemistry. TiO_2 has been used in many applications, such as water splitting for renewable energy, elimination of contaminants or harmful microbial organism in environmental treatment and selective conversion in chemical synthesis. Research on the behavior of benzene, which is a known human carcinogen emitted from both nature processes and human activities, in photocatalytic reaction over TiO_2 is significant in both environmental and industrial aspects. However, fundamental studies on this reaction are limited and there remain many questions about the detailed chemical mechanism on TiO_2 surface. In this study, we focused on reaction steps taking place on surface of TiO_2 particles in photooxidation of benzene.

The processes for oxidation of benzene on TiO_2 powders under UV-photoirradiation were studied with several chemical and physical methods. A systematic analysis of byproducts from benzene both in solution and on surface of TiO_2 was carried out. Byproducts were classified to phenolic compounds, carboxylic acids and polymeric substance. Of which, catechol and polymeric substance were found only on TiO_2 surface as the strongly adsorbed products. The adsorption of intermediates on TiO_2 was confirmed to be harmful to the photocatalytic reaction and the reason for coloration of TiO_2. The deactivation of TiO_2 during photocatalytic reaction is mainly caused by adsorbed phenolic products, especially by catechol. Although polymeric substance is not poisonous as phenolic products, it physically prevents the photocatalytic reactions.

By using isotope-tracing method, for the first time in the analysis of photocatalytic reactions, oxygen sources for photocatalytic reactions on TiO_2 particles was confirmed to be both O_2 and H_2O molecules. Their contributions on overall oxidation of benzene to phenol depend on TiO_2 structure, surface modification and reaction conditions. Rutile powders

showed higher contributions of O_2 in formation of phenol than did anatase powders. The relative contribution of O_2 increased with increase in O_2 partial pressure and decreased with addition of Pt particles. Experimental results suggest two mechanisms for phenol formation. The first one is oxygen-transfer pathway with the involvement of water as oxygen source. The other is hole-transfer pathway going through the formation of benzene cation which reacts with oxygen molecule and produce phenol in further steps.

In photooxidation of benzene, the formation of muconaldehyde as well as phenol as an initial product from benzene indicates that not only the hydroxylation pathway, which proceeds through phenolic compounds, but also the ring-opening pathway takes place. Of the two pathways, the ring-opening pathway was experimentally confirmed to contribute larger part in overall mineralization of benzene in the initial stage of the reaction. Muconaldehyde is produced slower but it is decomposed much faster than phenol. During photooxidation of benzene, phenol gradually accumulates and muconaldehyde is decomposed soon after its formation. Although the ^{18}O-tracing method is very useful for determining the origin of O in phenol molecules in photooxidation of benzene, it is not applicable to determination of origin of O in muconaldehyde and further oxidized byproducts. It is because of the fast O exchange between water and those byproducts, especially carbonyl compounds. Therefore, the detailed mechanism for formation of muconaldehyde is still under investigation. However, there are two possible mechanisms compatible with the obtained results can account for the formation of muconaldehyde. They are ozonization-like process with the involvement of ozone-like species produced on TiO_2 surface under UV irradiation and a process going through dioxetane species formed in coupling between benzene cation with superoxide anion.

Finally, the photooxidation of water over TiO_2 particles with O_2 molecules as electron scavenger was investigated by ^{18}O-tracing method. It is confirmed that the water photooxidation occurs on TiO_2 surface under UV irradiation. The evolution of O_2 increases as a result of the ease in accumulation of holes with addition of platinum particles and increase in pH of reaction solution. The synergism between anatase and rutile was also observed in

photooxidation of water. The oxidation of water is less competitive than oxidation of organic compounds. Rutile powders, which has lower photocatalytic activity in oxidation of organic compound, shows higher activity in formation of O_2 compared with anatase powders. This could be attributed to the difference in crystal structures between anatase and rutile.

Chapter 1: GENERAL INTRODUCTION

1.1 TiO_2 photocatalysis

Photocatalysis has been defined as the change in the rate of a chemical reaction or its initiation under the action of ultraviolet, visible, or infra-red radiation in the presence of a substance—the photocatalyst—that absorbs light and is involved in the chemical transformation of the reaction partners [1]. Of which, heterogeneous photocatalysis has been the most expanding field [2-10], since the first discovery in water photolysis into hydrogen and oxygen with using TiO_2 electrode by Fujishima and Honda in 1972.

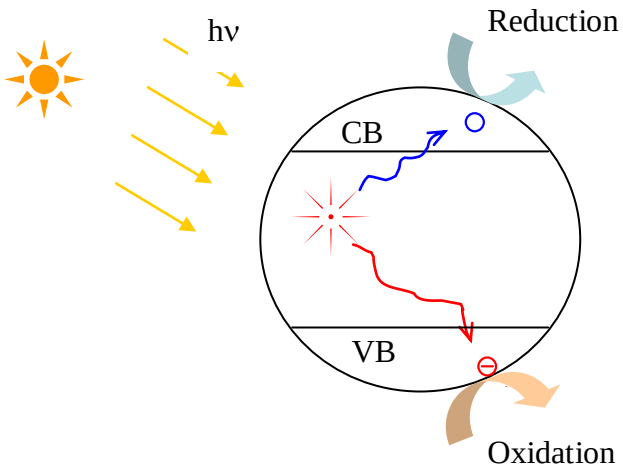

Fig. 1.1. Principle of photocatalysis

Photocatalyst is a catalyst that is able to produce, upon absorption of light, chemical transformations of the reaction partners. The excited state of the photocatalyst repeatedly interacts with the reaction partners forming reaction intermediates and regenerates itself after each cycle of such interactions [1]. Photocatalysts in heterogeneous photocatalysis are semiconductors such as TiO_2, ZnO, WO_3, Fe_2O_3, $SrTiO_3$, $CaTiO_3$, $KTaO_3$, Ta_2O_5, and ZrO_2.

In general, when a photon with energy higher than the band gap of a semiconductor is absorbed, a pair of electron and hole is generated in conduction band and valance band, respectively. A part of the photogenerated holes and electrons migrates to the semiconductor surface and initiates simultaneous oxidation and reduction reactions or chains of redox

reactions, as shown in Fig. 1.1. The recombination between photogenerated holes and electrons is ubiquitous in the bulk and on the surface of the photocatalyst particles. Much effort has been made to understand this complex reaction system and to make use of it efficiently. Many chemical and physical–methods have been used and several mechanisms have been proposed for photocatalysis [2-10].

Table 1.1. Physical parameters of anatase and rutile TiO_2 [2,11-15]

	Anatase	Rutile
Crystal structure	tetragonal D_{4h}^{19}-$P4_1/amd$ a = b = 3.782 Å, c = 9.502 Å	tetragonal D_{4h}^{14}-$P4_2/mnm$ a = b = 4.584 Å, c = 2.953 Å
Band gap energy	3.2 eV	3.0 eV
Density	3.89 g/cm^3	4.25 g/cm^3
Static dielectric coefficient	30	100
Donor state radius	15 Å	2.6 Å
Electron effective mass (m^*)	~ 1 m_o	~ 20 m_o

Among various semiconductors for photocatalysis, TiO_2 is almost the only material suitable for industrial use at present and also probably in the future. Most basic knowledge about photocatalysis has also been derived from extensive research works on TiO_2. This is because TiO_2 is the most abundant, photo-active, chemically and physically stable, and cheapest material. Moreover, it has been used as a white pigment from ancient times, and thus, its safety to humans and the environment is guaranteed by history. Anatase and rutile, two stable and common forms of TiO_2, have been studied extensively. Both of them are n-type semiconductors. Several physical and structural parameters of anatase and rutile TiO_2 are shown in Table 1.1.

Upon UV irradiation, pairs of electron and hole after being generated in few femtoseconds, migrate randomly in the bulk of TiO_2 particles. When they reach TiO_2 surface,

they can make chemical or physical changes in the interfacial atom layers, which are rich in defects due to the reconstruction of the TiO_2 crystal, and localize at sites with relatively lower energy. These sites are commonly called surface trapped holes and surface trapped electrons. Thermodynamically, these surface trapped holes and surface trapped electrons are more stable, longer lasting and less active than free holes and electrons. There are distributions in the energy of trapped holes and electrons. At low temperature, trapped electrons can be detected in the form of Ti^{3+}. As for surface trapped holes, several types of species, such as sub-surface oxygen radicals connected to surface hydroxyls (Ti–O˙–Ti–OH) surface oxygen radicals (Ti–O–Ti–O˙) generated from basic surface hydroxyls, lattice O˙ radical, etc. are postulated. Table 1.2 shows the characteristic time of primary processes on TiO_2 surface. These data indicate that the charge recombination in TiO_2 photocatalysts could be delayed because of the efficient charge trapping; the interfacial charge transfer processes are competitive to charge recombination; and photocatalytic reactions could be completed within μs to ms after the generation of the electron-hole pair. [2]

Table 1.2. Some characteristic times for primary processes in TiO_2 photocatalysis [2]

Primary process		Characteristic time
Charge carrier generation	$TiO_2 + h\nu \rightarrow e^- + h^+$	fs
Charge trapping	$h^+ \rightarrow h^+_{tr}$	< 200 fs
	$e^- \rightarrow e^-_{tr}$	< 150 fs
Charge recombination	$e^- + h^+$	1-25 μs
h^+ + donor	Methanol oxidation	~ 0.3 ns
	2-propanol oxidation	~ 3 ns
	Water oxidation	< 2 μs
e^- + acceptor	$O_2 \rightarrow O_2^{\cdot -}$	0.1 – 100 μs
	Pt → Pt….e-	2.3 ps

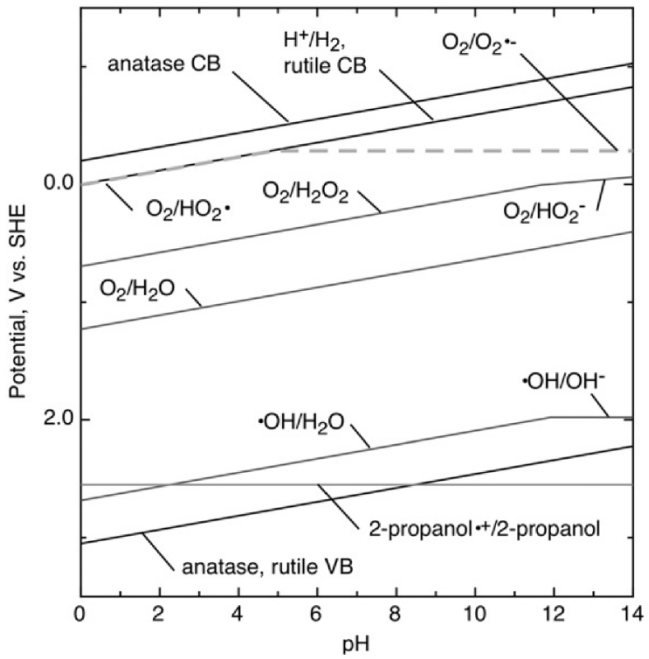

Fig. 1.2. Energy bands on TiO_2 versus solution pH values [2].

Fig. 1.2 shows the potential of band edges of TiO_2 in pH from 0 to 14 and in comparison with some electrode potential of several redox couples in aqueous solution. It can be seen that the conduction-band energy of rutile is coincident with the reversible hydrogen potential at all pH values, whereas that for anatase is more negative by 0.20 V. At lower pH values, the conduction band energy of rutile is also coincident with the reversible potential for O_2 reduction to hydroperoxyl radical $HO_2^{\cdot}$. But at higher pH, it deviates from the potential for O_2 reduction to superoxide radical anion $O_2^{\cdot -}$, which remains constant at 0.284 V. The conduction band energy of anatase is always more negative than that of rutile 0.2 V. The valence band energies for both rutile and anatase lie at approximately the same potential. When TiO_2 particle is irradiated with appropriate photons, oxygen evolution, hydroxyl radical production or organic oxidation at anode sites, and either oxygen reduction to superoxide, hydrogen peroxide or water, or reduction of the titanium dioxide itself, via hydrogen insertion, for example, at cathode sites can simultaneously take place. [2]

Much work has been done to clarify the oxidizing species generated on the irradiated TiO_2 surface in order to understand the detailed mechanism of photocatalysis and design

better photocatalytic systems. The widely accepted oxidizing species are holes, (both free and trapped), hydroxyl radicals ($HO^{\cdot}$), superoxide anion ($O_2^{\cdot -}$), and singlet oxygen ($^1O_2$). The involvements of hydrogen peroxide (H_2O_2) and molecular oxygen (O_2) are also proposed in the photocatalytic oxidation processes in various mechanisms. [2-10]

Holes: Both holes and trapped holes are considered as the primary oxidizing species in photocatalytic reactions. Because, the holes are trapped within picoseconds, most of the primary oxidation processes are caused by trapped holes. The direct oxidation by interface charge transfer between holes and substrates strongly depends on TiO_2 surface condition, interaction between TiO_2 surface and substrates, nature of substrate, and media.

$HO^{\cdot}$ radical: It is proposed that $HO^{\cdot}$ radicals are generated in the oxidation of either water or adsorbed hydroxide ion with photogenerated holes. It is also produced in photolysis H_2O_2 or reduction of H_2O_2 with photogenerated electrons. The $HO^{\cdot}$ involved oxidation processes are sometimes designated as indirect oxidation. However, there are still doubts about the existence of $HO^{\cdot}$ in photocatalytic reaction [16,17]

Superoxide anion, $O_2^{\cdot -}$: This anion is less important in initiating oxidation reaction because it is less active species compared with others. However, its formation in reduction of O_2 with photogenerated electron is essential for decrease in charge recombination and increase in photocatalytic reaction rate. It also can participate in secondary oxidative processes.

Singlet oxygen, $^1O_2$: Singlet oxygen is an important reactive oxygen species in atmospheric, biological and therapeutic processes, and is also used as a reagent in organic synthesis. It is proposed that singlet oxygen is produced in interaction between superoxide anions and holes. Thank to its long life, it can be an important oxidant in photooxidation of organics.

Oxygen, O_2: Oxygen molecules play important roles in photocatalytic reaction. They participate in chains of radical reactions through oganoperoxy radicals ($ROO^{\cdot}$). They also capture photogenerated electrons to suppress charge recombination and generate active

species such as superoxide anion and hydrogen peroxide. It is reported that, superoxide anion is favorably produced in reduction of O_2 on rutile surface, whereas, that for anatase is hydrogen peroxide. However, the reduction of O_2 by photogenerated electron on TiO_2 surface has not been well understood. The generation of superoxide has been recognized for a long time based on the EPR or chemiluminescence studies. The detection of surface-peroxo species is difficult and was just achieved by multiple internal reflection infrared spectroscopy [18,19].

Overall, strong oxidative property is dominant in a UV-photoirradiated TiO_2 suspension. Of the two commonly used TiO_2 forms, anatase possesses a higher photocatalytic activity than rutile does. However, the precise reasons for difference in activities have not been elucidated in detail. So far, three major active research topics in TiO_2-photocatalysis are water splitting for renewable energy, elimination of contaminants or harmful microbial organism in environmental treatment and selective conversion in chemical synthesis [2-10,21-23].

There is only one drawback of TiO_2. Because TiO_2 has a band gap larger 3 eV, it adsorbs photon in UV region that accounts only small part of solar energy (approximately 5%) on surface of the earth. Recently, intensive studies have been in progress to develop the existing materials or prepare new materials, which can be used under solar energy and hence shortening the time needed for the degradation. The development includes increasing the surface area, increasing the active sites, and increasing the absorption of photon energy and reducing the band gap energy.

1.2 Benzene and its toxicity

Benzene is a colorless, flammable and volatile liquid with a sweet odor. It is one of major pollutants coming from both natural processes and human activities. It ranks in the top 20 chemicals for production volume. Some industries use benzene as starting material or solvent, such as in production of plastics, resins, nylon and other synthetic fibers, rubbers, lubricants, dyes, detergents, drugs, and pesticides. Natural sources of benzene include emissions from volcanoes and forest fires. Benzene is also a naturally present in crude oil,

gasoline, and cigarette smoke. Table 1.3 is some sources of benzene in natural and human activities [24-27]

Table 1.3. Some sources of benzene in natural and human activities [27]

Natural sources	Industrial uses
- Crude oil	- Styrene (synthetic plastic and rubber products)
- Petroleum	- Phenols (resins)
- Cigarette smoke	- Cyclohexanes (fabrics such as nylon)
- Forest fires	- Maleic anhydride (polyester resins)
- Volcanoes	- Alkylbenzenes (detergents)
- Organic matter combustion	- Aniline
	- Chlorobenzenes
	- Intermediates (i.e. for drugs, dyes, pesticides)

Table 1.4. Threshold toxicity values for benzene [25]

	Dose	Signs and symptoms
Exposure via ingestion	125 mg/kg bw	Lethal dose
Exposure via inhalation	80 mg/m^3	No immediate clinical effects (8 hours)
	160 – 480 mg/m^3	Headache, lethargy, weakness (5 hours)
	1600 mg/m^3	Symptoms of illness (60 min)
	4800 mg/m^3	Serious symptoms (60 min)
	2400 mg/m^3	Dangerous to life (30 min)
	6400 mg/m^3	Central nervous system depression, cardiac arrhythmia, respiratory failure and death (5-10 min exposure)

Table 1.5. Environmental quality standards for benzene in Japan [26]

	Standards for human health	Measuring method
Air	Annual average ≤ 0.003 mg/m^3	Gas chromatograph-mass spectrometer or equivalent method.
Surface water	≤ 0.01 mg/L	-
Ground water	0.01mg/L	-
Soil	≤ 0.01 mg/l in sample solution	Leaching tests

Benzene has been indentified as a known human carcinogen. Breathing very high levels of benzene can result in death. Acute inhalation exposure to high levels of benzene may cause central nervous system effects such as dizziness, nausea, vomiting, headache, drowsiness, tremor, and loss of consciousness. These effects appear to be concentration dependent and reversible. Continuing exposure at sufficient concentrations can lead to the permanent suppression of bone marrow functioning so that can cause a decrease in red blood cells leading to anemia. It can also cause excessive bleeding and can affect the immune system, increasing the chance for infection. Long-term exposure to high levels of benzene in the air can cause leukemia, particularly acute myelogenous leukemia. This is a cancer of the blood-forming organs. Therefore, the use of benzene has been strictly restricted in whole over the world. Table 1.4 and 1.5 show threshold toxicity values and environmental quality standards for benzene regulated by Japan government. [24-34]

1.3 Recent research on photooxidation of benzene over TiO_2

The behavior of benzene in photocatalytic reaction over TiO_2 has been studied as a model of removal of aromatic compounds in the environmental chemistry in both gas phase and liquid phase. It is reported that benzene vapor is efficiently oxidized over UV photoirradiated TiO_2. CO_2 and CO are major detected products in gas phase [35-45]. However,

there are some reports on difficulty of decomposition of aromatic compounds using TiO_2 photocatalysts [35-38]. More precisely, aromatic compounds are decomposed more slowly than other organic compounds. In addition, during the photocatalytic reactions, the reaction rate is further lowered and TiO_2 powders are colored. Adsorption of intermediate products is thought to be the reason for the deactivation and coloration of TiO_2 particles, both of deactivation and coloration of TiO_2 are problematic for its practical application.

Selective photocatalytic reactions have also been attracted much research interest in the field of organic synthesis. Phenol has been reported as the sole initial product from benzene in photocatalytic reaction [21,44]. Yoshida et al. reported photocatalytic conversion of benzene to phenol as high as 90% [45]. Recently, ring opening reactions of aromatic compounds become one of the most studied photocatalytic reactions. We have reported that naphthalene is efficiently oxidized to 2-formylcinnamaldehyde in a mixed solvent of acetonitrile and water bubbled with molecular oxygen. In photocatalytic reaction of phenanthrene, biphenyl-2,2'-dicarbaldehyde has also reported as a main product [46,47]. The ring cleavage and formation of aldehydes from aromatic compounds have a great meaning in both fundamental research and practical applications. In this study, we chose benzene as a typical aromatic compound to investigate the ring-opening mechanism in photocatalytic reaction.

1.4 Research objectives

The research objectives in this study are:

1. Systematically studying benzene photooxidation, including analyzing byproduct both in liquid phase and on surface of TiO_2, investigating the influence of by-products from benzene on photocatalytic activity of TiO_2, determining oxygen sources in aqueous photooxidation of benzene.
2. Clarifying reaction mechanism for photocatalytic oxidation of aromatic compounds, which is not only meaningful in fundamental research but also applicable to industry and environmental treatment.

3. Studying photooxidation of water, which is present in most photocatalytic reactions, over TiO_2 particles by ^{18}O tracing method.
4. Clarifying the differences in photocatalytic activities of rutile and anatase TiO_2 based on the both photocatalytic oxidation of water and benzene.

1.5 Scope and outline of the thesis

Chapter 1

Fundamentals and applications of TiO_2 photocatalysis, sources and toxicities of benzene, and researches on photooxidation of benzene over TiO_2 photocatalysts are briefly reviewed. Based on the needs for deeper studies on photooxidation of benzene on TiO_2 photocatalyst, the research objectives of the thesis is pointed out.

Chapter 2

Byproducts in photooxidation of benzene over TiO_2 particles are analyzed and characterized carefully. The deactivation of TiO_2 photocatalysts during photooxidation of aromatic compounds, which is still mysterious in previous researches, is described and clearly clarified in this chapter.

Chapter 3

^{18}O tracing method is successfully applied to the study on photooxidation of benzene over TiO_2 particles. Both O_2 and H_2O molecules are confirmed to be the oxygen sources in this reaction. Their contributions depend on TiO_2 form, TiO_2 surface modification and reaction conditions. In the first time, the higher activity of anatase in photooxidation of organic compounds is attributed to the ease in formation of strong active oxygen species from water on the surface.

Chapter 4

In the first time, hydroxylation pathway and ring-opening pathway are experimentally confirmed as two parallel pathways in photooxidation of benzene. The important role of each pathway in overall mineralization of benzene is discussed, based on the results in experiments

using ^{13}C as isotope tracer. The difference in photo-activity of rutile and anatase is also described in this chapter.

Chapter 5

Photooxidation of water molecules on UV-photoirradiated TiO_2 particles in presence of molecular O_2 is studied by using ^{18}O-tracing method. Important results about O_2 formation on TiO_2 surface and differences between photocatalytic activities of rutile and anatase forms are discussed.

Chapter 6

Important results will be concluded and several research recommendations will be proposed.

References

[1] S. E. Braslavsky, *Pure Appl. Chem.*, 79, **2007**, 3, 293–465.

[2] A. Fujishima, X. Zhang and D. A. Tryk, *Surf. Sci. Rep.* 63, **2008**, 515-582.

[3] A. Fujishima, X. Zhang and D. A. Tryk, *Int. J. Hydrogen Energy.* 32, **2007**, 2664–2672.

[4] A. Fujishima, T. N. Rao and D. A.Tryk, *J. Photochem. Photobiol., C* 1, **2000**, 1–21.

[5] A. Fujishima and X. Zhang, *C. R. Chimie* 9, **2006**, 750–760.

[6] K. Hashimoto, H. Irie, and A. Fujishima*, Jpn. J. Appl. Phys.* 44 (12) **2005**, 8269–8285.

[7] M. R. Hoffmann, S. T. Martin, W. Choi, and D. W. Bahnemann, *Chem. Rev.* 95, **1995**, 69-96.

[8] M. A. Fox and M. T. Dulay, *Chem. Rev.* 83, **1995**, 341-357.

[9] A. L. Linsebigler, G. Lu and J. T. Yates, Jr., *Chem. Rev.* 95, **1995**, 735-758.

[10 A. Mills and S. L. Hunte, *J. Photochem. Photobiol., A* 108, **1997**, 1-35.

[11] S. Roberts, *Phys. Rev.* 76 (8), **1949**, 1215-1220.

[12] H. Tang, K. Prasad, R. Sanjines, P. E. Schmid and F. Levey, *J. Appl. Phys.* 75 (4), **1994**, 2042-2047.

[13] D. C. Cronemeyer, *Phys. Rev.* 87 (5), **1952**, 876-886.

[14] F. A. Grant, *Rev. Mod. Phys.* 31(3), **1959**, 646-674.

[15] H. P. R. Frederikse, *J. Appl. Phys.* 32 (10), **1961**, 2211-2215.

[16] O. I. Micic, Y. Zhang, K. R. Cromack, A. D. Trifunac and M. C. Thurnauer, *J. Phys. Chem.* 97, **1993**, 7277-7283.

[17] P. Salvador, *J. Phys. Chem. C* 1, **2007**, 17038-17043.

[18] R. Nakamura and Y. Nakato, *J. Am. Chem. Soc.* 126, **2004**, 1290-1298.

[19] R. Nakamura, A. Imanishi, K. Murakoshi and Y. Nakato, *J. Am. Chem. Soc.* 125, **2003**, 7443-7450.

[20] G. Palmisano, V. Augugliaro, M. Pagliaro and L. Palmisano, *Chem. Commun.,* **2007**, 3425 – 3437.

[21] V. Augugliaro, M. Litter, L. Palmisano and J. Soria, *J. Photochem. Photobiol., C* 7, **2006**, 127–144.

[22] S. B. Wang, H.M. Ang and M. O.Tade, *Environ. Int.* 33, **2007**, 694–705.

[23] M. Anpo, *Pure Appl. Chem.*, 72 (7), **2000**, 1265–1270.

[24 http://www.atsdr.cdc.gov/ (accessed June 7th **2010**)

[25] http://www.hpa.org.uk/ (accessed June 7th **2010**)

[26] http://www.env.go.jp/en/ (accessed June 7th **2010**)

[27] T. J. Atkinson, *Int. J. Hyg. Environ. Health* 212, **2009**, 1-10.

[28] H. Kajihara, S. Ishizuka, A. Fushimi, A. Masuda and J. Nakanishi, *Environ. Engg. and Policy* 2, **2000**, 1–9.

[29] R. Snyder, G. Witz, and B. D. Goldstein, *Environ. Health Perspect.* 100, **1993**, 293-306.

[30] R. Snyder and C. C. Hedli, *Environ. Health Perspect.* 104 (6), **1996**, 1165-1171.

[31] L. Fishbein, *Sci. Total Environ.* 40, **1984**, 189-218.

[32] D. V. Parke, *Environ. Health Perspect.* 104 (6), **1996**, 1123-1128.

[33] M. R. Lovern, M. J. Turner, M. Meyer, G. L. Kedderis, W. E. Bechtold and P. M. Schlosser, *Carcinogenesis* 18 (9), **1997**, 1695–1700.

[34] S. A. Kline, J. F. Robertson, V. L. Grotz, B. D. Goldstein, and G. Witz, *Environ. Health Perspect.* 101 (4), **1993**, 310-312.

[35] O. d'Hennezel, P. Pichat and D. F. Ollis, *J. Photochem. Photobiol., A* 118, **1998**, 197-204.

[36] H. Einaga, S. Futamura, T. Ibusuki, *Appl. Catal., B* 38, **2002**, 215–225.

[37] R. M. Alberici and W. F. Jardim, *Appl. Catal., B* 14, **1997**, 55-68.

[38] M. M. Ameen and G. B. Raupp, *J. Catal.* 184, **1999**, 112-122.

[39] S. Zhang, Z. Zheng, J. Wang and J. Chen, Chemosphere 65, **2006**, 2282–2288.

[40] H. Einaga, S. Futamura, T. Ibusuki, *J. Sol. Energy Eng.* 126, **2004**, 789-793.

[41] J. Zhong, J. Wang, L. Tao, M. Gong, L. Zhimin and Y. Chen, *J. Hazard. Mater.* B139, **2007**, 323-331.

[42] N. N. Lichtin and M. Sadeghi, *J. Photochem. Photobiol., A* 113, **1998**, 81-88.

[43] J. Chen, L. Eberlein and C. H. Langford, *J. Photochem. Photobiol., A* 148, **2002**, 183-189.

[44] H. Park and W. Choi, *Catal. Today* 101, **2005**, 291-297.

[45] H. Yoshida, H. Yuzawa, M. Aoki, K. Otake, H. Itoh and T. Hattori, *Chem. Comm.*, **2008**, 4634-4636.

[46] T. Ohno, K. Tokieda, S. Higashida, M. Matsumura, *Appl. Catal., A* 244, **2003**, 383-391.

[47] S. Higashida, A. Harada, R. Kawakatsu, N. Fujiwara and M. Matsumura, *Chem. Commun.*, **2006**, 2804-2806.

Chapter 2: THE DEACTIVATION OF TiO_2 DURING BENZENE PHOTOOXIDATION

During photooxidation of aromatic compounds, the rate of CO_2 evolution is gradually lowered, which is in contrast to the cases of other non-aromatic organic compounds, such as alcohols or acids. To clarify the reason for the decrease in activity of TiO_2, intermediates produced in the solution phase and on the surface of TiO_2 were analyzed using chemical and physical techniques. Several kinds of intermediates were identified: phenolic compounds, aldehydes, carboxylic acids, and polymeric substance. Of these products, catechol and other phenols species, which strongly adsorb on the surface of TiO_2 powder, were found to be responsible for the lowering of the photocatalytic activity of TiO_2. Meanwhile, polymeric substance gradually accumulates on TiO_2 surface. It was harmless to the TiO_2 activity but physically blocks benzene to come to TiO_2 surface. Also, oxidation of polymeric substance itself can be initiated by UV-Vis activation, and accounts for CO_2 evolution in prolonged photoirradiation.

2.1 Introduction

So far, many kinds of harmful organic substances have been mineralized into CO_2 and water by TiO_2-photocatalyzed reaction [1-4]. It would be very meaningful to construct a system for decomposing benzene or volatile aromatic compounds using photocatalysts because these compounds are highly toxic and carcinogenic and their concentrations in the environment are strictly limited. However, the deactivation and coloration of TiO_2 photocatalysts, especially in photooxidation of aromatic compounds, have been reported. This is problematic for practical application of TiO_2 powders. The reason can be attributed to the adsorption of intermediate products on surface of TiO_2 particles.

Surface charge transfer (CT) complexes formed between TiO_2 and phenolic compounds have been proposed as the cause of coloration of TiO_2. Alberici et al. [2] suggested that the species adsorbed on TiO_2 were responsible for the deactivation of TiO_2 photocatalysts during photocatalytic reactions of aromatic compounds. However, they did not determine the adsorbed products. Einaga et al. [3] analyzed the deactivated TiO_2 particles by means of IR spectroscopy and found “carbon deposits” on the surfaces of the particles. d’Hennezel et al. [5] extracted the species adsorbed on the TiO_2 surface with organic solvents and detected phenol, hydroquinone, and benzoquinone as intermediate products from benzene. However, Wu et al. [6] reported that species with phenoxy groups were formed on the TiO_2 surface and suggested that the products extracted from TiO_2 with organic solvents may not reveal the real products formed on the surface. We found that the products extracted with organic solvents are not the main cause of the deactivation and coloration of TiO_2 because, as described later, the TiO_2 powder after extraction of these intermediates products is colored and shows lowered photocatalytic activity. This means that there are considerable amounts of intermediate products that are not extracted from the TiO_2 surface by using conventional organic solvents.

We consider the identification of these products, which cannot be extracted with organic solvents, are important for the clarification of the deactivation of TiO_2 photocatalysts when used in the presence of aromatic compounds. In this study, therefore, we analyzed the

products formed in liquid and on the surface of TiO_2 in photooxidation of benzene. Based on obtained results, we discuss the cause of deactivation and coloration of the TiO_2 photocatalyst when used for the oxidation of benzene.

2.2 Experiments

TiO_2 powders ST-01, ST-21 and ST-41 obtained from Ishihara Sangyo, Ltd., NS-51 from Toho Titanium Co. Ltd., TIO-3 from Ishihara Sangyo Co. Ltd., MT-150A from Teika Co. Ltd. and P-25 Degussa from Nippon Aerosil Co. Ltd. were used as photocatalysts. Content of rutile phase and relative specific surface area of these TiO_2 powders are as follows: ST-01: 0%, 192.5 m^2/g; ST-21: 0%, 56.1 m^2/g; ST-41: 0%, 8.2 m^2/g; MT-150A: 100%, 110 m^2/g; TIO-3: 100%, 48.1 m^2/g; NS-51: 98.5%, 6.5 m^2/g and P-25: 26%, 49.2 m^2/g.

Benzene, phenol, catechol, hydroquinone, resorcinol, oxalic acid, maleic anhydride, malonic acid, acetic acid, sodium fluoride, and hydrogen chloride obtained from Wako Pure Chemical as guaranteed reagents were used without further purification.

All photocatalytic reactions were carried out at room temperature in 40 ml Pyrex glass tubes (1.5 cm in diameter) containing 100 mg of the TiO_2 powder and 5 ml of benzene. The gas phase of the tubes was filled with air. A 500 W high-pressure mercury lamp (Wacom BMO-500DY) was used as a light source, and the light beam was passed through a 34-filter (Kenko Co.) to eliminate deep UV components ($\lambda < 340$ nm) and through stainless-steel meshes to lower the light intensity to about 0.6 mW/cm^2. The reaction suspension was magnetically stirred during the reaction.

CO_2 evolution in the gas phase was monitored with a Shimadzu GC-8A gas chromatograph. Liquid phase was analyzed by an HPLC system equipped with a Hitachi L-7400 UV detector and 4.6×150 mm columns (GL-Sciences, Intersil ODS-3). The HPLC mobile phase was a mixture of acetonitrile and water (volume ratio of 1:1) with a flow rate of 0.5 ml per minute. The products were identified from the results of HPLC by comparing

retention times and UV-Vis adsorption spectra of the products with those of corresponding authentic compounds.

The TiO_2 powder samples that had been separated from the reaction solution and dried in ambient air at 80^oC for 3 h were analyzed for identification of adsorbed products. FTIR spectra of solid samples were recorded on a Nicolet Nesus 370S IR spectrometer with resolution of 2 cm^{-1}. UV diffuse reflectance spectra were obtained with a Shimadzu UV-2450 spectrophotometer equipped with an integrating sphere. For thermogravimetry (TG) and differential thermal analyses (DTA) of the samples, 20 mg of the powder sample was put in an opened pan in air and analyzed with a Bruker Thermal Analyzer (AXS TG-DTA 2000SA). Temperature was raised at a rate of 15^oC per minute. The products adsorbed on the TiO_2 powder were also analyzed after they were extracted from the TiO_2 surface. For the extraction, 25 mg of dried powder after photocatalytic reaction was ultra-sonicated in 2 ml of aqueous solution containing NaF (0.08 M) and HCl (0.72 M) for 2 hours at 40^oC, and then the liquid was analyzed by HPLC.

The adsorption isotherm of catechol on the TiO_2 powder was obtained as follows. TiO_2 powder (100 mg) was added to each of the catechol solutions in toluene (10 ml) with different concentrations. The suspensions were ultra-sonicated for 45 minutes at 40^oC to reach the equilibrium, and the concentration of catechol in the solution was determined by HPLC.

2.3 Results and discussion

2.3.1 CO_2 evolution from benzene and products in liquid phase

When organic compounds are decomposed by TiO_2-photocatalyzed reaction, CO_2 evolves. Time courses of CO_2 evolution from benzene samples containing different TiO_2 powders are shown in Fig. 2.1. High CO_2 evolution rates were obtained by using ST-01, ST-21, and P-25 powders. They have large specific areas and are chiefly made of an anatase phase. The high activity of P-25 powder may be partly attributed to the synergism between rutile and anatase phases [7]. In all cases, the CO_2 evolution rate decreased with irradiation

time, and the tendency was obvious for the powders with small specific surface areas (ST-41, TIO-3, and NS-51). This tendency suggests that intermediate products produced from benzene have negative effects on the photocatalytic activity of TiO_2 surface. With the production of these intermediates, the TiO_2 particles gradually changed from white to pale yellow and, then, brown, as discussed later.

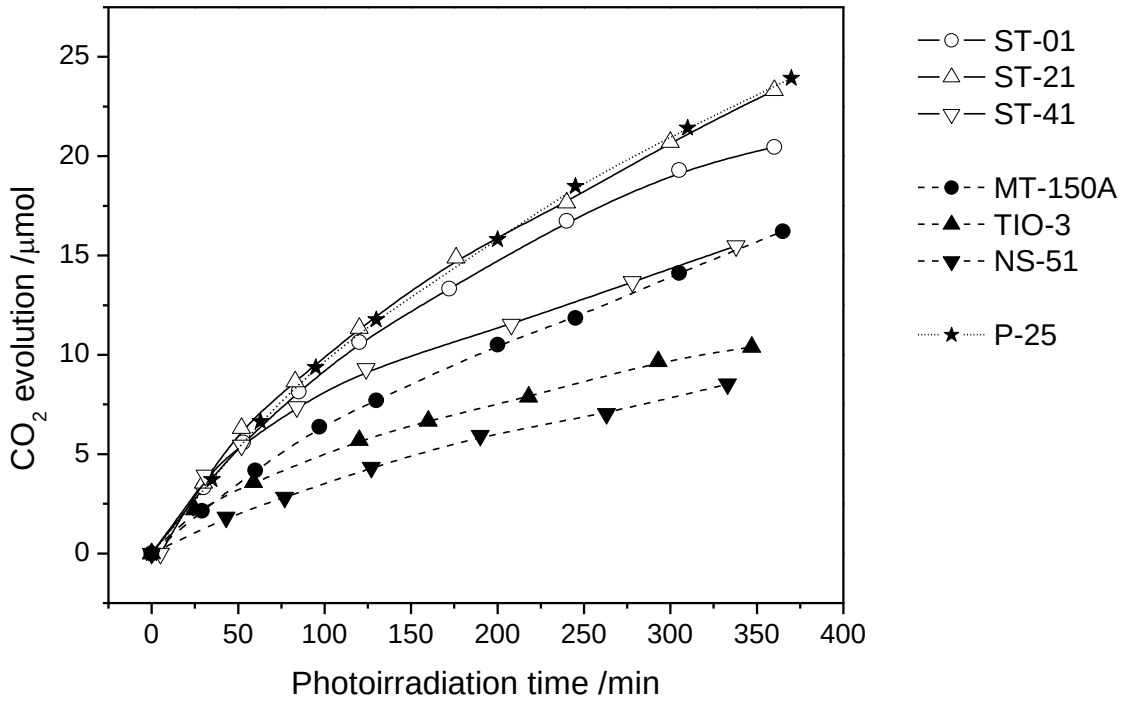

Fig. 2.1. Time courses of CO_2 evolution from pure benzene with several kinds of TiO_2 powders as photocatalysts.

The lowering of the CO_2-evolution rate with irradiation time was observed when benzene or some aromatic compounds were used as the samples, whereas the rate was constant for most of other organic materials as long as the components of the liquid do not change remarkably. To demonstrate the difference, the time courses of CO_2 evolution from pure benzene and pure acetic acid are compared in Fig. 2.2.

The lowering of CO_2-evolution rate from benzene with time suggests that some of the intermediate products from benzene have harmful effects on photocatalytic activity of TiO_2 particles. Therefore, we tried to determine products dissolved in liquid and also those

adsorbed on TiO_2 surface. In the following experiments, we mostly used ST-01 powder as photocatalyst. The reason we chosen ST-01 is that it is the most active and widely used TiO_2 powder in environmental treatment thank to its large specific surface area. Therefore, it allows us to fully investigate photooxidation of benzene in experiments carried out in a short time instead of in longer time with other TiO_2 powders.

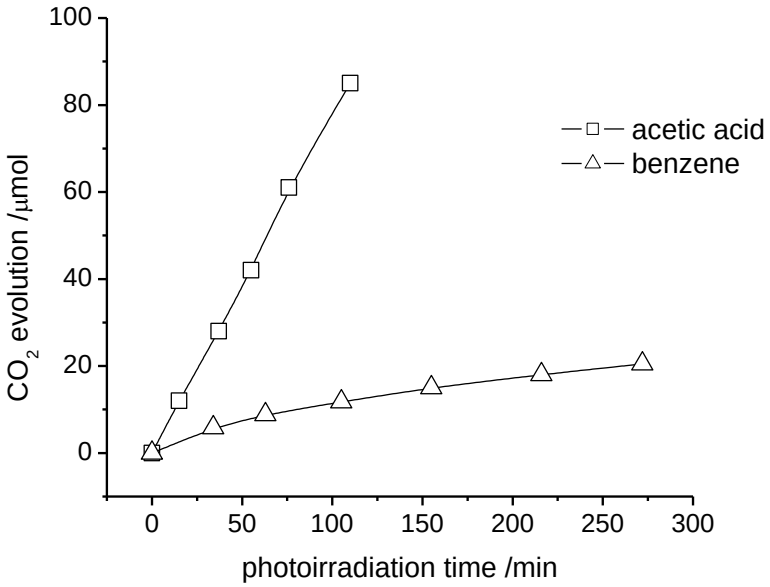

Fig. 2.2. CO_2 evolution by photocatalytic reaction of (a) pure benzene and (b) pure acetic acid using TiO_2 powder (ST-01) as a photocatalyst.

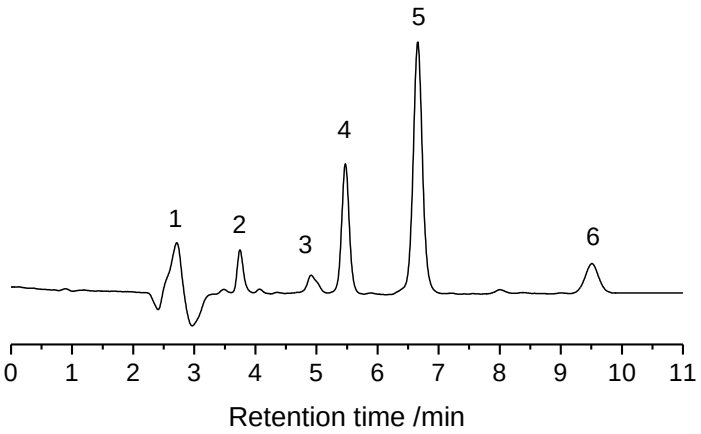

Fig. 2.3. A typical HPLC chromatogram of benzene after photoirradiation using TiO_2 powder (ST-01) as a photocatalyst.

In order to determine intermediate products from benzene, we periodically sampled small aliquots of the reaction liquid (benzene) during the photocatalytic reaction and analyzed them by HPLC. Typically, 6 peaks (Peaks 1 - 6) were observed in the HPLC chromatograms, as shown in Fig. 2.3. The valley observed after Peak 1 is an artifact, which appeared even when pure benzene was injected into the HPLC system. By comparing the retention times and UV-Vis spectra of the components with those of the authentic samples, four of these peaks were assigned to p-hydroquinone (Peak 2), muconaldehyde (Peak 3), p-benzoquinone (Peak 4), and phenol (Peak 5). These compounds were reported as products from benzene by the TiO_2-photocatalytic reaction [3, 5, 8]. Although Peak 1 was not identified, it is probably due to an acid or a mixture of acids produced from benzene; possible acids such as oxalic acid and formic acid, which can be produced from benzene, showed retention times almost at the same position. Peaks 1 - 5 grew for 30 minutes during photoirradiation and then started to decrease, whereas Peak 6, which appeared at the longest retention time, continued to grow. This last peak is probably due to dimeric species, i.e., hydroxybiphenyls and/or aromatic ethers. Production of these dimeric compounds from phenol in the TiO_2-photocatalyzed reaction was reported by Peiró et al. [9] and Ng et al. [10].

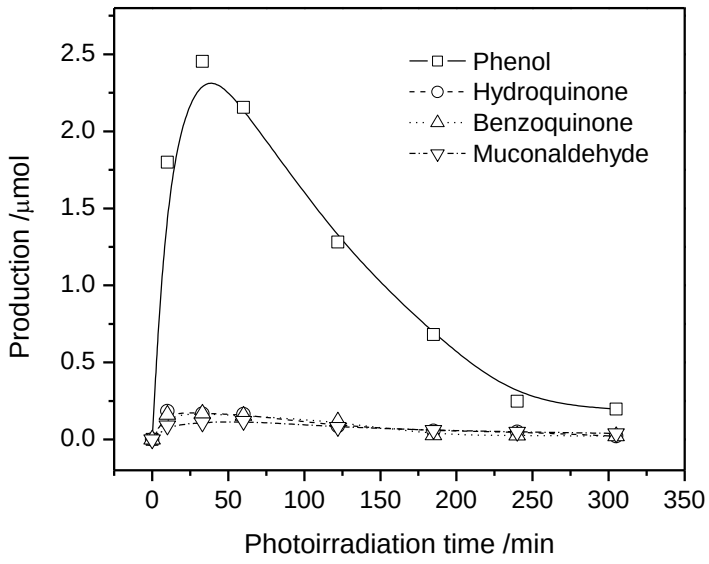

Fig. 2.4. Time course of phenol, hydroquinone and benzoquinone during photoirradiation using TiO_2 powder (ST-01) as a photocatalyst.

The time course of productions of phenol, hydroquinone, benzoquinone and muconaldehyde are shown in Fig. 2.4. During photoirradiation process, the dissolved by-products increased fast in early time as shown in Fig. 2.4, and after that, they started to decrease. The decrease in amount of by-product indicates the decrease in oxidation of benzene. There must be chemical deactivation of TiO_2 or physical inhibition of the contact between benzene and TiO_2 surface. Both of these reasons can prevent practical application of TiO_2.

2.3.2 Analysis of products adsorbed on TiO_2

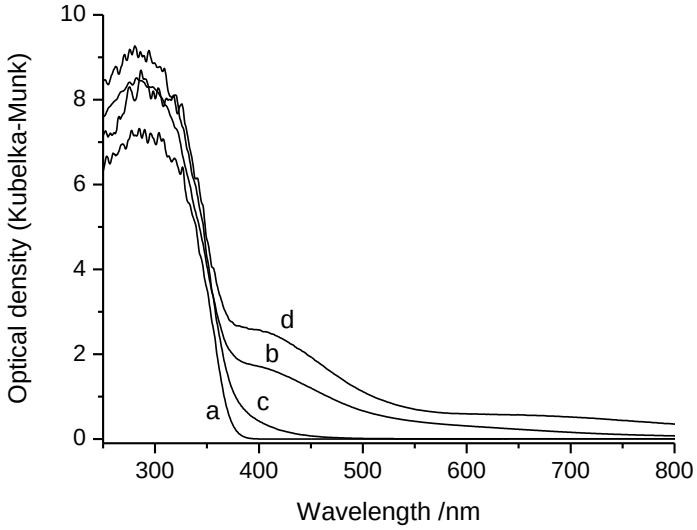

Fig. 2.5. Typical diffuse reflectance spectra of TiO_2 powder (ST-01) (a) before and (b) after photoirradiation for 35 minutes in benzene. Spectra (c) and (d) are of the TiO_2 powder on which phenol and catechol were adsorbed, respectively.

The deceleration of CO_2 evolution is probably related to the intermediate products which are not only dissolved in the liquid phase but also adsorbed on the TiO_2 surface. The adsorption of these intermediates was evident from coloration of the TiO_2 particles during photoirradiation. For analysis of the intermediates, the TiO_2 powder after photoirradiation was separated from benzene and dried in air. Diffuse reflectance spectra of the photoirradiated

TiO_2 powder and the same powder before photoirradiation are shown by curves (a) and (b) in Fig. 2.5. The results indicate that the intermediate products exist not only in the liquid but also on the surface of TiO_2.

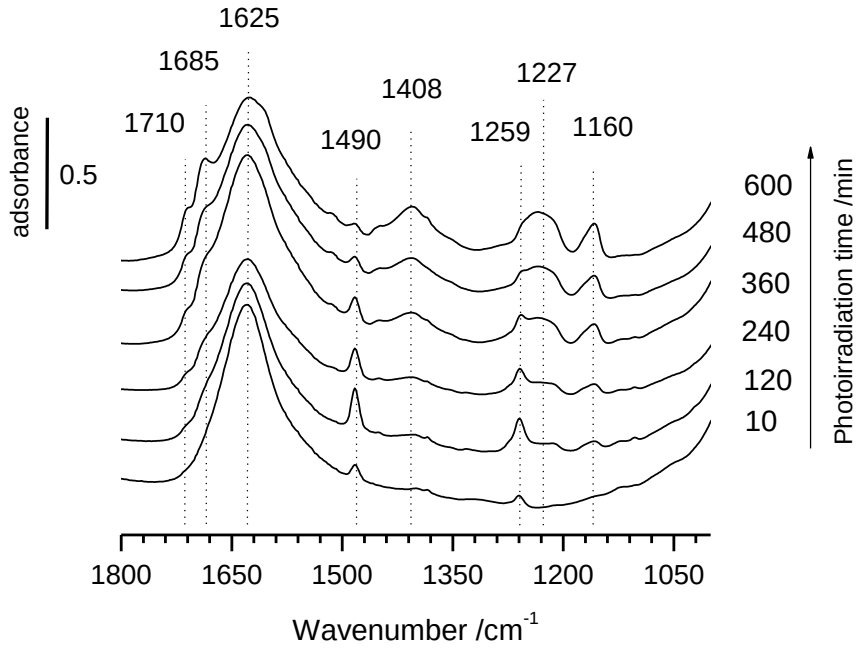

Fig. 2.6. FTIR spectra of TiO_2 (ST-01) powder after photoirradiation in benzene

Since the species adsorbed on TiO_2 powder are considered to have a stronger influence on the photocatalytic activity than those dissolved in solution, identification of the adsorbed species on TiO_2 is important. We therefore measured FTIR spectra for KBr discs containing the TiO_2 powder after photoirradiation. With increase in the irradiation time in benzene, two peaks at 1490 and 1259 cm^{-1}, which are typical peaks of C-C stretching vibration of benzene rings and C-O stretching vibration, increased and then started to decrease after photoirradiation for 240 minutes, as seen in Fig. 2.6. These peaks are due to phenolic compounds adsorbed on TiO_2 [6,11]. Three peaks at 1710 and 1685 and 1408 cm^{-1} became clear after 240 minutes. The peaks at 1710 and 1685 cm^{-1} are characteristic of asymmetric and symmetric stretching vibration of C=O double bonds, respectively [12]. The shift of these peaks to lower frequencies than normal positions suggests that these carbonyl groups are connected with a conjugated system or adsorbed on the surface of TiO_2. The peak at 1408 cm^{-}

[1] should be due to C-O-H bending. These results suggest that some acids are gradually formed on the surface of the TiO_2 powder. Two peaks observed at 1227 and 1160 cm^{-1}, which grew with irradiation time, are probably due to polymeric compounds formed from phenolic compounds on photoirradiated TiO_2 particles [10,13].

In order to identify the species adsorbed on TiO_2 after photoirradiation, we extracted them from the TiO_2 surface by immersing the TiO_2 powder after photoirradiation using organic solvents. We detected phenol, hydroquinone, and benzoquinone, as reported by d'Hennezel [5]. However, they cannot be the main cause of the deactivation and coloration of TiO_2 particles because the TiO_2 particles after extraction were strongly colored and showed a low level of photocatalytic activity.

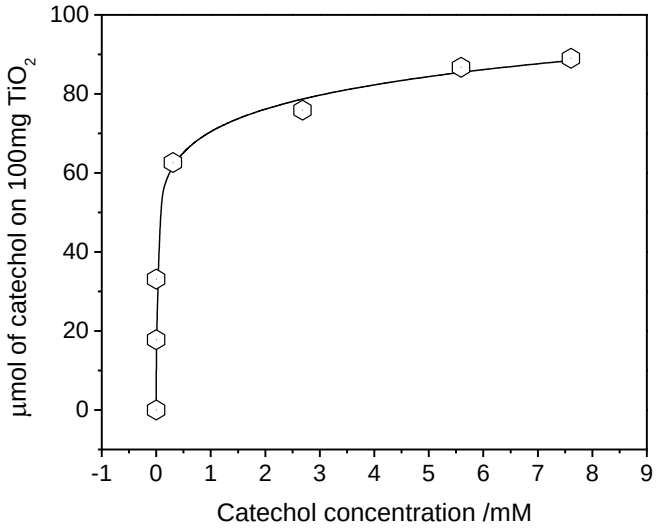

Fig. 2.7. Adsorption isotherm of catechol on TiO_2 (ST-01).

The species strongly adsorbed on TiO_2 particles must be identified to clarify the reasons for the deactivation and coloration of TiO_2. It is known that F^- is strongly adsorbed on TiO_2 and that TiO_2 gradually dissolves in HF solution [14,15]. Hence, the colored TiO_2 after photocatalytic reaction was immersed in an aqueous solution containing NaF (0.08 M) and HCl (0.72 M) for 30 min. Dissolution of TiO_2 was negligible during the treatment. The products extracted into the solution were analyzed by HPLC. There were two main products

in the HPLC chromatogram, which were assigned to phenol and catechol. Catechol has not been detected as a product from benzene by TiO_2-photocatalyzed reaction [5,6], probably due to the strong adsorption of catechol on TiO_2. Besides these species, several unidentified products were detected in the extraction solution. Judging from the retention times and UV-Vis spectra, we believe that they were carboxylic fragments produced by ring-opening reactions of benzene. Phenol was observed in large amounts both on TiO_2 and in benzene. In contrast, catechol was not found in solution phase, but detected in a larger amount as an adsorbed product on the surface of TiO_2. This is attributed to strong affinity of catechol to TiO_2 surface, which was proved by the adsorption isotherm of catechol, as shown in Fig. 2.7.

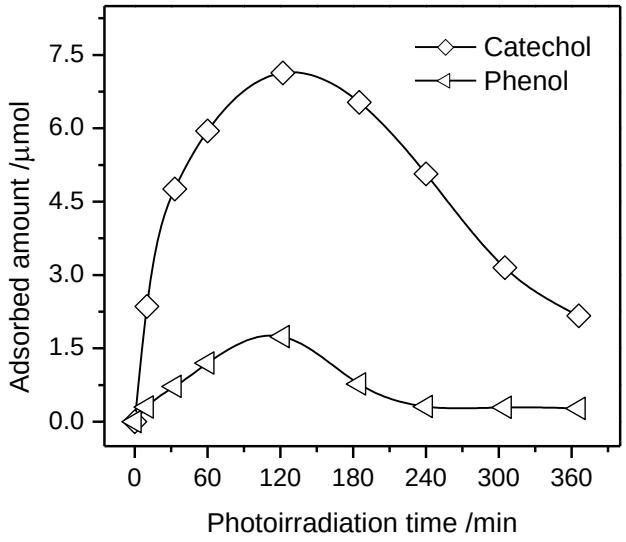

Fig. 2.8. Time course of production of catechol and phenol on TiO_2 (ST-01) powder. The products were extracted from dried samples (100 mg) of TiO_2 photoirradiated in benzene.

Fig. 2.8 shows amounts of phenol and catechol extracted from the ST-01 powder surface with increase in irradiation time. The amounts increased with increase in irradiation time in the early stage of the reaction, reached maximum values at about 120 minutes, and then started to decrease. This tendency is consistent with the tendency of the FTIR peaks at 1490 and 1259 cm^{-1}, which we attributed to phenolic compounds, observed for TiO_2 powders after

photoirradiation, as shown in Fig. 2.6. Compared with phenolic compounds in solution phase in Fig. 2.4, the decrease in phenolic compounds adsorbed on TiO_2 surface came little bit later.

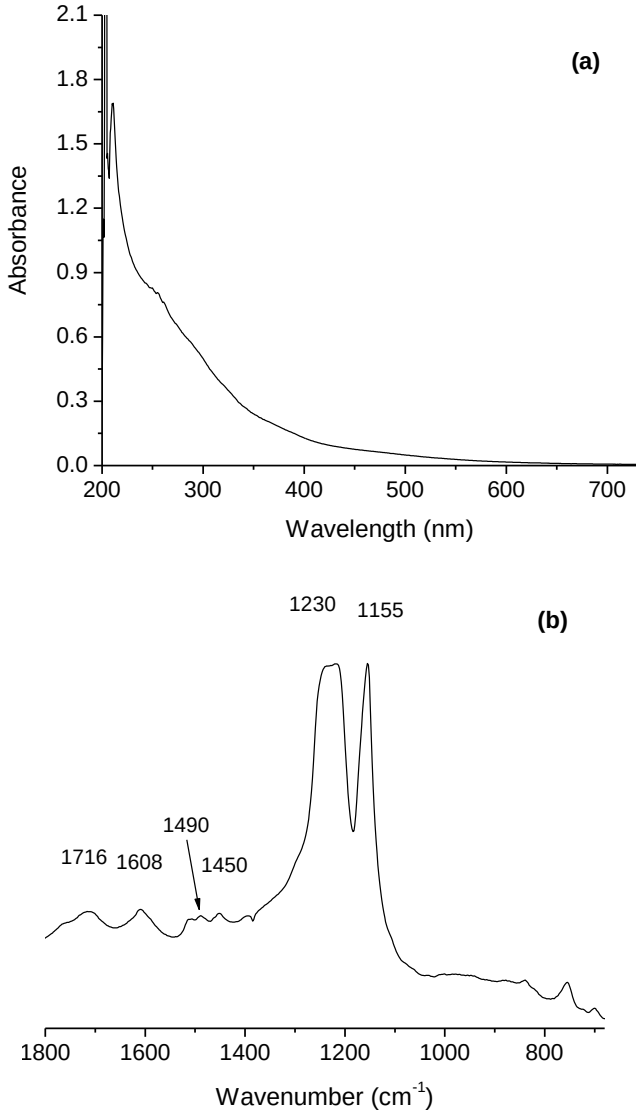

Fig. 2.9. UV-Vis (a) and FTIR (b) absorption spectra of polymeric substance separated from TiO_2 powder after 6 hours of photoirradiation in benzene.

It is notable that the coloration of TiO_2 particles remained even after extraction with the solution containing NaF and HCl, although the coloration after the treatment was much less. The coloration after the treatment was not reduced or eliminated by extraction with organic solvents. These results suggest that an insoluble substance such as a polymer remains on the TiO_2 surface after extraction with the solution containing NaF and HCl. In order to separate

this polymeric substance, we dissolved the used TiO_2 powder in HF (10 w%) solution. After TiO_2 was dissolved completely, we obtained a brown solid substance which was soluble in organic solvents such as acetone, acetonitrile. Fig. 2.9.a and b are UV-Vis and FTIR spectra obtained from this polymeric substance, respectively.

This polymeric substance with a wide range of strong absorption from UV to visible light, as shown in Fig. 2.9.a, accounts for the dark color of TiO_2 after long photoirradiation. The FTIR absorption spectrum in Fig. 4.8.b is consistent with those in Fig. 2.6. The two strong distinct peaks at 1230 cm^{-1} and 1155 cm^{-1} are characteristic to this polymer. These two peaks were assigned as asymmetric and symmetric stretching vibration of C–O–C bonds. The dominance of these peaks indicates that this polymeric substance is a kind of polyether or polyester. Peak at 1716 cm^{-1} is corresponding to stretching vibration of COO groups. Besides, the existence of benzene ring in this polymer is indicated by peaks at 1490 cm^{-1} and 1450 cm^{-1} which are characteristic of benzene frame vibrations.

Appearance of photoabsorption bands in the visible region after adsorption of catechol and phenol on TiO_2 powder, as shown in Fig. 2.5, suggests that they are chemisorbed on the surface of TiO_2 through the hydroxyl groups. The coloration of the TiO_2 particles is attributed to CT transition between the chemisorbed species and TiO_2 [11,16-18]. Liu et al. [16] and Rodriguez et al. [19] reported strong chemisorption of catechol on TiO_2. The strong adsorption of catechol on TiO_2 was supported by the adsorption isotherm as shown in Fig. 2.7. The two hydroxyl groups of catechol are thought to be responsible for its strong interactions with TiO_2. Presence of catechol on TiO_2 is important when the photocatalytic activity of TiO_2 is considered because it lowers the photocatalytic activity of TiO_2 [20]. Dimitrijevic et al. [18] suggested the possibility of driving photocatalytic reaction under visible light by utilization of CT excitation. However, the contribution of CT band excitation to the overall photocatalytic reaction is generally small [21]. We also confirmed that the rate of CO_2 evolution under visible light from catechol-adsorbed TiO_2 powder, which was suspended in benzene, was very slow.

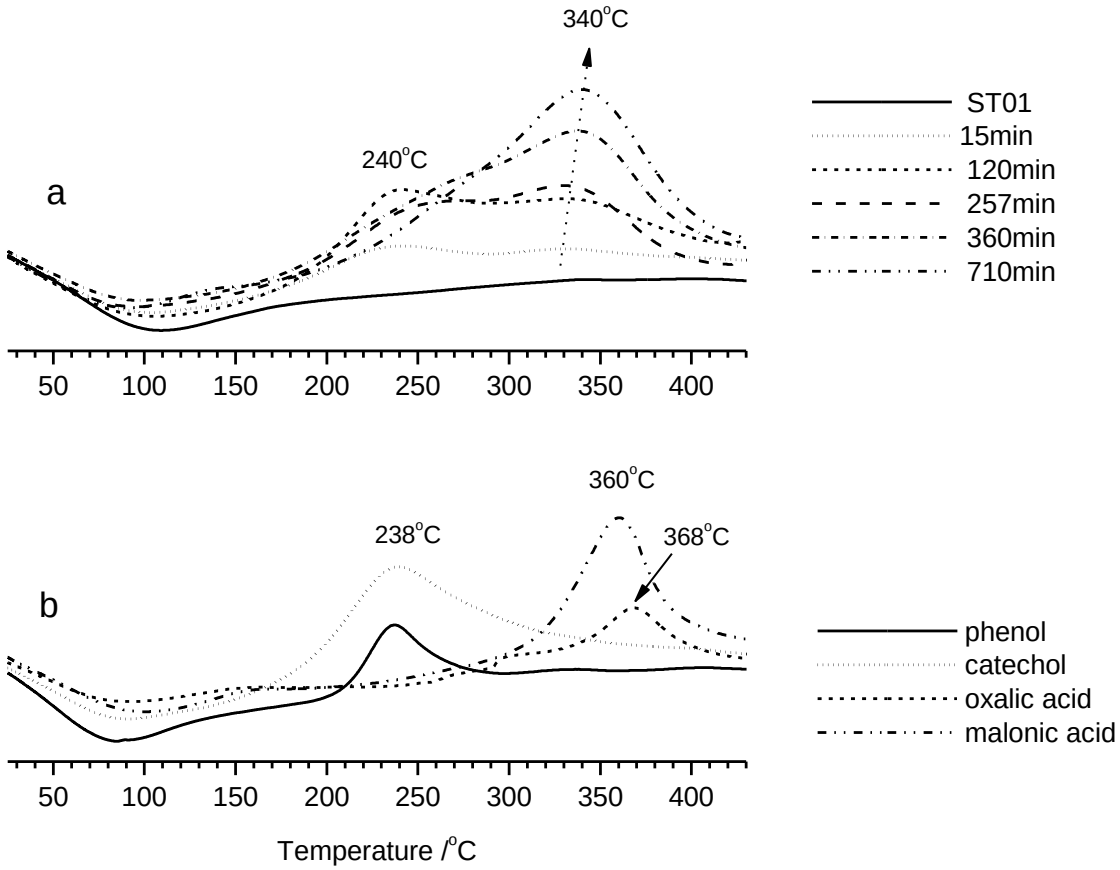

Fig. 2.10. (a) DTA curves for TiO_2 (ST-01) powder before and after photocatalytic reaction of benzene for different periods, (b) DTA curves for TiO_2 (ST-01) powder on which phenol, catechol, oxalic acid or malonic acid were adsorbed from aqueous solutions.

The products adsorbed on the photoirradiated TiO_2 powder were also analyzed by DTA in air. In the early stage of the photocatalytic reaction, two exothermic peaks were observed at 240 and 340°C, the former being the dominant in the initial state, as shown in Fig. 2.10.a. With increase in reaction time, the peak at 240°C increased and then started to decrease. The peak observed at 340°C continued to increase with increase in reaction time and became the dominant peak. The DTA curves for the TiO_2 powders on which phenol, catechol, oxalic acid, and malonic acid were adsorbed are shown in Fig. 2.10.b. From a comparison of these curves, the peak observed at 240°C in Fig. 2.10.a is attributed to phenolic compounds. The peak observed at 340°C in Fig. 2.10.a is probably due to polymeric substances because its change

with time is similar to the change in the FTIR peaks at 1227 and 1160 cm^{-1}, which we attributed to polymeric substances produced from phenolic compounds.

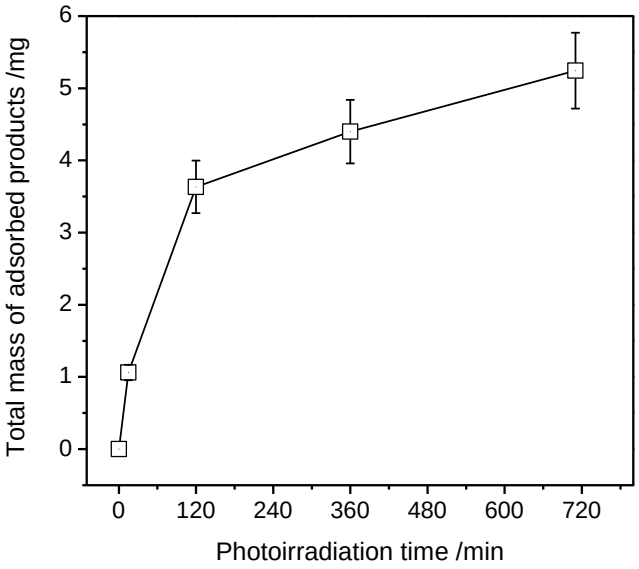

Fig. 2.11. Total mass of products adsorbed on 100 mg of TiO_2 (ST-01) powder. The mass was determined by TG measured over a temperature region from room temperature to 450°C; the mass change for the control sample was subtracted.

From the TG measurements we found that amounts of the products increased rapidly in the initial stage of the photocatalytic reaction and then increased at a much slower rate after photoirradiation for about 100 minutes, as shown in Fig. 2.11. The rapid increase is probably due to the adsorption of phenolic compounds and acids, whereas the slow increase after 100 minutes is probably due to the accumulation of polymeric substances.

From all of the above-described results, we conclude that there are three main products that are adsorbed on the photoirradiated TiO_2: phenolic compounds, carboxylic acids, and polymeric substances. The effect of them on photocatalytic activity of TiO_2 will be discussed below.

2.3.3 Effects of intermediate products on photocatalytic activity of TiO_2

To evaluate the effects of some compounds on the photocatalytic activity of TiO_2 for oxidation of benzene, we added phenol, hydroquinone, catechol, resorcinol or maleic anhydride to benzene and monitored the amount of CO_2 evolved during photoirradiation. The results in Fig. 2.12 show that the rate of CO_2 evolution was lowered by addition of phenol, catechol, hydroquinone, or resorcinol. In contrast, carboxylic acids such as maleic anhydride were easily oxidized on TiO_2 under photoirradiation, causing no lowering in the rate of CO_2 evolution.

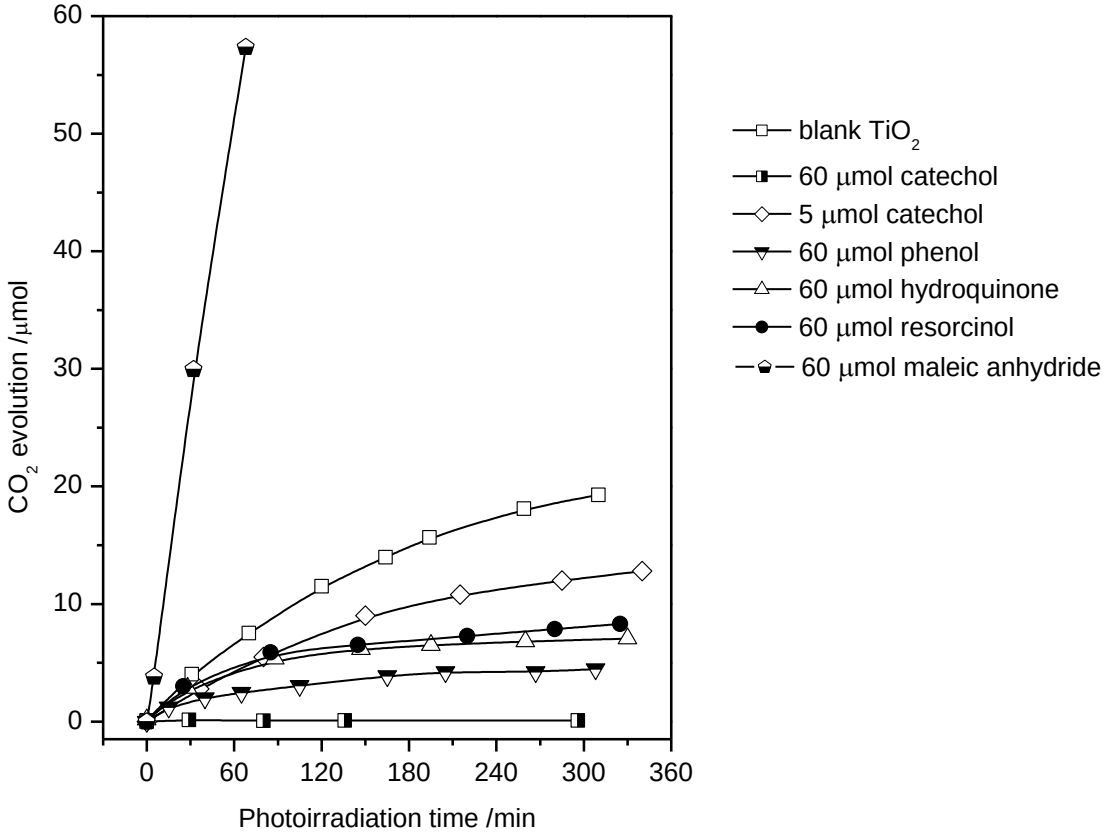

Fig. 2.12. CO_2 evolution by TiO_2 (ST-01) photocatalyzed reactions of pure benzene and benzene containing phenol, hydroquinone, catechol, resorcinol, or maleic anhydride. The amounts of the compounds added to 5 ml of benzene are shown above.

The largest deceleration effect was observed when catechol was added, and the effect decreased in the order of catechol, phenol, hydroquinone, and resorcinol. When 60 μmol of

catechol was added to 5 ml of benzene containing 100 mg of TiO_2, the evolution of CO_2 was totally suppressed. It has been reported that the strong surface complexation of catechol with TiO_2 allows it to cover the TiO_2 surface and that the adsorbed catechol resists oxidation by holes [20]. The suppression of CO_2 evolution by the addition of 60 μmol of catechol is attributed to this effect. Evolution of CO_2 was observed when the amount of catechol added was 5 μmol probably because there remained a surface area that was not covered by catechol. In this case, the initial rate of CO_2 evolution was about 5 μmol per hour. When photocatalytic reaction was carried out in authentic benzene, a similar reaction rate was observed after photoirradiation for about 60-75 min, as seen in Fig. 2.12. With this photoirradiation time, the amount of catechol adsorbed on TiO_2 (100 mg) was also about 5 μmol, as shown in Fig. 2.8. These results strongly suggest that deactivation of TiO_2 particles was due to the adsorption of catechol which was produced from benzene.

It is difficult to investigate the effect of polymeric substance on activity of TiO_2 in the same way we did for several small phenols such as catechol, phenol, hydroquinone and benzoquinone because this polymeric is unique for this reaction. Therefore, in order investigate the influence of this polymeric substance, we did two experiments. In the first one, we prolonged the photoirradiation and in the second one, we re-used TiO_2 powder, which was separated after prolonged photoirradiation, in a photooxidation of new benzene. CO_2 evolutions in these two experiments are shown in Fig. 2.13. As shown in this graph, CO_2 evolution rate, after the depression due to poisonous adsorbed phenols, recovered at long photoirradiation, after 400 min. After that, it kept constant at longer photoirradiation as long as O_2 was provided enough for the oxidation reaction. The recovery of CO_2 evolution rate was also indicated in the second experiment, in which the high CO_2 evolution rate kept unchanged from initial time of photoirradiation until 400 min.

This recover of CO_2 rate was consistent with the disappearance of phenolic compounds both in solution phase (Fig. 2.4) and adsorbed on TiO_2 surface (Fig. 2.8). Also, the decrease in phenolic byproducts in solution phase and on TiO_2 surface indicates the decrease in

photooxidation of benzene due to thick layer of polymeric substance has prevented the diffusion of benzene in solution to TiO_2 surface. And higher CO_2 evolution rate obtained at prolonged photoirradiation can be attributed to the photooxidation of polymeric substance. The role of TiO_2 becomes negligible at prolonged photoirradiation because polymeric layer itself, with the strong absorption in UV-Vis light as shown in Fig. 2.9.a, can burn under UV-Vis photoirradiation. However, the CO_2 evolution from auto-oxidation of this polymer was still much slower than that from photooxidation of small carboxylic acid such as acetic acid and maleic anhydride as shown in Figs. 2.2 and 2.13 respectively. Therefore, polymeric substance still has a bad effect on photocatalytic reactions, although it may be not chemically poisonous to the photocatalytic activity of TiO_2,

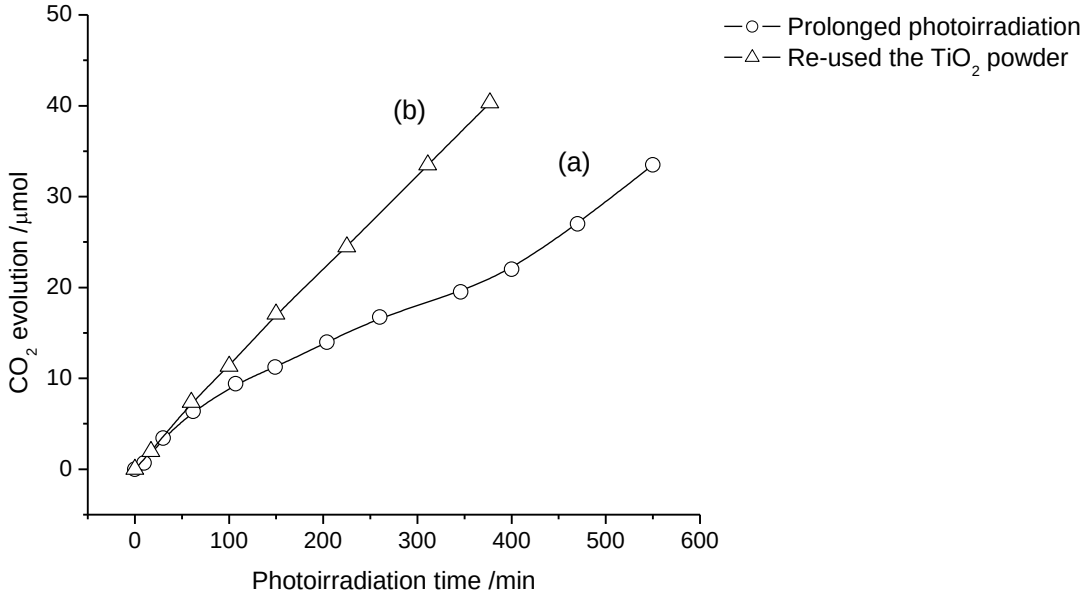

Fig. 2.13. Time courses of CO_2 evolutions in an experiment with prolonged photoirradiation (a) and an experiment using TiO_2 powder that was separated and then dried from the previous experiment (b). ST-01 was used as the TiO_2 powder.

Finally, the relation between the results described above and gas phase reactions should be discussed. In most practical applications of TiO_2 photocatalysts, they are used in a gaseous atmosphere containing very low concentrations of organic compounds under irradiation with a

much lower photon density. In the case of photocatalytic reaction carried out in air containing benzene molecules, TiO_2 powder gradually became colored after a long time. This suggests that compounds determined in authentic benzene in the present study are also produced in gas-phase reactions. However, the production of polymer compounds may not be significant in gas-phase system because the reaction rate is usually very slow due to the low concentration of benzene. Therefore, adsorbed phenolic compounds may be the main source of deactivation and coloration of TiO_2 powders.

2.4 Conclusions

We analyzed intermediate products from benzene in TiO_2-photoctalyzed reactions both in solution phase and on TiO_2 surface. The products formed in solution were phenol, p-hydroquinone, p-benzoquinone, muconaldehyde and some acids. On the surface of TiO_2, besides these compounds, catechol and a polymeric substance were formed. These substances adsorbed on TiO_2 surface were found to have a great effect on the photocatalytic activity. Adsorbed phenolic compounds chemically poison photocatalytic activity of TiO_2, whereas, polymeric substance block TiO_2 surface. Both of them are harmful to photocatalytic reactions.

References

[1] A. Fujishima, X. Zhang and D. A. Tryk, *Surf. Sci. Rep.* 63, **2008**, 515-582.

[2] R. M. Alberici and W. F. Jardim, *Appl. Catal., B* 14, **1997**, 55-68.

[3] H. Einaga, S. Futamura and T. Ibusuki, *Appl. Catal., B* 38, **2002**, 215-225.

[4] M. Mahbub Ameen and G. B. Raupp, *J. Catal.* 184, **1999**, 112-122.

[5] O. d'Hennezel, P. Pichat and D. F. Ollis, *J. Photochem. Photobiol., A* 118, **1998**, 197-204.

[6] W.C. Wu, L.F. Liao, C.F. Lien and J.L. Lin, *Phys. Chem. Chem. Phys.* 3, **2001**, 4456-4461.

[7] T. Ohno, K. Tokieda, S. Higashida and M. Matsumura, *Appl. Catal., A* 244, **2003**, 383-391.

[8] H. Park and W. Choi, *Catal. Today* 101, **2005**, 291-297.

[9] A. M. Peiró, J. A. Ayllón, J. Peral and X. Doménech, *Appl. Catal., B* 30, **2001**, 359-373.

[10] Y. H. Ng, S. Ikeda, T. Harada, S. Higashida, T. Sakata, H. Mori and M. Matsumura, *Adv. Mater.* 19, **2007**, 597-601.

[11] T. Rajh, L. X. Chen, K. Lukas, T. Liu, M.C. Thurnauer and D. M. Tiede, *J. Phys. Chem. B* 106, **2002**, 10543-10552.

[12] S. J. Hug and D. Bahnemann, *J. Electron Spectrosc. Relat. Phenom.* 150, **2006**, 208-219.

[13] M. Gattrell and S. W. Kirk, *J. Electrochem. Soc.* 140, **1993**, 903-911.

[14] C. Minero, G. Mariella, V. Maurino and E. Pelizzetti, *Langmuir* 16, **2000**, 2632-2641.

[15] T. Ohno, K. Sarukawa and M. Matsumura, *J. Phys. Chem. B* 105, **2001**, 2417-2420.

[16]. Y. Liu, J. L. Dadap, D. Zimdars and K. B. Eisenthal, *J. Phys. Chem. B* 103, **1999**, 2480-2486.

[17] N. M. Dimitrijevic, O. G. Poluektov, Z. V. Saponjic and T. Rajh, *J. Phys. Chem. B* 110, **2006**, 25392-25398.

[18] N. M. Dimitrijevic, E. Rozhkova and T. Rajh, *J. Am. Chem. Soc.* 131, **2009**, 2893-2899.

[19] R. Rodriguez, M. A. Blesa and A. E. Regazzoni, *J. Colloid Interface Sci.* 177, **1996**, 122-131.

[20] T. TachiKawa, Y. Takai, S. Tojo, M. Fujitsuka and T. Majima, *Langmuir* 22, **2006**, 893-896.

[21] S. Ikeda, C. Abe, T. Torimoto and B. Ohtani, *J. Photochem. Photobiol., A* 160, **2003**, 61-67.

Chapter 3: OXYGEN SOURCES FOR PHOTOOXIDATION OF BENZENE

Photocatalytic oxidation of benzene to CO_2 was studied in aqueous solutions using different kinds of TiO_2 powders. Isotopic oxygen tracers ($H_2{}^{18}O$ and ${}^{18}O_2$) were used to investigate the oxidation process. Phenol was produced as a main intermediate in solution phase. When anatase powders, which showed high activity for oxidation of benzene, were used, 70-90% of oxygen introduced into phenol was from water. On the other hand, when rutile powders were used, only 20-40% of the oxygen was from water. The rest was from molecular oxygen in both cases. The rate of phenol production by using molecular oxygen was nearly the same between anatase and rutile powders. Hence, the high activity of anatase powders for photooxidation of organic compounds is attributed to their high activity for utilizing water as the oxygen source. The processes using water and molecular oxygen as the oxygen sources are respectively ascribed to oxygen transfer and hole transfer processes in the initial step of benzene oxidation.

3.1 Introduction

It is well known that in photocatalysis, photogenerated holes and electron upon absorption of appropriate photon can migrate to the semiconductor surface and initiate simultaneous oxidation and reduction reactions or chains of redox reactions. Much effort has been made to deepen the understanding of this complex reaction system and to make use of it efficiently. Several mechanism models have been proposed on the basis of experimental results obtained by chemical and physical methods [1-5]. The higher catalytic activity of anatase particles than rutile particles in decomposition of organics has been mostly attributed to its higher conduction band level (larger band gap) [1-6]. However, the photocatalytic reaction mechanism is still unclear, because, for example, rutile particles are more active than anatase particles in oxidation of water, which necessitates very strong oxidation power [7,8]. Hence, clarification of the mechanism of this reaction is very important from both theoretical and practical aspects.

The aim of this chapter is to clarify the processes of benzene photooxidation on TiO_2 in aqueous solution. Products from benzene was carefully studied and the photocatalytic reaction mechanism was studied by isotopic tracing methods using a stable isotope of oxygen (^{18}O) included in $H_2{}^{18}O$ and $^{18}O_2$. The movement of these isotopic atoms was traced in phenol, which is the most produced intermediate in solution phase, and CO_2 evolved. From the results, we obtained useful insights into the difference between activities of rutile and anatase particles as photocatalysts.

3.2 Experiments

Six kinds of TiO_2 powders were used as photocatalysts. They were NS-51 from Toho Titanium Co. Ltd., TIO-3 from Catalysis Society of Japan, and CR-EL, ST-41, ST-21 and ST-01 from Ishihara Sangyo Ltd. The contents of rutile and specific surface areas of these powders are shown in Table 5.1. Benzene, phenol, p-hydroquinone and p-benzoquinone were obtained from Wako Pure Chemical. Pure water containing 10% $H_2{}^{18}O$ was from Cambridge

Isotope Laboratories, Inc. Oxygen gas containing 99% $^{18}O_2$ was from Isotec Co. All of the chemicals were guaranteed reagents and used without further purification.

All of the photooxidation reactions were carried out in a closed Pyrex tube containing 20 mg of TiO_2 powder, 0.1 ml of benzene, 2 ml of water and 14 ml of gas phase at atmospheric pressure. The gas phase was either air or oxygen. The reaction solution was stirred with a magnetic stirrer to suspend the TiO_2 powder and photoirradiated with UV-Vis light from a 500 W high-pressure mercury lamp (Wacom BMO-500DY). The reaction temperature reached a stable temperature of about 40^{o}C after 30 min of photoirradiation. To make an aqueous reaction solution saturated with benzene, 0.1 ml of benzene was added to the reaction system. The dissolved part of benzene in the reaction solution was in equilibrium with the vaporized part in gas phase. In order to trace an oxygen isotope in the products, either 10% $H_2{}^{18}O$ containing water or $^{18}O_2$ was used as the oxygen isotope source.

Intermediate products in reaction solutions were analyzed with an HPLC system equipped with a Hitachi L-7400 UV detector and 4.6 $\times$ 150 mm columns (GL-Sciences, Intersil ODS-3). The HPLC mobile phase was a mixture of acetonitrile and water (volume ratio of 1:1), which was flowed at a rate of 0.5 ml/min. The products were identified from the HPLC results by comparing retention times and UV-Vis absorption spectra of the products with those of corresponding authentic compounds.

CO_2 evolution and amount of oxygen in the gas phase were monitored with Shimadzu GC-8A gas chromatographs. Contents of ^{18}O to the total amounts of oxygen included in phenol, CO_2 and O_2 were determined with a GCMS-QP2010S system.

3.3 Results and discussion

3.3.1 Product analysis

When aqueous suspensions containing TiO_2 and benzene were irradiated by UV light, some intermediate species must be produced before complete mineralization into CO_2. The procedure for analyzing byproducts in solution phase was the same with that described in the

previous chapter. The number of byproducts obtained in aqueous solution was not different from that obtained in benzene solution as shown in the previous chapter. But the production rates of each byproducts and CO_2 was different. In general, the photooxidation rate in aqueous media was higher and the deactivation of TiO_2 was not much severe as in benzene solution. This is consistent with the reports showing that H_2O can accelerate photocatalytic reaction [1-3]. However, the involvement of H_2O in photocatalytic reaction is still controversial. In solution phase, we found that phenol accounted for the major part of dissolved products, which is indicated in the typical HPLC chart shown in Fig. 3.1.

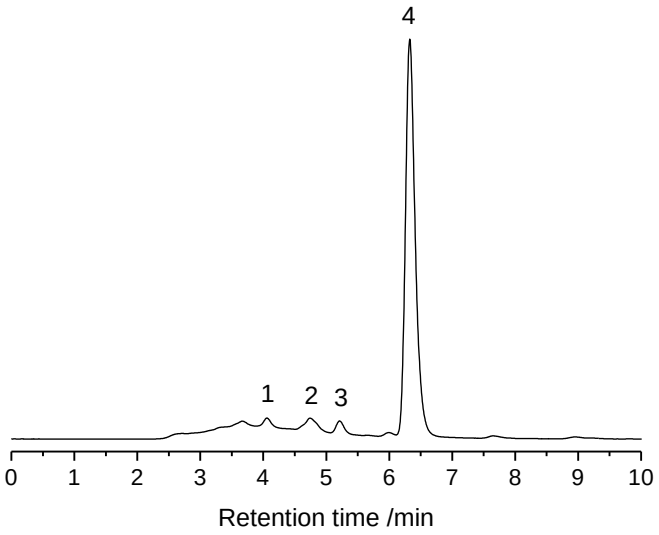

Fig. 3.1. A typical HPLC chromatogram obtained from liquid phase analysis. Peaks 1 – 4 are peaks of hydroquinone, muconaldehyde, benzoquinone and phenol respectively. All the main byproducts have already been reported in literature [9-12].

3.3.2 Photooxidation of benzene in labeled water

Since the amount of phenol is much larger than the amounts of other products and it is the only product containing one oxygen atom, phenol is often considered to be the initial product of the photocatalytic oxidation of benzene [10-12]. It has been proposed that phenol is produced as a result of reaction with an $HO^{\cdot}$ radical, which is produced by oxidation of an

OH group on TiO_2 by a photogenerated hole [1-5,10-12]. However, there are some reports against the production of $HO^{\cdot}$ radical on photoirradiated TiO_2 [13,14]. It is therefore important to identify the origin of the oxygen atom introduced into phenol, which will also give insights into the mechanism of oxidation of organic compounds on TiO_2 photocatalysts. In the present study, we examined the origin of the oxygen introduced into phenol by using ^{18}O-enriched water (10% $H_2{}^{18}O$) as the solvent and analyzed the content of ^{18}O in the phenol. As a complementary study, we also used labeled dioxygen (100% $^{18}O_2$) as the electron acceptor.

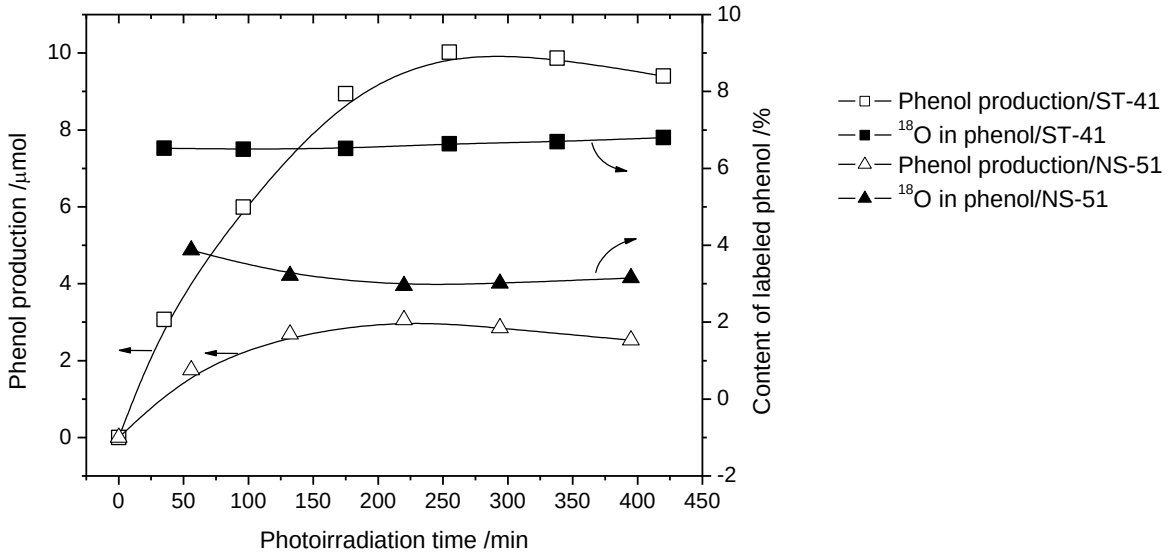

Fig. 3.2. Time courses of photocatalyzed production of phenol from benzene and contents of phenol containing ^{18}O. Photocatalyses were carried out in ^{18}O-enriched water (10% $H_2{}^{18}O$) using ST-41 and NS-51 powders.

In the series of experiments using ^{18}O-enriched water, normal air was filled in the gas phase of the test tube. The production of phenol in solution, evolution of CO_2 and amount of remaining O_2 in the gas phase were determined by means of HPLC and GC, and the inclusion of ^{18}O in them was traced by GC-MS.

Fig. 3.2 shows that the concentration of phenol initially increases with photoirradiation time. The rate of phenol production is higher for ST-41 (anatase) than for NS-51 (rutile).

Similar results were obtained using other anatase and rutile powders, the characteristics of which are shown in Table 3.1. This result is consistent with the results of previous studies showing that anatase powders show higher photocatalytic activity than that of rutile powders. After reaching maximum values at about 250 min, the concentration of phenol gradually decreases. This decrease is due to the photocatalytic decomposition of phenol and decrease in the concentration of dissolved benzene in the aqueous solution and the decrease in the amount of oxygen added to the reaction tube. The contents of labeled phenol (phenol with an ^{18}O atom) are about 6.7% for ST-41 and about 3.0% for NS-51. These contents are almost constant, although the initial value for NS-51 is slightly higher than the stationary value. It is important that these contents are between 10%, which is the content of $H_2{}^{18}O$ in water used, and 0.2 %, which is the content of ^{18}O included in normal air. The stationary contents of labeled phenol for experiments using several TiO_2 powders are shown in Table 3.1. The results show that the content of labeled phenol is between 1.7 % and 9.0% and that the content is lower for rutile powders than for anatase powders.

Table 3.1. Characteristics of some TiO_2 powders and contents of labeled phenol in the phenol produced from benzene by photocatalysis in ^{18}O-enriched water (10% $H_2{}^{18}O$).

Powders	Content of rutile (%)	Specific surface area (m^2/g)	Content of labeled phenol (stationary value) (%)
ST-41	<0.1	8.2	6.7
ST-21	<0.1	56.1	9.0
ST-01	<0.1	192	8.6
NS-51	98.6	6.5	3.0
CR-EL	>99.9	7.1	3.2
TIO-3	>99.9	48.1	1.7

The oxygen-exchange rate between phenol and water and that between phenol and molecular oxygen were experimentally confirmed to be slow, as shown in Supporting Information. Therefore, the results showing that the content of labeled phenol is between 1.7 % and 9.0% indicate that oxygen atoms are introduced into phenol from both H_2O and O_2 during phenol formation. The results also indicate that the contribution of water is larger for anatase powders than for rutile powders.

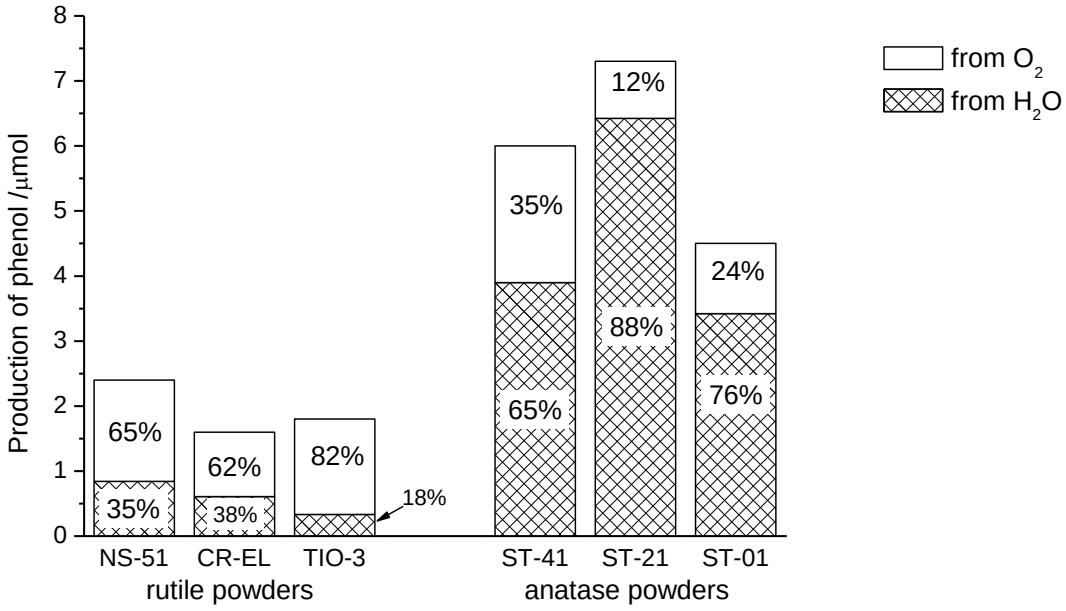

Fig. 3.3. Amounts of phenol produced from benzene by photoirradiation for 100 min in ^{18}O-enriched water (10% $H_2{}^{18}O$) using several TiO_2 powders and percentage of phenol produced using water as the oxygen source, which was calculated on the basis of the results shown in Table 3.1.

Anatase powders produce larger amounts of phenol than do rutile powders after photoirradiation for 100 min, as shown in Fig. 3.3. This result is consistent with results of previous studies showing that anatase powders are more active as photocatalysts for oxidizing organic compounds [1-3]. From simple calculation based on the contents of labeled oxygen in phenol, we can determine the ratio of the oxygen sources for producing phenol by the photocatalytic reaction. The contributions of H_2O and O_2 to the production of phenol for these rutile and anatase powders are shown in Fig. 3.3 for different TiO_2 powders. The marked

difference between anatase and rutile powders is that anatase powders produce very large amounts of phenol using water molecules as the oxygen source, compared with rutile powders. On the other hand, the amounts of phenol produced using oxygen molecules as oxygen source are nearly the same between anatase and rutile powders. Hence, the high efficiency of phenol production using water as the oxygen source is attributed to the high photocatalytic activity of anatase powders.

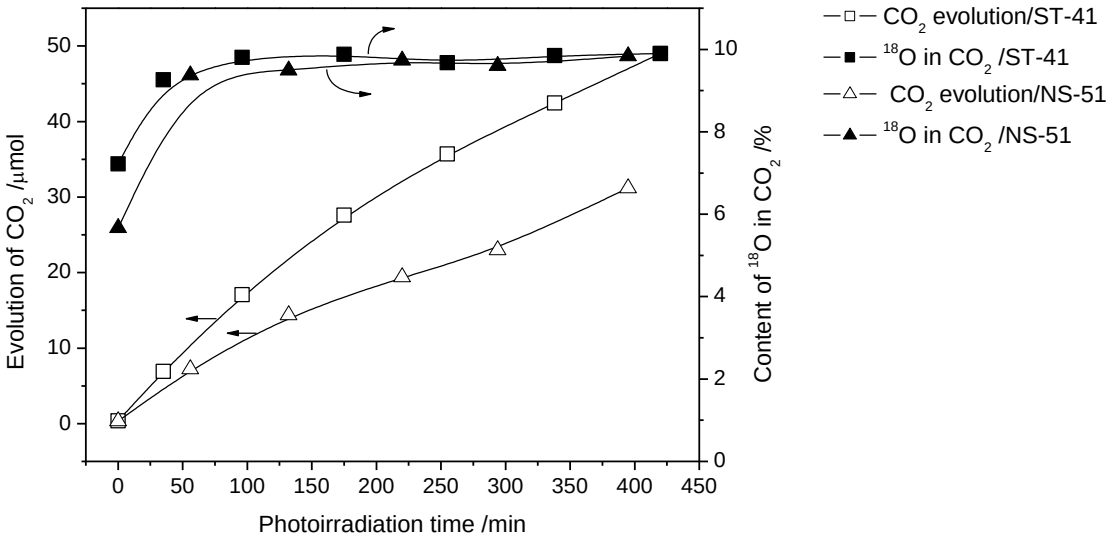

Fig. 3.4. Time courses of CO_2 evolution from benzene and contents of ^{18}O in oxygen atoms of the CO_2. Photocatalyses were carried out in ^{18}O-enriched water (10% $H_2{}^{18}O$) using ST-41 and NS-51 powders.

The rates of CO_2 evolution from benzene using ST-41 (anatase) and NS-51 (rutile) powders are compared in Fig. 3.4. CO_2 evolution started upon photoirradiation and continued with photoirradiation time. The immediate evolution of CO_2 is consistent with the result obtained in Chapter 4 that ring-opening pathway contribute most in benzene photooxidation over TiO_2, as will discussed later. The content of ^{18}O in oxygen atoms of CO_2 reached 10%, which is the same as the content of $H_2{}^{18}O$ in the water used as the solvent. However, this does not mean that the oxygen source for CO_2 production is solely water. This is because of the oxygen exchange between CO_2 and H_2O, which is reported to be a considerably fast process

[16]. The lower contents of ^{18}O in oxygen atoms of CO_2 seen at very short irradiation (less than 25 min) in Fig. 3.4 are due to natural CO_2 molecules adsorbed on the surface of the TiO_2 powders before starting the reactions

The production of CO_2 is accompanied by decrease in the amount of oxygen in the gas phase, as shown in Fig. 3.5. The rate of O_2 consumption is nearly the same or even slightly faster than the rate of CO_2 evolution, as shown in Fig. 3.4. This fact indicates that O_2 is used as a chief oxygen source in the whole processes of oxidation of benzene except the process for producing phenol from benzene, especially on anatase powders. The slightly larger consumption of O_2 than the amount of CO_2 observed is due to the accumulation of some intermediate species in the reaction system. Therefore, the process for producing phenol from benzene on TiO_2 powders, especially on anatase powders, is considered to be a unique process of photocatalytic reactions.

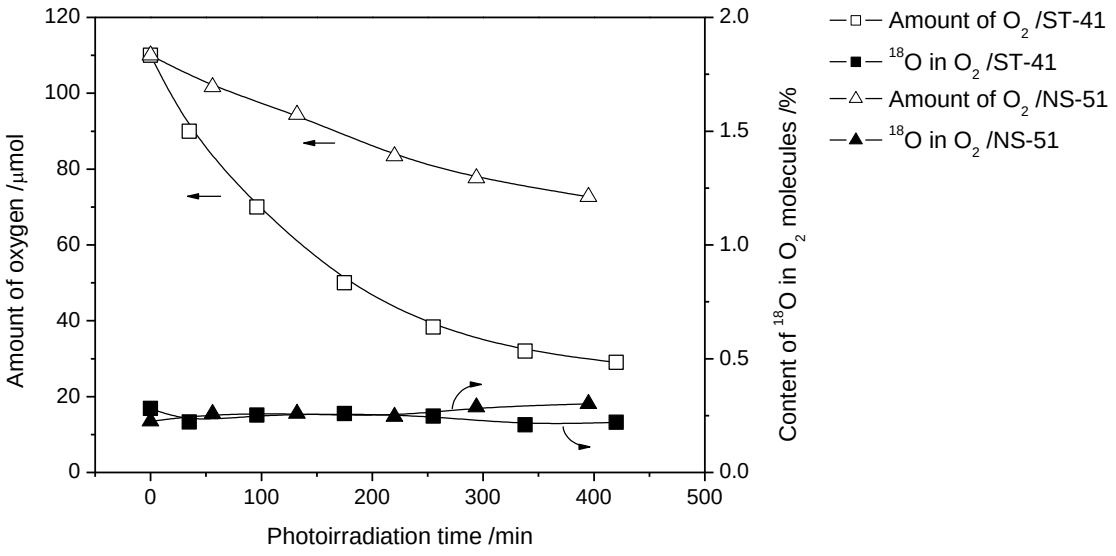

Fig. 3.5. Time courses of the amount of O_2 in the gas phase of test tubes during photocatalyses of benzene in O-enriched water (10% $H_2{}^{18}O$) using ST-41 and NS-51 powders and contents of ^{18}O in O_2 molecules.

The content of ^{18}O in oxygen molecules during photooxidation of benzene over both rutile and anatase hardly changed during photoirradiation (Fig. 3.5). This result indicates that

neither O-exchange between H_2O and O_2 molecules nor evolution of O_2 from photooxidation of water took place.

3.3.3 Photooxidation of benzene in labeled oxygen atmosphere

In order to further confirm the above results about the origin of O atoms introduced into phenol, we carried out the reaction in an atmosphere of pure $^{18}O_2$, which was filled in the gas phase of the test tube, using normal water as the solvent. The results obtained using ST-41 (anatase) and NS-51 (rutile) powders as the photocatalysts are shown in Figs. 3.6 and 3.7.

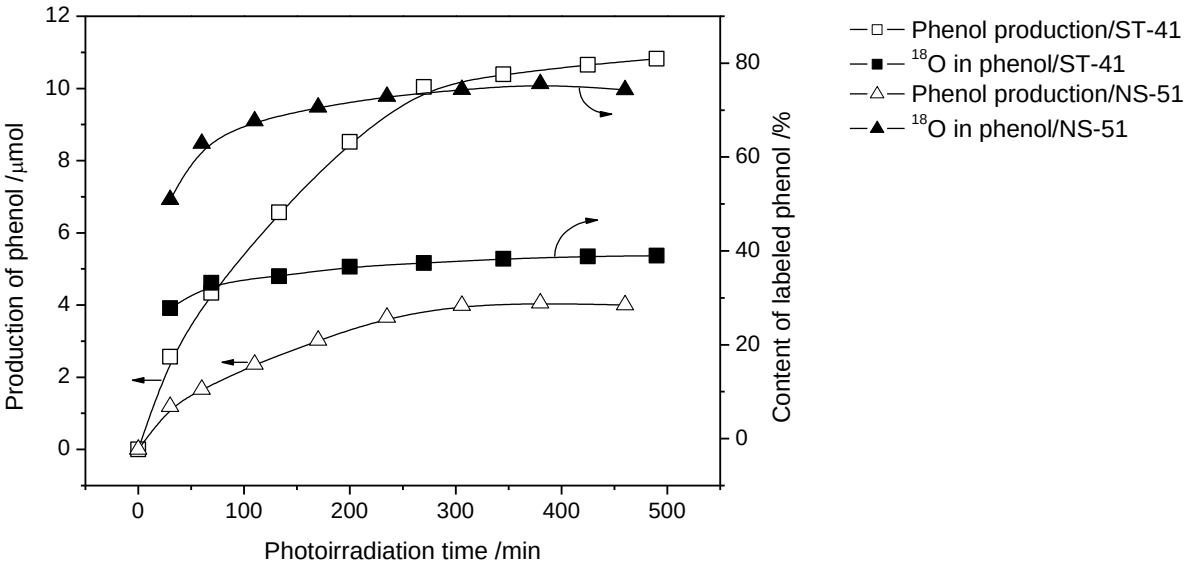

Fig. 3.6. Time courses of photocatalyzed production of phenol from benzene and contents of phenol containing ^{18}O. Photocatalyses were carried out in normal water under $^{18}O_2$ atmosphere using ST-41 and NS-51 powders.

When the reaction was carried out under the $^{18}O_2$ atmosphere instead of normal air, the mineralization rate was increased almost twice the rate obtained in air, which is shown in Fig. 3.4. This is ascribable to the enhanced electron removal from the photoirradiated TiO_2 particles due to the increased concentration of the electron acceptor, i. e., O_2 or $^{18}O_2$. Except this point, other tendencies were nearly equivalent to those observed in the reaction carried out in normal air. The contents of ^{18}O in phenol produced in $^{18}O_2$ atmosphere were 40% and

75% for ST-41 and NS-51, respectively, as shown in Fig. 3.6. These percentages mean that the contributions of O_2 (or $^{18}O_2$) to the production of phenol are 40% and 75% for ST-41 and NS-51, respectively, which are closed to the percentages determined for the reactions in air.

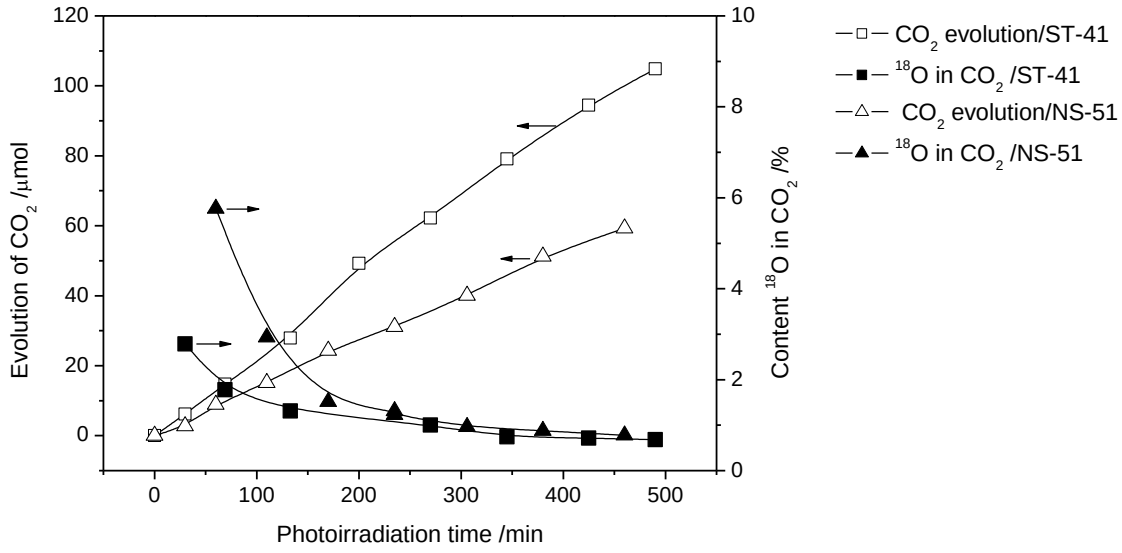

Fig. 3.7. Time courses of CO_2 evolution from benzene and contents of ^{18}O in oxygen atoms of the CO_2. Photocatalyses were carried out in normal water under $^{18}O_2$ atmosphere using ST-41 and NS-51 powders.

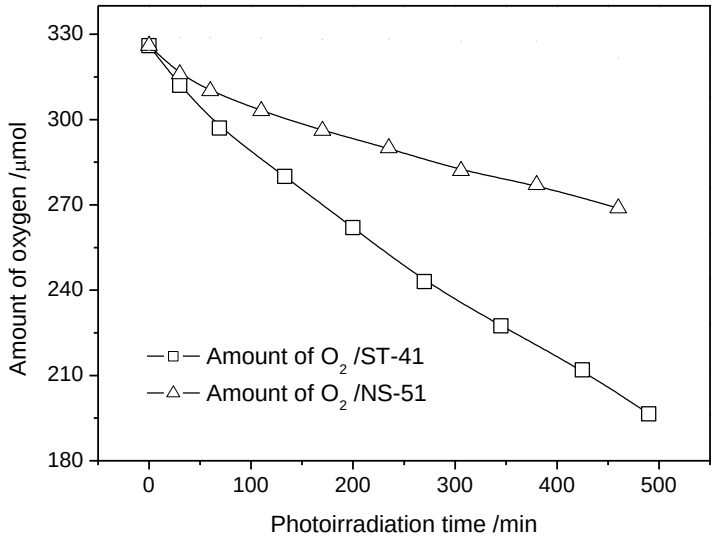

Fig. 3.8. Time courses of the amount of O_2 ($^{18}O_2$) in the gas phase of test tubes during photocatalyses of benzene. Photocatalyses were carried out in normal water under $^{18}O_2$ atmosphere using ST-41 and NS-51 powders.

The high content of ^{18}O in CO_2 in the initial period of the reaction, as shown in Fig. 3.7, suggests that a large amount of oxygen atoms used for the oxidation of benzene is supplied from O_2 (or $^{18}O_2$). However, the content decreased with time and finally reached the value of ^{18}O in water due to the exchange of O atoms between CO_2 and water, as discussed before.

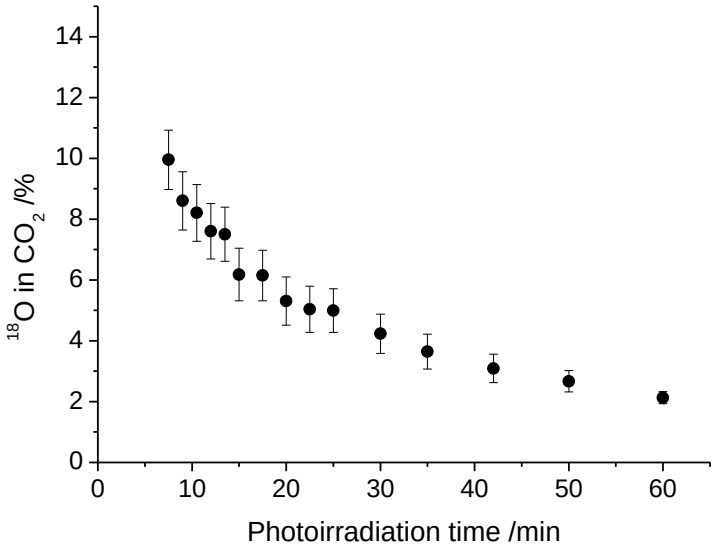

Fig. 3.9. Time course of ^{18}O content in the oxygen atoms of CO_2 photocatalytically produced from benzene using ST-41 in normal water under $^{18}O_2$ atmosphere.

Fig. 3.9 shows the change in the content of ^{18}O in oxygen atoms of CO_2 molecules generated from benzene using ST-41 in the initial period of the reaction. The contribution of O_2 as the source of oxygen to the production of phenol was about 35%, as shown in Fig. 3.3. If the contribution of O_2 for the oxidation of benzene to CO_2 takes place only in the production of phenol, the content of ^{18}O in CO_2 should be about 3% because 12 oxygen atoms are used for oxidation of benzene to CO_2 molecules. The much higher content observed in the initial period, as shown in Fig. 3.9, suggests that large amount of O_2 ($^{18}O_2$ in this experiment) directly participate in either the oxidation of byproducts from phenol to CO_2 or ring-opening pathway from benzene to muconaldehyde and finally to CO_2. This result is in good agreement with the later discussion about formation of muconaldehyde on TiO_2 in Chapter 4.

3.3.4 Influence of addition of Pt particles and partial pressure of oxygen

In order to investigate the influence of Pt particles added in photocatalytic reaction on TiO_2, mixture of NS-51 or ST-41 powder with 8 w% Pt were used in similar experiments above. The results of phenol production after 200 min photoirradiation in experiments using NS-51 or ST-41 with or without Pt addition and either normal air - 10% H_2O^{18} water or $^{18}O_2$ atmosphere - normal water are shown in Fig. 3.10.

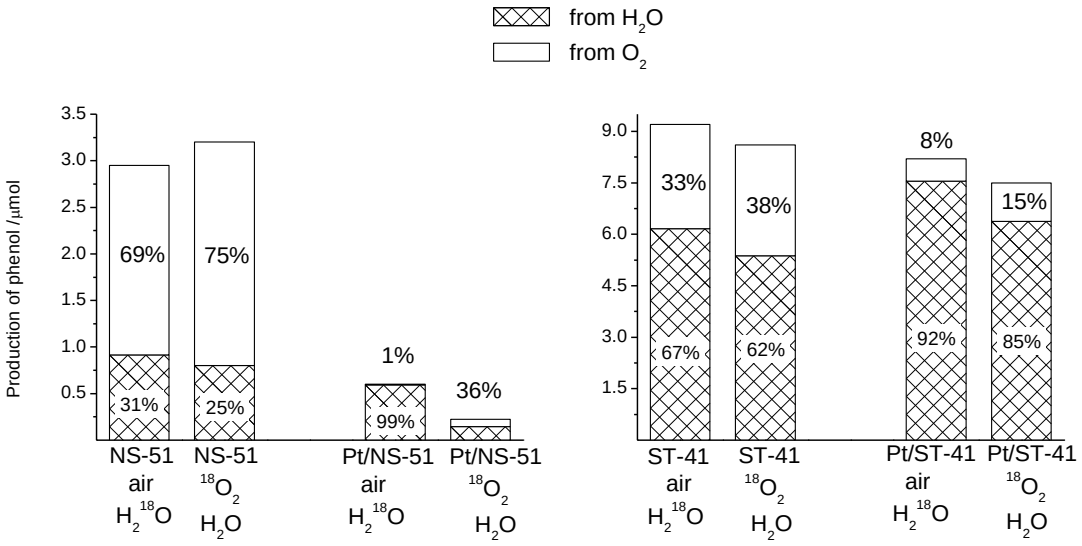

Fig. 3.10. Production of phenol after 200 min photoirradiation on NS-51 and ST-41 with and without addition of Pt particles in experiments using air or O_2 atmosphere. The percentage of phenol with O coming from water or oxygen molecules is also shown in this figure.

The positive influence of addition of Pt particles on photocatalytic reaction on TiO_2 surface has been reported in literature [1-3], and also confirmed later in photooxidation of water in Chapter 5. Although photocatalytic reaction rates are increased with the addition of Pt powder, the amount of phenol as a byproduct in solution phase did not increase but, in the mater of fact, did decrease as shown in Fig. 3.10. This is the result of the competition between formation and decomposition of phenol in the reaction systems containing a limited amount of benzene. In order to know the influence of presence of Pt particle on decomposition of phenol,

we did photooxidation of phenol in aqueous suspension of TiO_2 with and without Pt addition. The reaction rates of phenol, O_2 and CO_2 of these experiments are shown in Table. 3.2.

Table 3.2. Reaction rates of phenol, O_2 and CO_2 in photooxidation of phenol over TiO_2 with and without Pt addition.

	C_6H_6O	+ **O_2**	$\rightarrow$ **CO_2**	
NS51	-0.036	-0.064	0.041	(μmol/min)
NS51-Pt	-0.258	-0.291	0.120	(μmol/min)
ratio NS51-Pt/NS51	7.17	4.55	2.92	(times)
ST41	-0.072	-0.138	0.104	(μmol/min)
ST41-Pt	0.102	-0.226	0.146	(μmol/min)
ratio ST41-Pt/ST41	1.42	1.64	1.40	(times)

As shown in Table 3.2, the disappearance rate of phenol increase 7.17 times when Pt powder was added to rutile NS-51 powder. This sharply increase in disappearance rate of phenol was accompanied by a sharply increase in consumption rate of O_2, 4.55 times. Meanwhile, the addition of Pt powder to anatase ST-41 powder increased the disappearance rate of phenol and consumption rate of O_2 only 1.42 and 1.62 times respectively. The special selectivity for removal of phenol on rutile TiO_2 has been also shown in Table 4.2 in Chapter 4. This accounts for the result shown in Fig. 3.10. Production of phenol obtained in photooxidation of benzene decreased much when Pt particles were added. Although rutile NS-51 has a great power in removal of phenol, its overall photocatalytic activity still is lower than that of anatase ST-41. This is indicated in Table 3.2 that CO_2 evolution rate in case of using NS-51 is still lower than that in case of using ST-41.

From Fig. 3.10, it can be seen that addition of Pt powder influenced on not only production of phenol but also the contributions of water and O_2 molecules to phenol formation. The addition of Pt powder decreased much contribution of O_2 as oxygen source to

phenol formation. When Pt particles are in contact with TiO_2 particles, the primary reduction of O_2 by photogenerated electrons on Pt particles takes place far from the primary oxidation of benzene by photogenerated holes on TiO_2 particles. Therefore, there is less chance for formation of phenol with oxygen atom coming from O_2 molecule. The involvement of O_2 molecules as oxygen source is also confirmed in Fig. 3.10, which shows that the content of phenol with O atom from O_2 molecules increased when O_2 atmosphere was used instead of air in the gas phase.

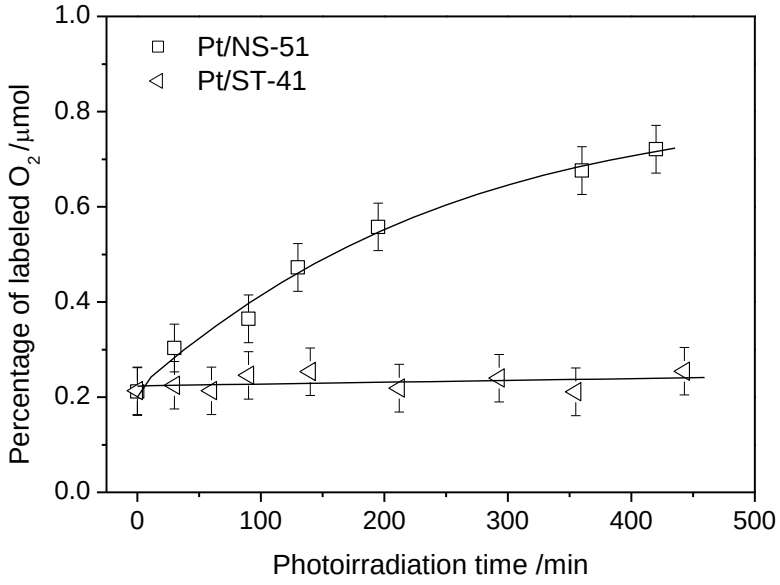

Fig. 3.11. Time courses of content of ^{18}O in the gas phase of test tubes during photocatalyses of benzene in O-enriched water (10% $H_2{}^{18}O$) using ST-41 and NS-51 powders with addition of 8 w% Pt particles.

As discussed above, the complete photooxidation of water to O_2 is less competitive than photooxidation of organic compounds. However, Fig. 3.11 shows that, O_2 evolution was still able to occur in presence of benzene with the help of Pt particles over TiO_2. The evolution of O_2 occurred only in case of rutile NS-51. It is confirmed that rutile has a higher ability in producing O_2, although anatase has a higher power for mineralizing organic compounds. This result is consistent with the result in photooxidation of water in Chapter 5. That rutile is more active for water oxidation may be related to the activity and stability of surface active oxygen

species formed on rutile and anatase under UV photoirradiation. As discussed in Chapter 5, O_2 evolution is a result of accumulation of trapped holes on TiO_2 surface. The trapped holes on rutile may be less oxidative, but have higher tendency to join to each other, which facilitates the formation of O_2 molecules. Meanwhile, the trapped holes on anatase have fewer trends to join to each other, but are more oxidative for oxidation of organic compounds. That is why phenol with O atom from water is produced much more on anatase than on rutile. It is that differences in structural properties determine the differences in photocatalytic activity between anatase and rutile.

3.3.5 Discussion on phenol formation mechanism

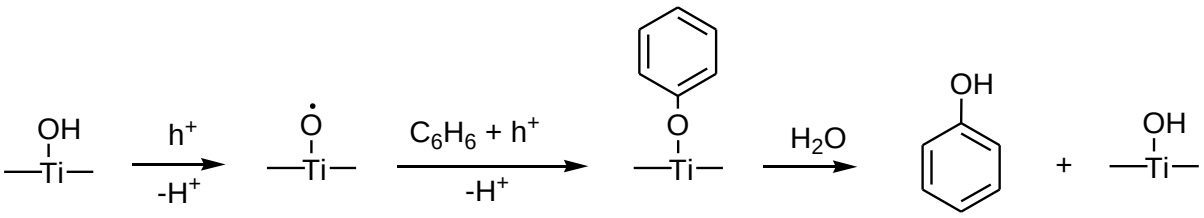

Scheme 3.1. A possible mechanism for production of phenol from benzene through an oxygen transfer process using water as the oxygen source.

In general, the initial photooxidation of organic compounds has been considered to be due to either oxygen transfer [1-5,11,12] or hole transfer [10,15] from TiO_2 to substrates. The former is often assumed to occur though $HO^{\cdot}$ radicals, although the generation of $HO^{\cdot}$ radicals on photoirradiated TiO_2 is still controversial [13,14]. In the case of benzene photooxidation, it has been widely considered that the oxygen transfer is the only way to produce phenol [4,5,11,12]. The results showing that, although not at 100% efficiency, phenol is produced by using water as the oxygen source, as can be seen in Fig 3.3, suggest that the oxygen transfer process does exist in the phenol production, especially on anatase particles. A possible process is shown in Scheme 3.1. Besides Ti-$O^{\cdot}$ shown in Scheme 3.1, $HO^{\cdot}$ radicals,

Ti-OO· or more complicated surface peroxides can be the source of oxygen to be transferred to benzene [1-3,17-21].

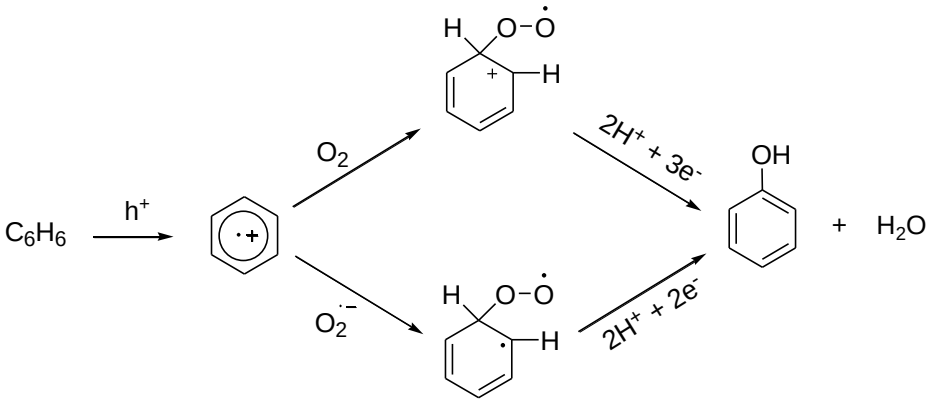

Scheme 3.2. A possible mechanism for production of phenol from benzene through a hole transfer process using O_2 as the oxygen source.

Importantly, however, the experimental results show that phenol can also be produced using O_2 as the oxygen source, as can be seen in Fig. 3.3. This indicates that phenol can be produced by a route different from the oxygen transfer process. The contribution of oxygen molecules as the oxygen source to oxidation of organic compounds on photoirradiated TiO_2 has been proposed in some kinds of oxidation reactions. They are mostly observed for the reactions between aliphatic radicals and an oxygen molecule [1-4,10]:

$$R\cdot + O_2 \rightarrow ROO\cdot$$

In the case of benzene, it seems more reasonable to consider that benzene cation radicals, which are formed by the hole transfer mechanism, are the species to react with oxygen, as shown by Scheme 3.2. The peroxide radical formed as a result of the reaction between the benzene cation radical and an O_2 molecule can be converted to phenol through reductive processes, for which a variety of intermediates produced before conversion into CO_2 may be used as reductants. In addition to molecular oxygen, $O_2^{\cdot-}$ produced by reduction of O_2 on TiO_2 may also be used in the reaction with benzene cation radicals.

A marked difference was observed in photocatalytic activity for the oxidation of benzene between rutile and anatase powders, as shown in Fig. 3.3. The difference is attributed to the different activities of anatase and rutile powders for the oxidation of benzene to phenol. On anatase particles, benzene is oxidized to phenol efficiently by Scheme 3.1 using water as the oxygen source, whereas Fig. 3.13 using O_2 as the oxygen source contributes to a lessened degree, as shown in Fig. 3.3. On the other hand, on rutile particles, the contribution of Scheme 3.1 to benzene oxidation is much smaller. Hence, the ease in oxidation of benzene to phenol by Scheme 3.1 on anatase particles is attributed to its high activity for oxidation of benzene to CO_2. We speculate that the energy levels and/or the atomic configuration on the surface of the anatase particles are the reason for their efficient production using water as the oxygen source, as has been discussed in relation to the higher photocatalytic activity of anatase particles [6]. As for the surface atomic arrangement, we speculate that anatase particles have a more irregular structure on the surface than do rutile particles because they are manufactured at lower temperatures than are rutile particles. These irregular sites may contribute to the formation of Ti-$O^{\cdot}$, Ti-$OO^{\cdot}$, or more complicated surface peroxides on the surface, which are then used for forwarding the process represented by Scheme 3.1.

Rutile powders are known to be good photocatalysts for oxidizing water into molecular oxygen in the presence of good electron acceptors such as Fe (III) ions [7,8]. However, we found that in the oxidation of benzene using molecular oxygen as the electron acceptor, the route using water as the oxygen source (Scheme 3.1) is not efficient on rutile powders, as shown in Fig. 3.3. The difference probably arises from the difference in the mechanisms of these two processes. In the case of oxidation of water, a pool of holes (or accumulation of peroxides) and strong electron acceptors are necessary to enable the 4-electron transfer process for liberating molecular oxygen, whereas oxidation of benzene is driven by a 1-electron transfer process that does not need a pool of holes.

Finally, it should be noted that $HO^{\cdot}$ radicals can be produced by reduction of O_2. If the $HO^{\cdot}$ radicals produced from O_2 on TiO_2 contribute to the production of phenol, this provides

another explanation for the contributions of water and O_2 to the production of phenol on photoirradiated TiO_2. However, this is unlikely because $O_2^{\cdot -}$ is the chief product from O_2 on rutile powders, whereas hydrogen peroxide, which can easily be converted to $HO^{\cdot}$ radicals, is the chief product from O_2 on anatase powders [22]. Therefore, if $HO^{\cdot}$ radicals produced from O_2 contribute to phenol production, this process must be advantageous for anatase powders. This contradicts the experimental results shown in Fig. 3.3. The ease in producing $O_2^{\cdot -}$on rutile powders may be responsible for the large contribution of O_2 to production of phenol on rutile powders by Fig. 3.3 because $O_2^{\cdot -}$ has higher reactivity with benzene cation radicals than does O_2.

3.4 Conclusions

By using isotope-tracing methods we successfully determined the origin of oxygen introduced into phenol that is produced from benzene by photocatalyzed reaction. For efficient oxidation of benzene, the path using water as the oxygen source is considered to be important. However, it was also found that molecular oxygen can be a source of oxygen introduced into phenol which is more important on rutile powders than on anatase powders. Since benzene is a basic organic compound, the results are important in deepening the understanding of photocatalytic reactions of organic materials on TiO_2 photocatalyst. The results also demonstrate that ^{18}O-tracing methods are useful for clarifying the mechanism of photocatalytic reactions. However, it is difficult to apply ^{18}O-tracing methods to carbonyl compounds because the rates of oxygen exchange between water and carbonyl compounds are too fast to identify the source of oxygen atoms introduced into them.

Supporting Information

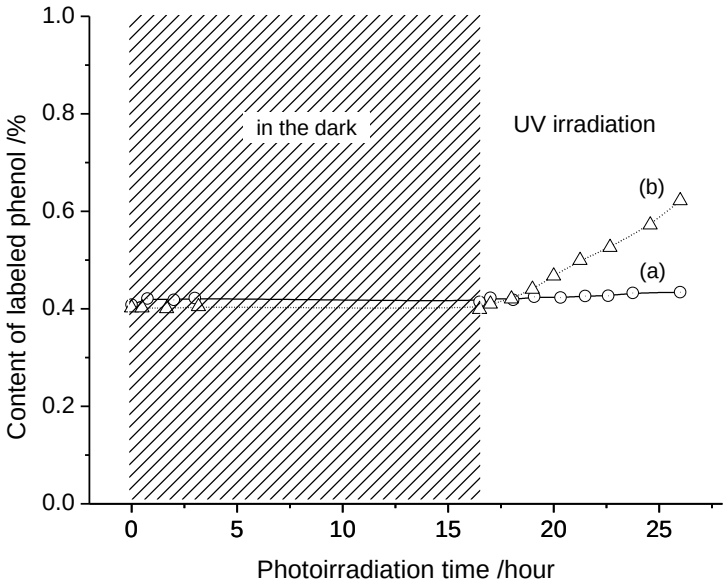

Fig. Changes of content of phenol due to O-exchange (a) between phenol and $H_2{}^{18}O$ and (b) between phenol and $^{18}O_2$ in aqueous solution with and without UV irradiation. These two experiments used phenol (21 μmol) in water (2 ml, normal or containing 10% $H_2{}^{18}O$) equilibrated with gas phase (14 ml, $^{18}O_2$ or normal air)

References

[1] A. Fujishima, X. Zhang and D. A. Tryk, *Surf. Sci. Rep.* 63, **2008**, 515-582.

[2] A. M. Fox and T. M. Dulay, *Chem. Rev.* 93, **1993**, 341-357.

[3] R. M. Hoffmann, S. T. Martin, W. Choi and W. D. Bahnemann, *Chem. Rev.* 95, **1995**, 69-96.

[4] G. Palmisano, V. Augugliaro, M. Pagliaro and L. Palmisano, *Chem. Commun.* **2007**, 3425-3437.

[5] Y. Shiraishi and T. Hirai, *J. Photochem. Photobiol. C* 9, **2008**, 157-170.

[6] L. Kavan, M. Grätzel, S. E. Gilbert, C. Klemenz, and J. Scheel, *J. Am. Chem. Soc.* 118, **1996**, 6716-6723.

[7] R. Abe, K. Sayama and H.Sugihara, *J. Phys. Chem. B* 109, **2005**, 16052-16061.

[8] T. Ohno, D. Haga, K. Fujihara, K. Kaizaki and M. Matsumura, *J. Phys. Chem. B* 101, **1997**, 6415-6419 errata, 101, **1997**, 10605.

[9] T. D. Bui, A. Kimura, S. Ikeda and M. Matsumura, *Appl. Catal. B* 94, **2010**, 186-191.

[10] O. d'Hennezel, P. Pichat and D. F. Ollis, *J. Photochem. Photobiol. A* 118, **1998**, 197-204.

[11] H. Einaga, S. Futamura and T. Ibusuki, *Appl. Catal. B* 38, **2002**, 215-225.

[12] H. Park and W. Choi, *Catal. Today* 101, **2005**, 291-297.

[13] O. I. Micic, Y. Zhang, K. R. Cromack, A. D. Trifunac and M. C. Thurnauer, *J. Phys. Chem.* 97, **1993**, 1211-1283.

[14] P. *J.* Salvador, *Phys. Chem. C* 111, **2007**, 17038-17043.

[15] F. Soana, M. Sturini, L. Cermenati and A. Albini, *J. Chem. Soc. Perkin Trans. 2*, **2000**, 699-704.

[16] M. J. Welch, J. F. Lifton and J. A. Seck, *J. Phys. Chem.* 73 [10], **1969**, 3351-3356.

[17] T. Ohno, Y. Masaki, S. Hirayama and M. Matsumura, *J. Catal.* 204, **2001**, 163-168.

[18] R. Nakamura and Y. Nakato, *J. Am. Chem. Soc.* 126, **2004**, 1290-1298.

[19] T. Ohno, T. Mitsui and M. *J.* Matsumura, *Photochem. Photobiol. A* 160, **2003**, 3-9.

[20] C. Minero, G. Mariella, V. Maurino and E. Pelizzetti, *Langmuir* 16, **2000**, 2632-2641.

[21] T. Hirakawa, K. Yawata and Y. Nosaka, *Appl. Catal. A* 325, **2007**, 105-111.

[22] H. Goto, Y. Hanada, T. Ohno and M. Matsumura, *J. Catal.* 225, **2004**, 223-229.

Chapter 4: TWO INITIAL PRODUCTS AND PARALLEL PATHWAYS OF BENZENE PHOTOOXIDATION

TiO_2-photocatalyzed oxidation of benzene was studied in aqueous solution and in pure benzene. Muconaldehyde as well as phenol was identified, for the first time, as an initial product from benzene by TiO_2 photocatalysis. Formation of muconaldehyde is a direct result of aromatic ring cleavage on TiO_2 surface. The ring-opening pathway and hydroxylation pathway, which are the two parallel pathways of photooxidation of benzene, account for 10 % and 90% total benzene photodecomposition respectively. Since muconaldehyde is easily oxidized on photoirradiated TiO_2, CO_2 evolved from the benzene solution in the initial time period is formed mostly via the muconaldehyde path.

4.1 Introduction

With many advantages, TiO_2 has been widely used for mineralization of pollutants in environmental treatment [1-3]. It is well known that most of organic compounds are mineralized into CO_2 and water on photoirradiated TiO_2. This is true for benzene. It is also known that phenol is produced from benzene on TiO_2 photocatalyst [4-10]. Hence, it is reasonable to think that benzene is first oxidized to phenol, which is finally converted into CO_2 after many oxidation steps, as shown in the upper route of Scheme 1.

However, a question arises concerning the process because phenol is rather difficult to be oxidized on TiO_2 photocatalyst. After continued reaction, phenol produced from benzene accumulates in the system and hinders the reaction of benzene [4-6]. Meanwhile, the evolution of CO_2 takes place immediately upon photoirradiation. The question is whether phenol is the intermediate producing CO_2 on TiO_2 photocatalyst. Other products reported to be produced from benzene are hydroquinone, *p*-benzoquinone and catechol, which can be produced from phenol [4-10]. Albeit in a small amount, we observed muconaldehyde as described in previous chapters. We also observed the production of 2-formylcinamaldehyde from naphthalene [11-12]. In this chapter, we investigate the possibility of mineralization of benzene on TiO_2 photocatalysts not passing through phenol, and pay special attention to the role of muconaldehyde as the intermediate.

4.2 Experiments

Photocatalytic Reaction. Photocatalytic reactions were carried out in closed Pyrex tubes filled with reaction solution (2 ml) and normal air in the gas phase (14 ml). The reaction solution was an aqueous suspension containing TiO_2 powder (10 mg/ml) and an excessive amount of benzene (0.1 ml). In some experiments, instead of the aqueous solution, pure benzene was used, to which TiO_2 powder (10 mg/ml) was added. The suspension was vigorously stirred and irradiated by UV light from a 500 W high-pressure mercury lamp

(Wacom BMO-500DY) during the photocatalytic reaction. Note that the pure benzene used contained water at about 0.003%.

In order to obtain larger amounts of the products for their characterization, the photooxidation reaction was carried out in large scale in pure benzene solution. The reaction solution was filtered, concentrated, and then, run through a silica gel column. Products were separated out of the mixture with the eluents of n-hexane and chloroform.

Ozonation of Benzene. In order to compare oxidation of benzene in photocatalytic process with in ozonation one, we carried out ozonation reactions in 15ml pure dichloromethane solutions containing 0.5 M benzene. The reaction solutions were kept below 5^{o}C in an ice bath during being bubbled with ozone/air from an ozone generator (Nihon Ozone Corp., 1.5 g ozone per hour). After bubbling with ozone for 30 min, the solution was bubbling with argon gas and its temperature gradually increased to room temperature. Byproducts in the obtained solution were analyzed by HPLC without any further chemical treatment.

Analyses of Products. During photocatalytic reactions, small aliquot samples were periodically analyzed by a HPLC system equipped with a Hitachi L-7400 UV detector and 4.6 $\times$150 mm columns (GL-Sciences, Intersil ODS-3). The HPLC mobile phase was a mixture of acetonitrile and water (volume ratio of 1:1) with a flow rate of 0.5 ml per min. The products were identified from the results of HPLC by comparing retention times and UV-Vis adsorption spectra of the products with those of corresponding authentic compounds. Separated products were subjected to NMR spectrometer (JEOL JNM-AL400). CO_2 evolution in the gas phase was monitored with a Shimadzu GC-8A gas chromatograph. Contents of materials labeled with ^{13}C atoms produced in the aqueous solution and $^{13}CO_2$ in the gas phase were determined by using a Shimadzu GCMS-QP2010S system.

Materials Used. Two kinds of TiO_2 powders (ST-21 and ST-41) were obtained from Ishihara Sangyo, Ltd. NS-51 powder from Toho Titanium Co. Ltd. and TIO-3 powder from Ishihara Sangyo Co. Ltd. The content of the rutile phase and the relative specific surface area

of these TiO_2 powders are shown in Table 1. Benzene, phenol, p-hydroquinone and p-benzoquinone, n-hexane, chloroform, and dichloromethane were obtained from Wako Pure Chemical. Labeled phenol ($^{13}C_6H_5OH$, 99%), and labeled benzene ($^{13}C_6H_6$, 99%) were obtained from Cambridge Isotope Laboratories, Inc. All of the chemicals were guaranteed reagents and used without further purification.

4.3 Results and discussion

4.3.1 Product analysis and characterization

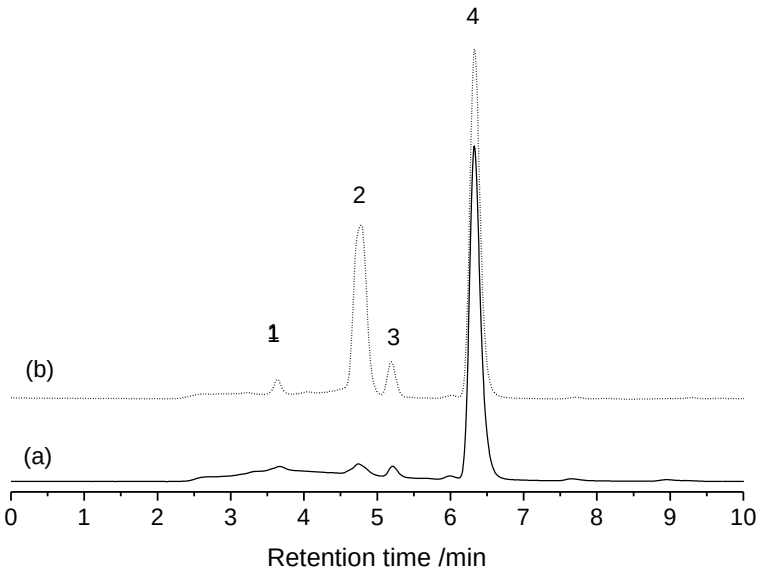

Fig. 4.1. Typical HPLC charts of the products formed from benzene after photoirradiation for 300 min using ST-41 powder as the photocatalyst in (a) aqueous solution and (b) pure benzene.

After photoirradiation of an aqueous solution of benzene, in which TiO_2 particles were suspended, production of hydroquinone (Peak 1), *p*-benzoquinone, (Peak 3) and phenol (Peak 4) in the solution was confirmed by HPLC, as shown in Fig. 4.1a. The production of these compounds from benzene has been known, of which phenol is observed in the largest amount in the reaction solution [4-10]. Carboxylic acids are produced before production of CO_2, which formed a broad HPLC band over the retention time from 2.5 to 4.0 min. In addition to these products, we reported muconaldehyde (Peak 2) as a product from benzene.

The amount of muconaldehyde produced in solution is usually very small compared with the amount of phenol if we compare the ratio after photoirradiation for a long time because it decomposes fast by the successive photocatalytic reaction, as discussed later. Probably for this reason, the production of muconaldehyde from benzene by TiO_2-photocatalyzed reaction has long been overlooked or ignored. Although the production of muconaldehyde from benzene by TiO_2-photocatalyzed reaction has not been reported, production of 2-formylcinamaldehyde from naphthalene is known [11-12]. Hence, cleavage of aromatic rings into dialdehydes is considered to be a common process for photocatalytic reactions of aromatic compounds. In this study, we paid attention to the production of muconaldehyde because it gives deep insights into the mineralization of benzene and other aromatic compounds by TiO_2-photocatalysis.

Production of muconaldehyde from benzene becomes apparent, when the reaction is carried out in pure benzene, as shown in Fig. 4.1 b. This may be due to an excessive amount of benzene as the reactant and a rapid separation of muconaldehyde produced from TiO_2 surface due to its good solubility in benzene. In addition, production of phenol is suppressed to some extent in pure benzene because water plays important role in the production of phenol from benzene [6,9,10].

To obtain detailed information about the process for the production of muconaldehyde from benzene, we carried out TiO_2-photocatalyzed reaction in pure benzene and identified the product as follows. After UV irradiation for 300 min, TiO_2 powder was separated from the reaction solution by centrifugation and benzene was vaporized to thicken the solution. The obtained concentrated solution was run through a silica gel column using at first n-hexane and then chloroform, as the eluents. The part containing muconaldehyde was obtained after changing the eluent to chloroform. The sampled part was concentrated and analyzed by GC-MS and NMR systems.

The GC chromatogram revealed that the thus obtained sample contained muconaldehyde and phenol at nearly the same amounts, as shown in Fig. 4.2 a. The two peaks, (I) at 10.6 min

and (II) at 11.2 min, are two isomers of muconaldehyde (MW =110), both of which show the same mass spectrum with a parent peak at 110, as shown in Fig. 4.2 b. When GC chromatograms were obtained after keeping the sample solution for a few days, peak (I) decreased to a very low level, whereas peak (II) increased. This result suggests that they are isomers of muconaldehyde.

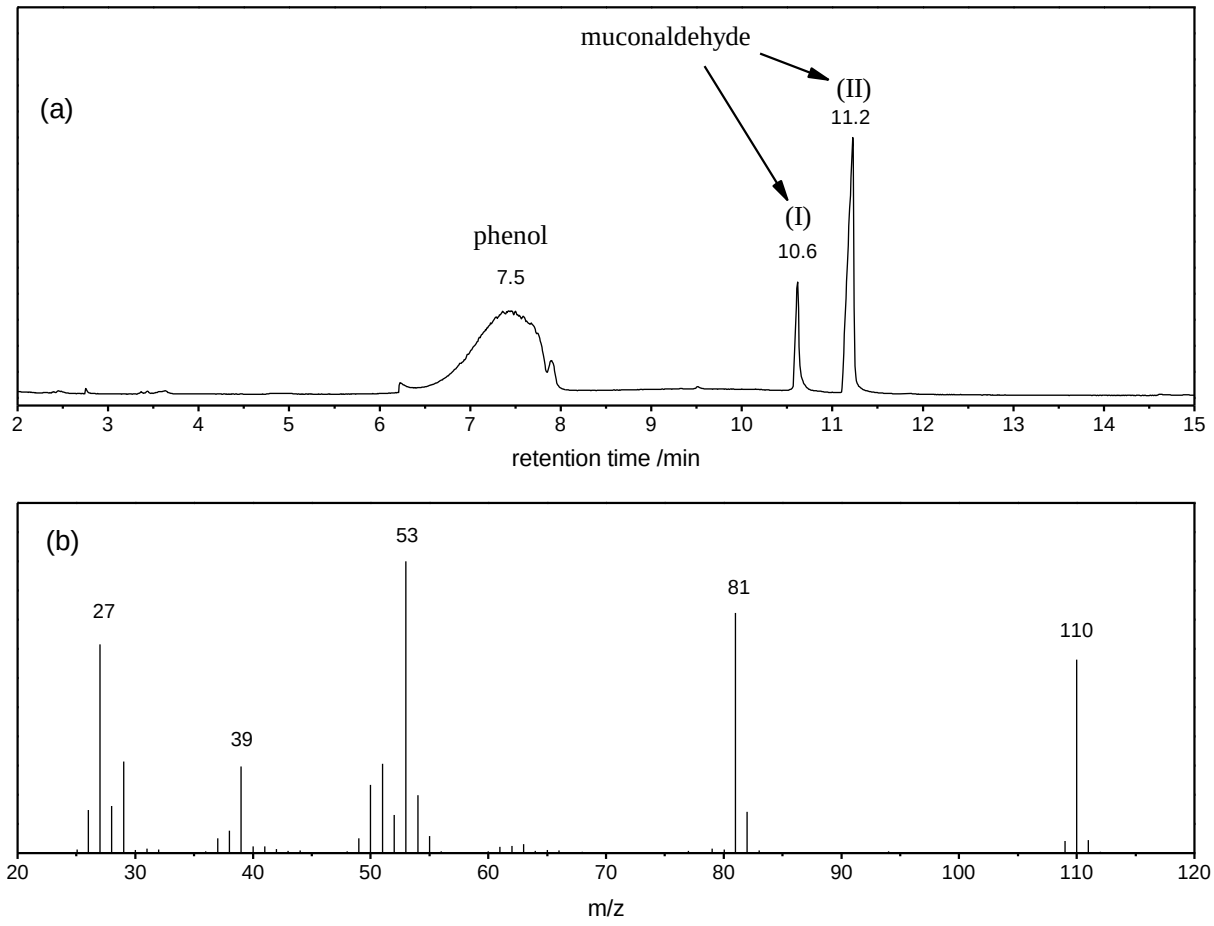

Fig. 4.2. (a) Typical gas chromatogram of the products obtained from pure benzene after photoirradiation for 300 min using ST-41 powder as the photocatalyst and (b) a mass spectrum of the component showing the peak (I) or (II) in the gas chromatogram. The samples were extracted from benzene using a silica gel column and n-hexane and chloroform as eluents.

The ^{1}H NMR spectra of the extract shows that they are *cis, trans*-muconaldehyde for peak (I) and *trans, trans*-muconaldehyde for peak (II); therefore, *cis, trans*-muconaldehyde

isomerizes to *trans, trans*-muconaldehyde with time, which is thermodynamically more stable. ^{13}C NMR spectra of the products also support the identification, as shown in the Supporting Information. The isomerization of muconaldehyde suggests that *cis, cis*- isomer was produced before the *cis, trans*-isomer, although we could not monitor the process because it took more than a day for preparing the samples for the GC-MS and NMR measurements. Note that we confirmed the production of muconaldehyde from benzene in the reaction carried out in aqueous solution of benzene from the comparison of the UV-Vis spectra and the HPLC retention times of the products.

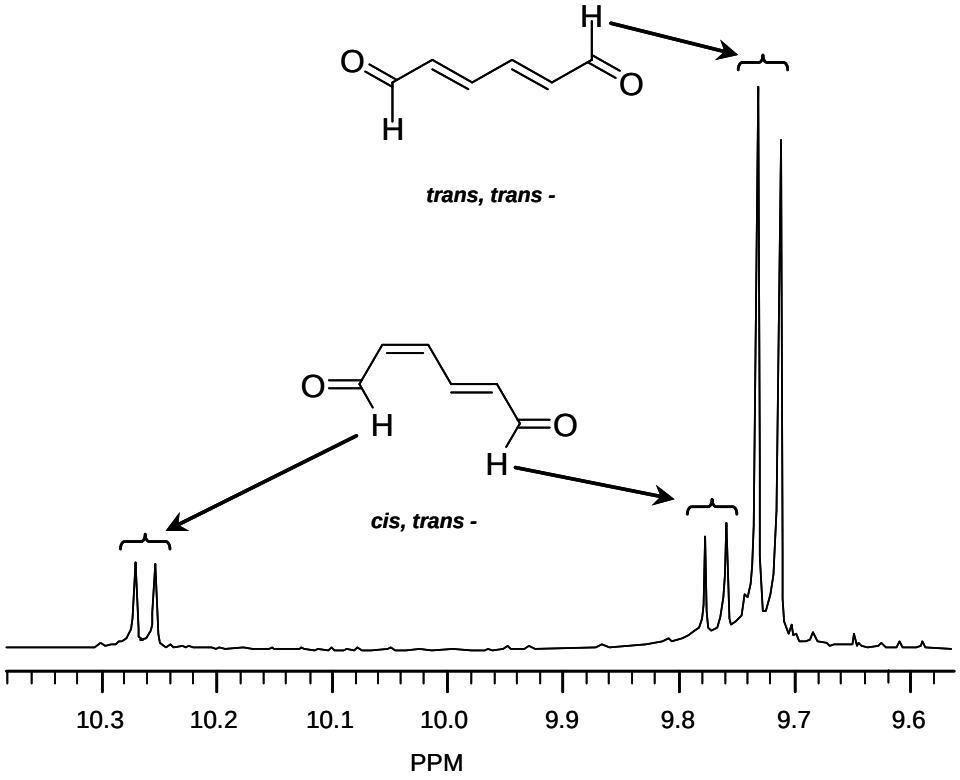

Fig. 4.3. ^{1}H NMR spectrum of muconaldehyde included in the extract from benzene after photoirradiation for 300 min using ST-41 powder as the photocatalyst. Two pairs of doublet peaks at around 10.26 and 9.77 ppm are due to two protons of two –CHO groups in *cis,trans*-muconaldehyde. The doublet peak at around 9.72 ppm are due to two protons of two equivalent –CHO groups in *trans,trans*-muconaldehyde. For more details about ^{1}H NMR and ^{13}C NMR data, see Supporting Information.

4.3.2 Two pathways for decomposition of benzene by TiO_2-photocatalysis

The formation of phenol from benzene has most often been explained by the model in which $HO^{\cdot}$ radical is used as the oxidant [7-10]. However, the mechanism is not so straightforward because the formation of $HO^{\cdot}$ radicals on photoirradiated TiO_2 is a controversial process [13,14]. In addition, in Chapter 3, we found that a part of phenol produced from benzene uses molecular oxygen as the oxygen source. Hydroquinone, *p*-benzoquinone, catechol and polymer-like products from benzene are considered to be the successive products from phenol by the mechanism by which phenol is produced, although the complexity remains in the mechanism.

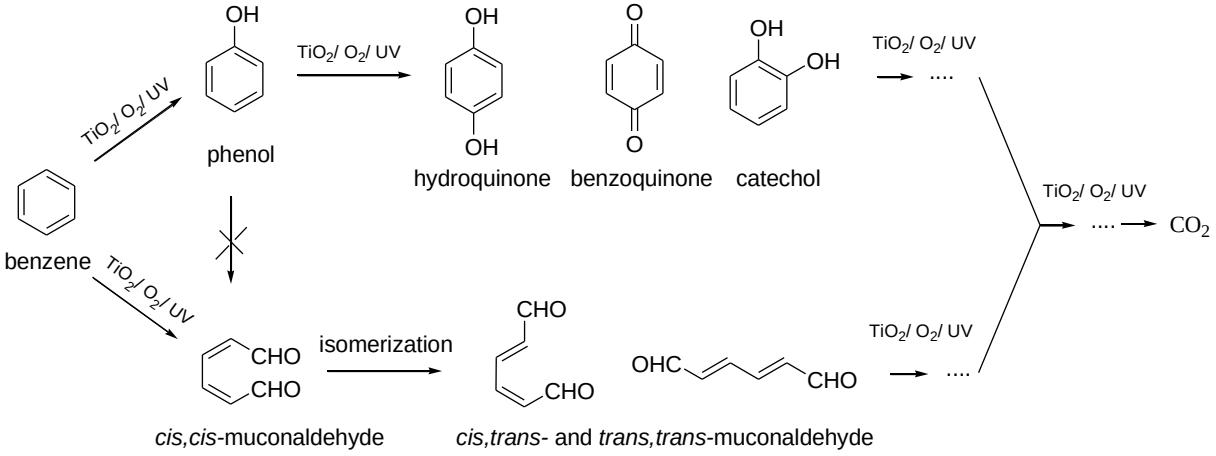

Scheme 4.1. Two pathways for decomposition of benzene by TiO_2-photocatalyzed reaction: (a) a pathway via phenol and (b) a pathway via muconaldehyde.

Here, a question arises about whether muconaldehyde, which is another simple product from benzene, is produced via phenolic compounds such as phenol and catechol or it is produced from benzene directly. To obtain the answer, we conducted photocatalytic reaction of phenol in aqueous solution containing phenol and TiO_2 particles. As a result, we obtained p-hydroquinone and p-benzoquinone as the main products formed in the solution and catechol on the TiO_2 surface, but importantly no muconaldehyde was detected in the solution. This means that muconaldehyde as well as phenol is the initial stable product from benzene; i.e.,

benzene undergoes oxidative decomposition in two parallel pathways. The first one is a phenolic pathway that goes through formation of phenol before the complete mineralization into CO_2. The second one is a ring-opening pathway that produces muconaldehyde as the first product, which have not been reported. The two pathways are summarized in Scheme 4.1. It is reasonable to consider that the same products are produced in the two pathways in the successive steps before CO_2 evolution. In other word, the aromatic ring of the compounds formed by the phenolic pathway has to be cleaved before CO_2 evolution.

4.3.3 Time courses of productions of phenol, muconaldehyde and CO_2

In the following experiments we carried out the reaction in aqueous solution of benzene and monitored the amounts of phenol and muconaldehyde produced in the solution. We also monitored the amounts of O_2 and CO_2 in the gas phase during the reaction. Fig. 4.4 shows the results obtained using ST-41(anatase) and NS-51 (rutile) powders as the photocatalysts. In both cases, as the CO_2 evolved (Fig. 4.4 a), the amount of O_2 decreased (Fig. 4.4 b). The rates were higher for ST-41 than NS-51, indicating that ST-41 is more active for mineralization of benzene. The amount of CO_2 evolved for 300 min was about half the amount of O_2 consumed. This indicates that a large part of the oxygen atoms were taken up in the intermediates produced from benzene. It is important to note that CO_2 evolved upon the UV irradiation without delay. The immediate evolution of CO_2 suggests that at least some of the products from benzene are oxidized more easily than benzene itself. As the reaction continued, the rates for CO_2 evolution and O_2 consumption decreased gradually. These tendencies are attributed to the decreases in the concentrations of benzene and O_2 in the reaction system. In addition, the deactivation of the photocatalysts by the phenolic products may also contribute to the lowered rate to some extent as described in Chapter 2.

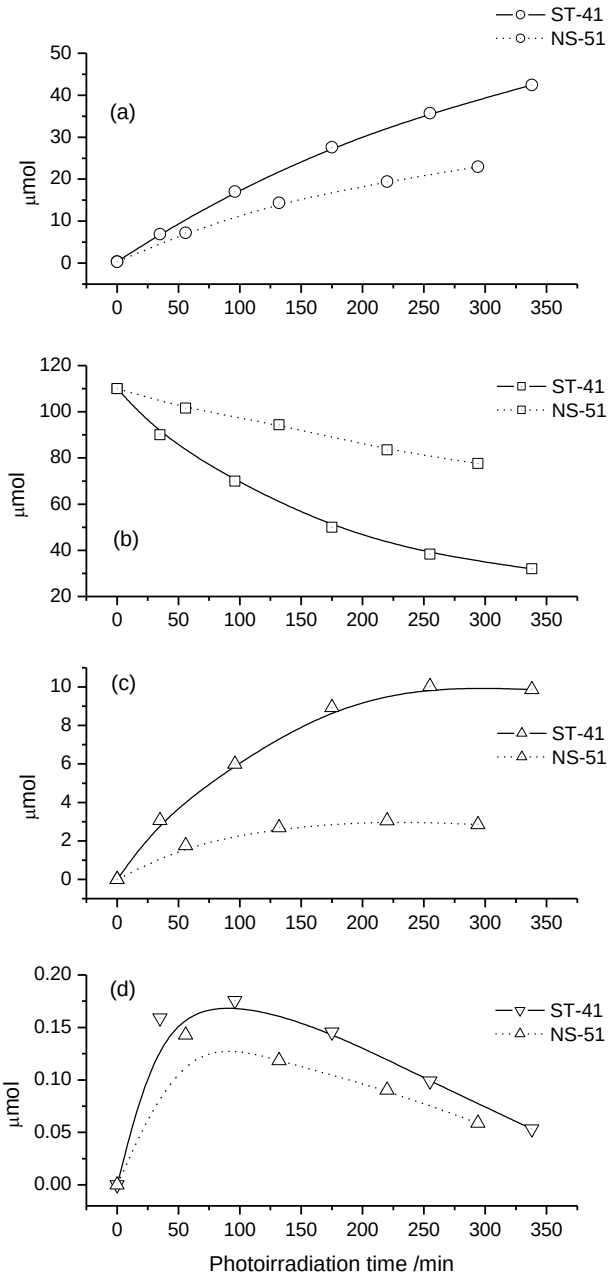

Fig. 4.4. Time courses of the amounts of (a) CO_2, (b) O_2, (c) phenol, and (d) muconaldehyde in the reaction system during photocatalyzed reaction of benzene in aqueous solution using ST-41 and NS-51 powders as photocatalysts.

The rates for phenol production (Fig. 4.4 c) and muconaldehyde production (Fig. 4.4 d) show somewhat different tendencies from the rates for CO_2 evolution and O_2 consumption. This suggests that these products undergo further reactions. The fact that the concentration of

muconaldehyde increases in a short time and reaches a maximum after photoirradiation for about 100 min suggests that it is decomposed easily. The concentration of muconaldehyde is determined by the concentrations of benzene and molecular oxygen in the system after reaction for a short time period. After photoirradiation for 300 min, the concentration of muconaldehyde in solution is about only 1% the amount of phenol. However, the initial rate of increase in the amount of muconaldehyde is about 10% of the rate of increase in the amount of phenol, as shown in Table 4.1. This suggests that although the amount of muconaldehyde accumulating in the solution is very small compared with that of phenol, its production cannot be neglected when we consider the mineralization process of benzene by TiO_2-photocatalysis. The initial rates for the production of phenol, muconaldehyde and CO_2, which were determined from the slope of their changes, using 4 kinds of TiO_2 photocatalysts are summarized in Table 4.1.

Table 4.1. Characteristics of TiO_2 powders used as photocatalyst and initial rates for production of phenol, muconaldehyde and CO_2 from aqueous solution of benzene under photoirradiation.

Photocatalyst	Crystalline Structure	Specific surface area (m^2/g)	Initial production rates (nmol/min)		
			Phenol	Muconaldehyde	CO_2
ST-41	Anatase	8.2	88.1	9.0	173.0
ST-21	Anatase	56.1	121.7	17.3	189.5
NS-51	Rutile	6.5	31.4	3.1	105.6
TIO-3	Rutile	48.1	17.5	1.7	96.5

4.3.4 Production and decomposition rates of phenol and muconaldehyde

To determine the rates for production of phenol and muconaldehyde and also for decomposition of them in more accurately, we conducted the TiO_2-photocatalyzed reaction in

an aqueous suspension of benzene, to which isotope compounds had been added. Fig. 4.5 shows the result obtained by adding 16 μmol of labeled phenol ($^{13}C_6H_5OH$) to 2 ml aqueous suspension containing 0.1 ml benzene and 20 mg ST-41 powder. The amount of normal phenol produced from benzene increased continuously during photoirradiation. On the other hand, labeled phenol, which had been added to the solution, decreased very slowly with photoirradiation time. This result suggests that phenol is rather stable in this reactions system, which is consistent with our previous result in Chapter 2, which showed that phenolic compounds are difficult to decompose by TiO_2-photocatalysis.

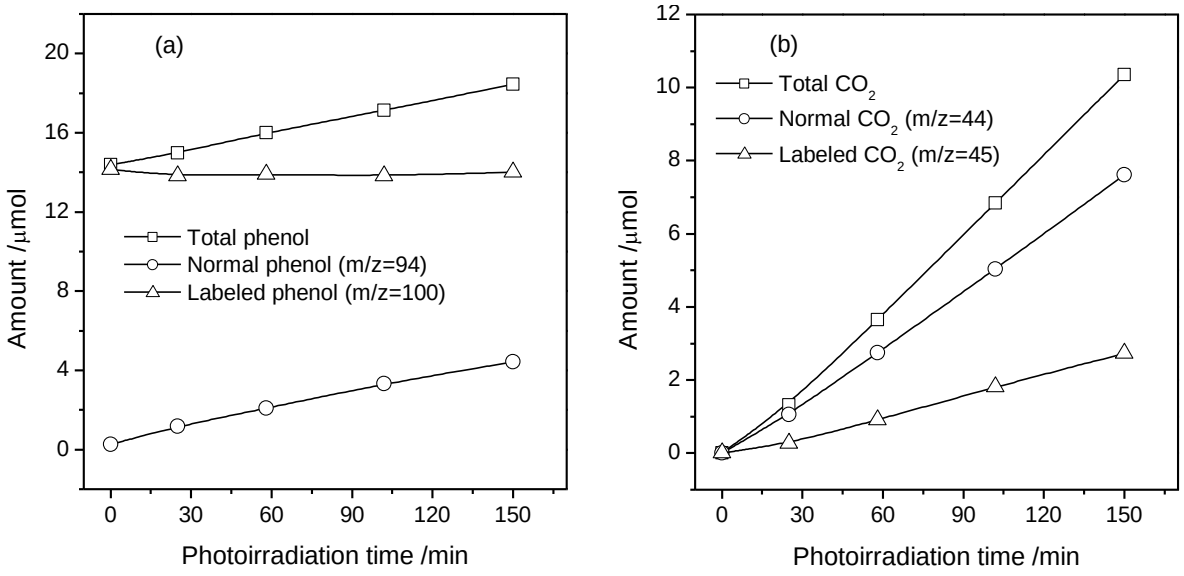

Fig. 4.5. Time courses of the changes in the amounts of (a) phenol and (b) CO_2 in the reaction system containing 2 ml aqueous suspension of 0.1 ml benzene and 20 mg ST-41 powder, to which 16 μmol of labeled phenol ($^{13}C_6H_5OH$) was added. Before the photoirradiation, the system was kept in the dark in 45 min in order for adsorption equilibrium takes place. The amount of labeled phenol adsorbed on TiO_2 before the photoirradiation were shown in Table 4.2.

As for the increase in the amount of CO_2 in the gas phase, Fig. 4.5 b shows that only about 20% of CO_2 produced contains a ^{13}C atom, which comes from labeled phenol added to the solution. This result evidences that the phenolic route (the upper line of Scheme 4.1) is not

the main path for the production of CO_2 from benzene at least under the experimental conditions. The reaction rates obtained with 4 kinds of TiO_2 powders, which are listed in Table 4.1, are shown in Table 4.2. The production of phenol is faster with anatase-form TiO_2 powders than with rutile-form TiO_2 powders, irrespective of their particle sizes (see Table 4.1). This is the tendency observed generally for the photocatalytic reactions of organic compounds [1-3]. However, the inactivity of anatase-form TiO_2 for the consumption of phenol seems to be very unique. One reason for this inactivity is that phenol (labeled) was adsorbed on the surface, the amount of which is shown in Table 4.2.

Table 4.2. Amount of labeled phenol adsorbed on TiO_2 before the photoirradiation and initial rates of the changes in the amounts of phenol and CO_2 in the system containing 2 ml aqueous suspensions of 0.1 ml benzene and 20 mg TiO_2 powders, to which 16.0 μmol of labeled phenol ($^{13}C_6H_5OH$) was added.

Photocatalyst (*)	Amount of labeled phenol adsorbed on TiO_2 before the photoirradiation (μmol)	Rates for the changes in amounts of phenol and CO_2 (nmol/min)			
		normal phenol	labeled phenol	normal CO_2	labeled CO_2
ST-41	1.2	30.0	0.4	51.0	18.0
ST-21	1.9	38.0	0.9	75.0	41.0
NS-51	1.7	8.0	17.5	26.0	16.0
TIO-3	1.8	6.0	15.1	14.0	9.0

* Characteristics of the powders are shown in Table 4.1.

Under photoirradiation, the labeled phenol molecules were gradually decomposed and replaced with normal phenol produced. Since the phenol molecules are produced on the surface of TiO_2, they are easily adsorbed on the surface. Therefore, under photoirradiation, the ratio of normal phenol to labeled phenol on the TiO_2 surface should be much higher than that in solution. This tendency is more apparent for anatase-form powders than rutile-form powders because larger amounts of phenol are produced on anatase powders. As another

reason, we found that the net decomposition rate of phenol is somewhat slower on anatase powders than on rutile powders, as shown in the Supporting Information. The inactivity of anatase-form powders for the decomposition of phenol may arise from the chemisorption of phenol on the surface of anatase-form TiO_2 [15].

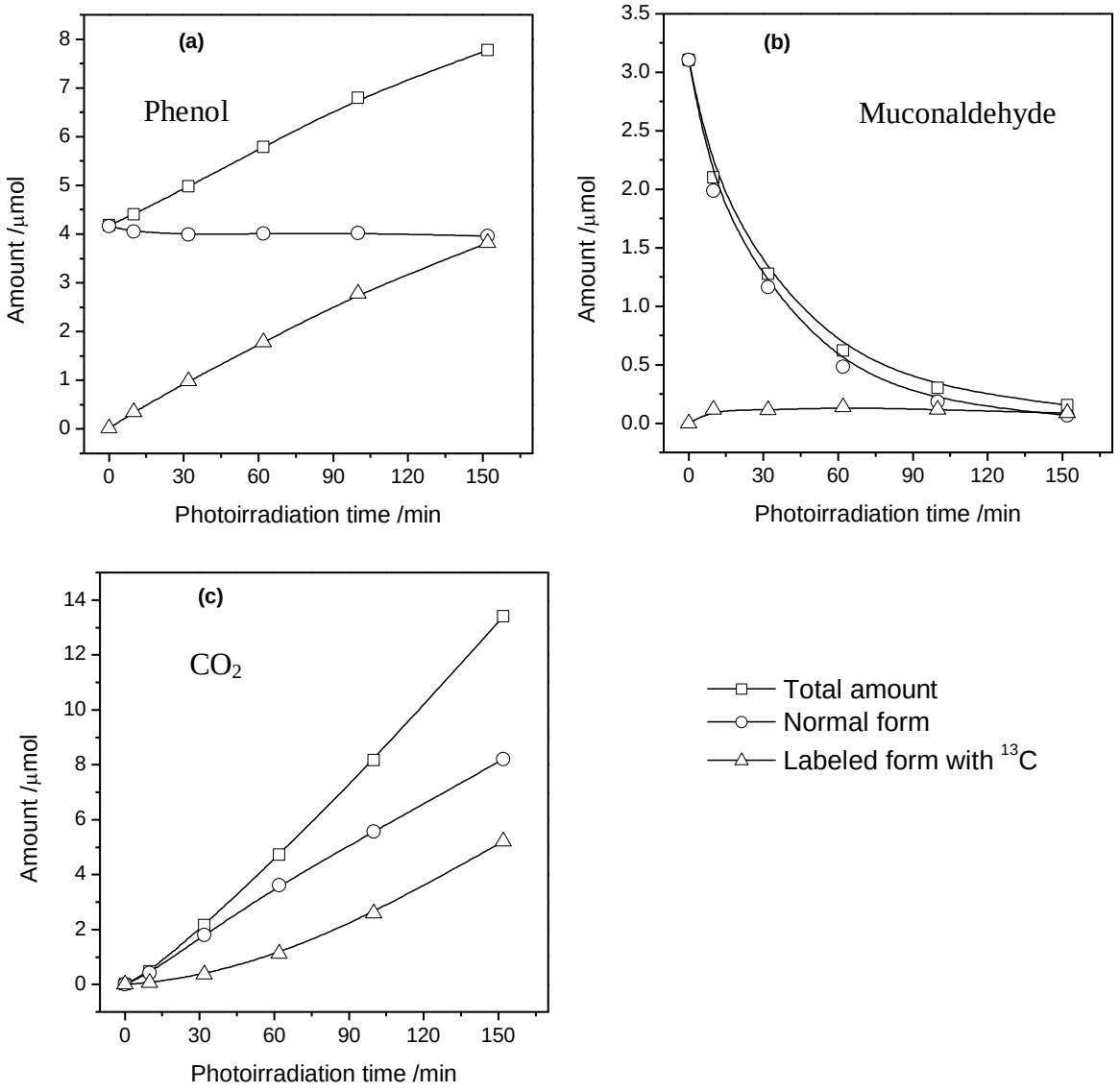

Fig. 4.6. Time courses of the changes in the amounts of (a) phenol, (b) muconaldehyde, and (c) CO_2 in the system containing 2ml aqueous suspension of 0.1 ml labeled benzene ($^{13}C_6H_6$) and 20mg ST-41, to which 3.5 μmol of muconaldehyde ($^{12}C_6H_6O_2$) and 4.5 μmol of phenol ($^{12}C_6H_5OH$) and ST-41 powder were added. Before the photoirradiation, the system was kept in the dark in 45 min in order for adsorption equilibrium takes place.

Important thing is that the production rates for $^{12}CO_2$ (from benzene) are faster than the production rates for $^{13}CO_2$ (from $^{13}C_6H_5OH$), irrespective of the TiO_2 powders, as shown in Table 4.2. Since large amounts of labeled phenol (1.23 to 1.88 μmol) were adsorbed on the TiO_2 surface, the rates are scarcely affected by the replacement of labeled phenol with normal phenol during the experiments for determining the rates. Therefore, the result strongly suggests that the production of CO_2 occurs mostly via the path without passing phenol, i.e., the muconaldehyde pathway is more favorable than the phenolic pathway.

Table 4.3. Initial rates of the changes in the amounts of phenol and muconaldehyde in the system containing 2 ml aqueous solution of 0.1 ml benzene and 20 mg TiO_2 powders, to which 3.5 mol of muconaldehyde ($^{12}C_6H_6O_2$) and 4.5 μmol of normal phenol ($^{12}C_6H_5OH$) were added.

Photocatalyst (*)	Rates for the changes in amounts of phenol and muconaldehyde (nmol/min)			
	labeled phenol	normal phenol	labeled muconaldehyde	normal muconaldehyde
ST-41	27.0	0.9	3.0	110.0
NS-51	11.0	7.4	1.0	45.0

* Characteristics of the powders are shown in Table 4.1.

In order to further clarify the contribution of muconaldehyde to the production of CO_2, we added muconaldehyde (about 3.5 μmol), which had been synthesized by TiO_2 photocatalysis from pure benzene, to the aqueous solutions containing labeled benzene ($^{13}C_6H_6$) and performed the photocatalysis. As the gas chromatogram reveals (see Fig. 4.3), the muconaldehyde ($^{12}C_6H_6O_2$) sample we prepared contained normal phenol ($^{12}C_6H_5OH$) also. Fig. 4.6 shows the result obtained with ST-41 powder (anatase). While labeled phenol ($^{13}C_6H_5OH$) is constantly produced, phenol ($^{12}C_6H_5OH$) is decomposed very slowly (Fig. 4.6 a). This tendency is the same as that seen in Fig. 4.5. On the other hand, as shown in Fig. 4.6 b, the added muconaldehyde ($^{12}C_6H_6O_2$) decreases very rapidly in about 100 min, during which the labeled muconaldehyde ($^{13}C_6H_6O_2$) is produced in a manner similar to the result

shown in Fig. 4.4 d, i.e., the concentration of labeled muconaldehyde reaches a maximum at about 60 min. In this case, most of CO_2 produced in the initial period is $^{12}CO_2$, and the production of $^{13}CO_2$ shows a delay time, as shown in Fig. 4.6 c. These results indicate that although the efficiency of the production of muconaldehyde is lower than that of phenol, it is decomposed on the TiO_2 photocatalyst very easily. In the experiment, if all the muconaldehyde molecules added was totally decomposed to CO_2, the amount of CO_2 evolved should be about 19 μmol. Compared with this amount, the amount of CO_2 evolved during 150 min is about 8 μmol. This is simply because there are many oxidation steps for the complete oxidation of muconaldehyde into CO_2. The absence of an induction period for the evolution of $^{12}CO_2$ suggests that the intermediates formed from muconaldehyde ($^{12}C_6H_6O_2$) before CO_2 evolution can be oxidized as easily as or more easily than muconaldehyde. The initial rate of decomposition of muconaldehyde is much faster than the rates for the other processes, as shown in Table 4.3. This is why the evolved CO_2 composed mostly of $^{12}CO_2$ in the initial period, as shown in Fig. 4.6 c.

4.3.5 Mechanism for the oxidation of benzene into muconaldehyde

The formation rate of phenol is about 10 times that of muconaldehyde irrespective of the kind of TiO_2 powders, as shown in Tables 4.1. Therefore, we speculate that about 90 % of total benzene will be decomposed via phenol route (the upper route of Scheme 4.1) and about 10% via the muconaldehyde route (the lower route shown in Scheme 4.1). However, concerning the CO_2 evolution from benzene, the situation is different. This is because, if benzene in the system is completely oxidized into CO_2, about 90% of CO_2 must be produced via the phenolic pathway. When the oxidation proceeds partially or at the beginning stage of the reaction, most of CO_2 can be produced via muconaldehyde, whereas phenol accumulates in the system. The muconaldehyde path should be more important for anatase-form powders than for rutile-form powders because they show high activity for oxidizing benzene into muconaldehyde and low activity for the oxidation of phenol. Therefore, the process via

muconaldehyde is important when we consider the whole process of mineralization of benzene by TiO_2-photocatalysis.

Concerning the mechanism of the production of phenol from benzene, we have described in Chapter 3 that there are two processes. One uses water as the oxygen source and the other uses molecular oxygen as the oxygen source Scheme 3.1 and 3.2, the former process being more important. Since the production of muconaldehyde from benzene is independent of the process of phenol production, the mechanism must be different from that of phenol production. The clarification should be of great importance in understanding the basic process of photocatalytic reaction of aromatic compounds on TiO_2 photocatalysts. However, the isotope method we used for clarifying the oxygen source for the production of phenol cannot be applied to the production of muconaldehyde because the O atom in carbonyl compounds exchanges with that in a water molecule very fast [16].

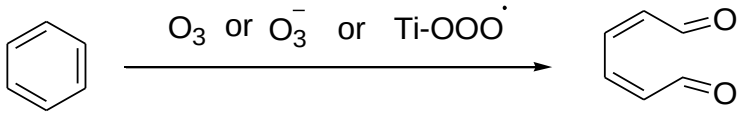

Scheme 4.2. Illustration of muconaldehyde formation by an ozonization process

To find the clue to the production of muconaldehyde from benzene, we oxidized benzene using different oxidants, and we found that muconaldehyde is produced very efficiently by the ozonation reaction without using reductants such as metallic zinc. In this case, muconaldehyde and/or other successive products play the role of the reductant. This finding suggests that muconaldehyde is produced using ozone or ozone-like species formed on the surface of TiO_2, as represented by Scheme 4.2. Although there have been no report, as far as we know, about the production of ozone on photoirradiated TiO_2 powders, production of ozone on anodically biased TiO_2 electrodes is recently reported [17]. It is likely that the same process occurs on photoirradiated TiO_2 particles. Our speculated process for the production of ozone on photoirradiated TiO_2 is shown in Scheme 4.3. The mechanism is

consistent with our finding that 2-formylcinamaldehyde is produced from naphthalene on a photoirradiated TiO_2 anode [11].

Another possible mechanism for the production of muconaldehyde from benzene on TiO_2 photocatalyst is the process represented by Scheme 3.3, in which dioxetane is assumed to be the intermediate. The formation of dioxetane has often been considered as the product from alkenes and aromatic compounds, although there have been no evidence for supporting formation of dioxetane on the surface of TiO_2 photocatalyst.

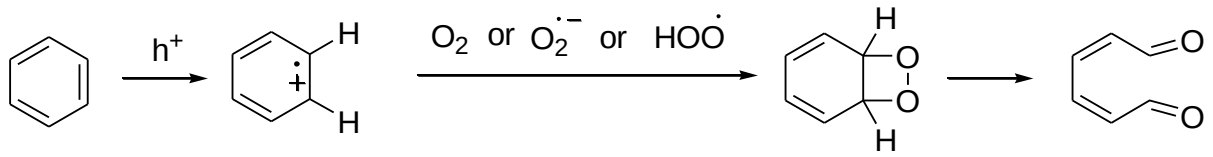

Scheme 4.3. Illustration of muconaldehyde formation by process through dioxetane species

Schemes 4.2 and 4.3 are compatible with the experimental results we obtained. In TiO_2 photocatalysis, it is assumed most often that $HO^{\cdot}$ radicals produced from water are the oxidant for oxidation of organic compounds. However, we found that in the case of CO_2 evolution from benzene, the process not involving $HO^{\cdot}$ radicals is most important, although we cannot identify the exact mechanism. We assume that similar processes are involved in many other TiO_2-photocatalized reactions, on which the details of the mechanism have not been studied.

4.4 Conclusions

We found that muconaldehyde as well as phenol is produced from benzene on TiO_2 photocatalysts as the intermediate before its mineralization. The productions of muconaldehyde and phenol from benzene on TiO_2 photocatalysts account for 10 % and 90 % of total benzene decomposition, respectively. However, muconaldehyde is decomposed much faster than phenol on TiO_2 photocatalysts. As a result, phenol accumulates in the system and muconaldehyde mostly leads to CO_2 production when benzene added is incompletely oxidized. Therefore, the path of muconaldehyde is important in the mineralization of benzene.

The two intermediates are produced from benzene by independent processes. Although the production of muconaldehyde is very fundamental for the reaction of benzene, it has been overlooked. Since benzene is the most basic aromatic compound, the results obtained in this study are important not only for benzene but also for other aromatic compounds. This also gives fundamental information about the process occurring on TiO_2 photocatalysts.

Supporting Information

- UV absorption spectrum of muconaldehyde

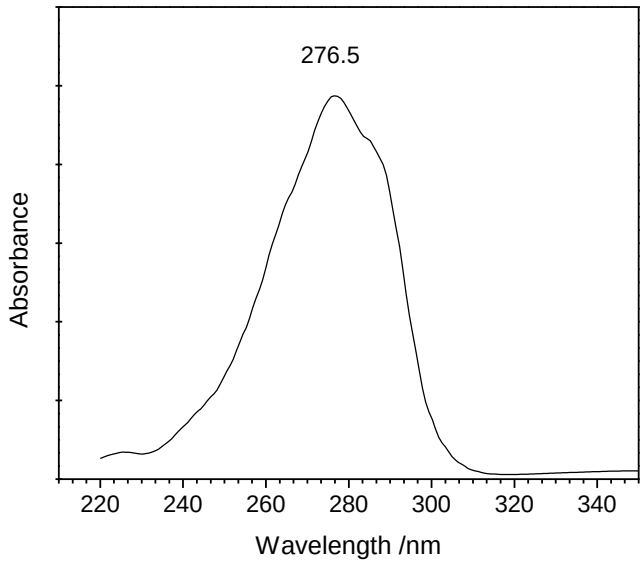

- NMR data of *cis,trans*- and *trans,trans*- muconaldehyde

cis,trans-muconaldehyde: ^{1}H NMR (400 MHz, $CDCl_3$): δ, ppm 10.26 (1H, d, J_{1-2}=6.6 Hz, H-1), 9.77 (1H, d, J_{5-6} = 7.8 Hz, H-6), 8.05 (1H, dd, J_{4-5} = 15.3 and J_{3-4} = 11.8 Hz, H-4), 7.07 (1H, t, J_{3-4} = 11.8 and J_{2-3} = 11.4 Hz, H-3), 6.42 (1H, dd, J_{4-5} = 15.3 and J_{5-6} = 7.8 Hz, H-5), 6.26 (1H, dd, J_{2-3} = 11.4 and J_{1-2} = 6.6 Hz, H-2); ^{13}C NMR (400 MHz, $CDCl_3$) : δ, ppm 193.0 (C-6), 189.6 (C-1), 142.5 (C-4), 141.8 (C-3), 136.5 (C-5), 133.2 (C-2).

trans trans-muconaldehyde: ^{1}H NMR (400 MHz, $CDCl_3$) : δ, ppm 9.72 (2H, d, J_{1-2} = 7.9 Hz, H-1 and H-6), 7.29 (2H, dd, J_{2-3} = 11.5 and J_{3-5} = 3.2 Hz, H-3 and H-4), 6.52 (2H, ddd, J_{2-3} = 11.5, J_{1-2} = 7.9 and J_{2-4} = 3.2 Hz, H-2 and H-5); ^{13}C NMR (400 MHz, $CDCl_3$) : δ, ppm 192.6 (C-1 and C-6), 146.0 (C-3 and C-4), 138.0 (C-2 and C-5).

References

[1] A. Fujishima, X. Zhang and D. A. Tryk, *Surf. Sci. Rep.* 63, **2008**, 515-582.

[2] A. M. Fox and T. M. Dulay, *Chem. Rev.* 93, **1993**, 341-357.

[3] R. M. Hoffmann, S. T. Martin, W. Choi and W. D. Bahnemann, *Chem. Rev.* 95, **1995**, 69-96.

[4] M. Mahbub Ameen and Gregory B. Raupp, *J. Catal.* 184, **1999**, 112-122.

[5] O. d'Hennezel, P. Pichat and D. F. Ollis, *J. Photochem. Photobiol. A* 118, **1998**, 197-204.

[6] H. Einaga, S. Futamura and T. Ibusuki, *Appl. Catal. B* 38, **2002**, 215-225.

[7] R. M. Alberici and W. F. Jardim, *Appl. Catal., B* 14, **1997**, 55-68.

[8] H. Park and W. Choi, *Catal. Today* 101, **2005**, 291-297.

[9] N. N. Lichtin and M. Sadeghi, *J. Photochem. Photobiol., A* 113, **1998**, 81-88.

[10] H. Yoshida, H. Yuzawa, M. Aoki, K. Otake, H. Itoh and T. Hattori, *Chem. Comm.*, **2008**, 4634-4636.

[11] T. Ohno, K. Tokieda, S. Higashida and M. Matsumura, *Appl. Catal., A* 244, **2003**, 383-391.

[12] F. Soana, M. Sturini, L. Cermenati and A. Albini, *J. Chem. Soc. Perkin Trans. 2* **2000**, 699-704.

[13] O. I. Micic, Y. Zhang, K. R. Cromack, A. D. Trifunac and M. C. Thurnauer, *J. Phys. Chem.* 97, **1993**, 1211-1283.

[14] P. *J.* Salvador, *Phys. Chem. C* 111, **2007**, 17038-17043.

[15] T. TachiKawa, Y. Takai, S. Tojo, M. Fujitsuka and T. Majima, *Langmuir* 22, **2006**, 893-896.

[16] M. J. Welch, J. F. Lifton and J. A. Seck, *J. Phys. Chem.* 73 (10), **1969**, 3351-3356.

[17] K. Kitsuka, K. Kaneda, M. Ikematsu, M. Iseki, K. Mushiake, T. Ohsaka, Electrochim. Acta 55, **2009**, 31–36.

Chapter 5: PHOTOOXIDATION OF WATER ON PHOTOIRRADIATED TiO_2 IN THE PRESENCE OF MOLECULAR OXYGEN

Oxygen exchange between H_2O and O_2 over photoirradiated TiO_2 was confirmed by using oxygen isotope tracing method. This result indicated that both the oxidation of H_2O and reduction of O_2 simultaneously take place on TiO_2 surface. Of two processes, oxidation of H_2O is slower and rate-determining process. The effects of TiO_2 structure, pH, light intensity, amount of added Pt on water oxidation have been studied.

5.1 Introduction

The role of TiO_2 in heterogeneous photocatalysis as an ideal photocatalyst has been confirmed in its practical application in water splitting for renewable energy, eliminating contaminants or harmful microbial organism for environmental treatment and selective conversion in chemical synthesis [1-6]. In most application, TiO_2 is used in the presence of O_2 and water molecules as either media or adsorbed species. Therefore, it is worth studying the behavior of O_2 and H_2O on photoirradiated TiO_2. Photo-generated electron-hole pairs on conduction band and valance band of TiO_2 are strong enough to initiate redox reactions. $HO^{\cdot}$, $O_2^{\cdot -}$ and H_2O_2 which have been confirmed to be produced from interaction between electron-hole pairs with adsorbed oxygen and water account for strong oxidative property of aqueous TiO_2 suspension irradiated by UV light [1-3, 7-10]. However, the detail of formation of these active oxygen species on surface of TiO_2 is still unclear. Especially, whether $HO^{\cdot}$ radical is generated on TiO2 surface under UV irradiation is still controversial [11,12]. In this chapter, by using labeled water, we investigated the oxidation of water on photoirradiated TiO_2. The obtained result has been discussed to elucidate an insight view on photocatalysis.

5.2 Experiments

Pure water containing 10% $H_2{}^{18}O$ purchased from Cambridge Isotope Laboratories, Inc. was used as labeled oxygen source. Hydrogen peroxide 30% solution, benzene and phenol obtained from Wako Pure Chemical Industries Co. were used as guaranteed regents. Rutile powder NS-51 (specific area of 6.5 m^2/g) from Toho Titanium and anatase powder ST-41 (8.2 m^2/g), ST-01 (192 m^2/g) from Ishihara Sangyo were used as photocatalysts. In experiments investigating the effect of Pt particles, a mixture of lab-made black-Pt powder and TiO_2 were used. In experiments investigating the synergy effect between anatase and rutile, mixtures of ST-01 and NS-51, with content of NS-51 ranging from 0 to 100 %, were used.

All the reactions were carried out in ^{18}O-enriced water (2 ml) a closed Pyrex tube (15 ml) and under photoirradiation of UV light with selected wavelength of 365nm from a 500 W

super pressure mercury lamp (Wacom, BMO-500DY). The UV light intensity was adjusted by using stainless-steel masks. The intensity of UV light was measured by the Eppley thermopile purchased from The Eppley Laboratory, Inc., USA. In photo-induced Fenton reactions, 0.2 ml H_2O_2 solution (30 w%) were added in the reaction solution. In photocatalytic reactions, 20 mg photocatalyst was added to the reaction solution.

The content of labeled oxygen in the gas phase was analyzed in a gas chromatograph GC-2010, Shimadzu connected with a mass detector GCMP-2014S, Shimadzu.

5.3 Results and discussion

5.3.1 Photo-induced Fenton reactions and photocatalytic reactions

It is widely understood that UV-photoirradiated aqueous suspension of TiO_2 is very oxidative. Almost all organic compounds are completely mineralized by photocatalytic reaction over TiO_2 particles [1-5]. The non-selective oxidation of photocatalytic reaction is similar with that of Fenton reaction, which is characterized by $HO^{\cdot}$ radical-involved mechanism. Also, hydrogen peroxide, H_2O_2, has been reported to be produced in aqueous suspension of TiO_2 [9,10]. This leads to a simplification that photocatalytic reaction is one kind of Fenton reaction. And, the role of TiO_2 in photocatalytic reaction is underestimated. In the following experiments, we want to point out the important difference between photocatalytic reaction and Fenton reaction in photooxidation of water.

In photo-induced Fenton reaction, the H_2O_2 solution in enriched water (10% $H_2{}^{18}O$) was irradiated. The content of O^{18} in form of O_2 released from photolysis of hydrogen peroxide was measured. We found that this content did not change with time, as shown in Fig. 5.1. It suggested that there was no isotopic exchange between water and hydrogen peroxide and the released O_2 was purely from H_2O_2 molecule. This result was consistent with the thermal decomposition of hydrogen peroxide carried out by M. Anbar et al [13] and M. R. Tarasevich et al [14]. It suggests the mechanism of photolysis of hydrogen peroxide like that:

$$H_2O_2 \xrightarrow{\text{UV light}} 2HO^{\cdot} \qquad (1)$$

$$OH^{\cdot} + H_2O_2 \Leftrightarrow H_2O + HOO^{\cdot} \quad (2)$$

$$HOO^{\cdot} + OH^{\cdot} \rightarrow O_2\uparrow + H_2O \quad (3)$$

$$HOO^{\cdot} + HOO^{\cdot} \rightarrow H_2O_2 + O_2\uparrow \quad (4)$$

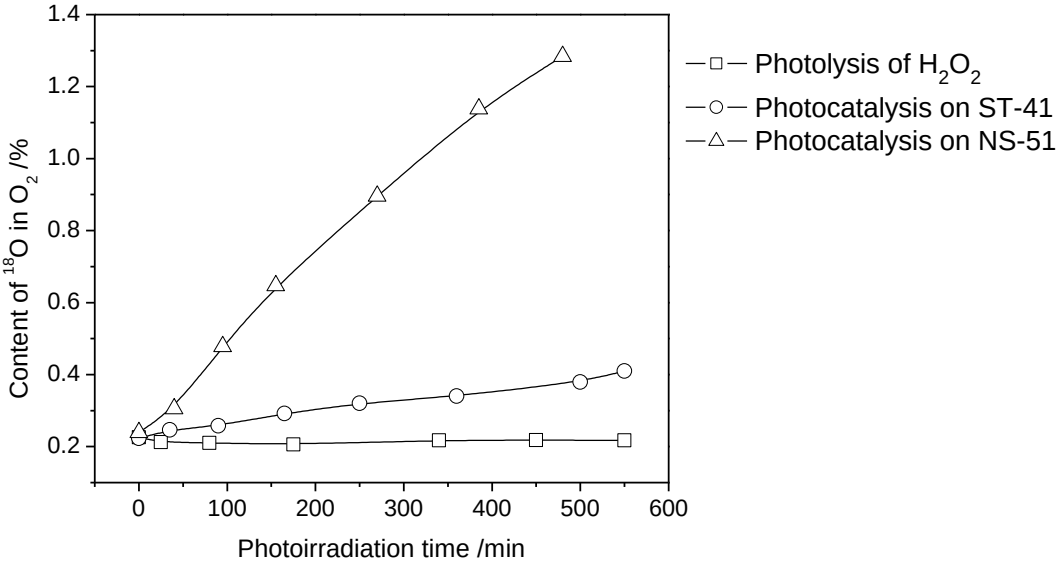

Fig. 5.1. Evolution of O^{18} in form of O_2 in gas phase from photolysis reaction of H_2O_2 and photocatalytic reactions using ST-41 and NS-51 as photocatalysts. In all the reactions, water containing 10% $H_2{}^{18}O$ is used as a solvent and no steal mask was used.

The result also suggests that the possibility for the oxygen isotopic exchange between water and hydrogen peroxide in (5), (6) and (7) was negligible. Therefore, the $HO^{\cdot}$-involved mechanism does not induce oxygen evolution from water.

$$OH^{\cdot} + H_2{}^{18}O \rightarrow H_2O + H^{18}O^{\cdot} \quad (5)$$

$$OH^{\cdot} + {}^{18}OH^{\cdot} \rightarrow HO\text{-}{}^{18}OH \quad (6)$$

$$H_2O_2 + {}^{18}OH^{\cdot} \rightarrow HO\text{-}{}^{18}OH + HO^{\cdot} \quad (7)$$

In photocatalytic reaction using rutile NS-51 or anatase ST-41 powders, we observed the evolution of O_2 molecules containing ^{18}O, when the suspensions in labeled water were photoirradiated with UV light, as shown in Fig. 5.1. This indicates that the photooxidation of water occurred. The evolution of ^{18}O in form of O_2 molecules did not occur in solution phase

as shown in photo-Fenton reactions, which have been thought to share many similarities with photocatalytic reactions [1-3]. Therefore, this result clearly shows that the photooxidation of water took place on TiO_2 surface under UV photoirradiation. Total amount of oxygen in gas phase in these experiments did not change with photoirradiation time. It means that two simultaneous processes took place on TiO_2 surface. One is consumption of O_2 in the reactions initiated by photogenerated electrons. The other is generation of O_2 in complete oxidation of water initiated by photogenerated holes. The two processes are illustrated in Scheme 5.1.

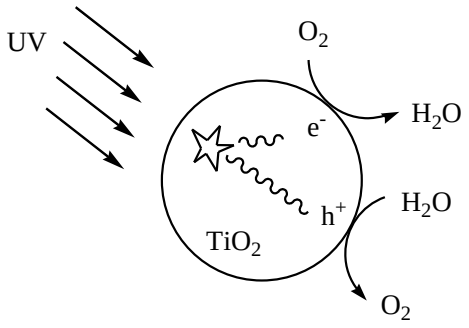

Scheme 5.1. Exchange reactions on photoirradiated TiO_2 particles

From Fig. 5.1, it is noticeable that NS-51 (rutile) powder has much higher activity in decomposition of water than ST-41 (anatase) powder. Both two photocatalysts used have small and comparable specific surface areas. Therefore, the difference in the activity can be attributed to the difference in their structures. It suggests that rutile surface is more favorable for oxidation of water to oxygen than anatase surface. This result is also consistent with the report by R. Abe et al. that rutile have a unique selectivity for O_2 evolution [15]. However, it is important to note here that rutile has higher photocatalytic activity only for water oxidation. In photooxidation of organic compounds, anatase has been confirmed to have higher activity than rutile as shown in previous Chapters. The reasons for these phenomena have not clearly clarified yet.

5.3.2 Effects of Pt particles, pH, light intensity and anatase-rutile synergism

It is known that Pt particles, when in contact with TiO_2 particles, can attract photogenerated electron and catalyze the reduction reaction [2-3, 6]. The depletion of photo-generated electron in TiO_2 particles in contact with Pt particles reduces the recombination of electron hole pairs and enhances the overall photocatalytic reactions. That is why the addition of platinum powder increased the evolution of labeled oxygen and the quantum yield (Fig. 5.2). This result can also be explained in detail when the primary processes on TiO_2 are considered. As discussed in Chapter 1, upon generation, holes can be trapped efficiently on TiO_2 surface. The depletion of electrons that occurs when TiO_2 particles are in contact with Pt particles enhances the accumulation of trapped holes. As a result, intermediate species with O-O bonding on TiO_2 surface are formed. These species are oxidized further to O_2 molecules.

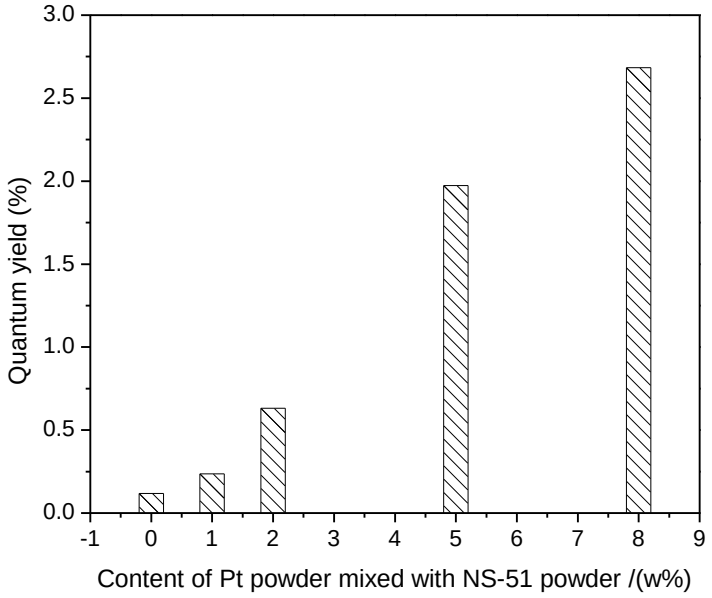

Fig. 5.2. The dependence of quantum yield on weight content of Pt particles mixed with the photocatalyst. No steal mask was used.

In order to investigate the influence of light intensity on evolution of oxygen, we used mixture of NS-51 with 8% Pt as the photocatalyst and light intensity was increased from 10 to 120 mW/cm^2 s. Results in Fig. 5.3 shows that the quantum yield increases with light intensity from 10 to 70 mW/cm^2 s and then decreases at higher light intensities. This suggests complicated physics and chemistry on surface of TiO_2. The obtained efficiency is a result of

competition between the gathering of holes and the recombination of holes with electrons. When light intensity is increased, density of trapped holes on TiO_2 surface increases; probability for formation of O-O bonding species increases; and quantum yield increases. It indicates that the gathering of holes in form of O-O bonding species requires a certain degree of accumulation holes on TiO_2 surface. However, when light intensity too high, the recombination of excessive generated electrons and holes leads to the decrease in quantum yield. This result is consistent with report by J. Tang [16], that production of oxygen in water oxidation needs four holes and takes about 1 s; and different from oxidation of methanol, which requires 1 hole and within only 10 ns.

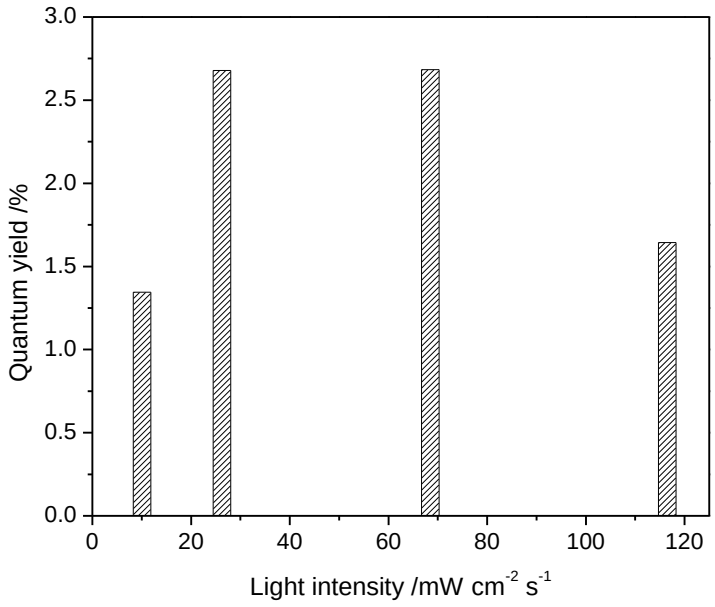

Fig. 5.3. Quantum yield versus light intensity (λ_{max} = 365 nm). Mixture of NS-51 8w% Pt was used as photocatalyst. The insensitive of the light was adjusted to lower values by using appropriate number of steal masks.

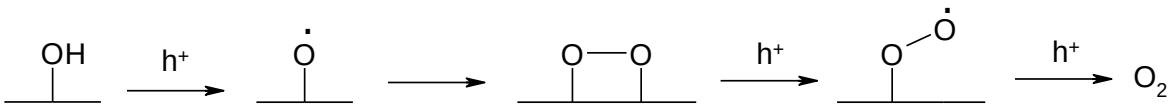

Scheme 5.2. Schematic illustration for the accumulation of four holes on TiO_2 surface leading to formation of O_2 molecule

Scheme 5.2 is schematic illustration of O_2 evolution as a result of accumulation of holes. Before the release of O_2, there must be several intermediate surface species corresponding to the accumulation of two or three holes. The higher activity in O_2 evolution on rutile surface may be attributed to the ease in formation of such intermediate species. It suggests that the determining factor for difference in photocatalytic activities of rutile and anatase is not the difference in band edge positions, but the difference in structural property. We suppose that these species play important roles not only in splitting of water but also in multi-hole reactions which can be utilized in selective oxidation of organic substrates. We have discussed about competition between photooxidation of organic compounds and photooxidation of water in Chapter 3.

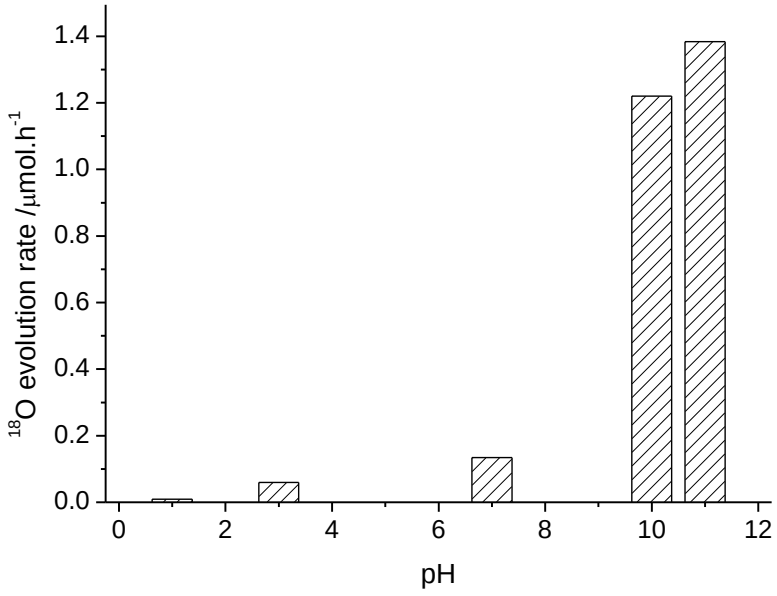

Fig. 5.4. ^{18}O evolution rates versus pH of solutions in experiments using 20 mg NS-51 mixed with 8% Pt in 2 ml water containing 10% $H_2{}^{18}O$. pH was adjusted by NaOH (1 M) or HCl (1 M) solutions. No steal mask was used.

The effect of pH on evolution rate of O_2 has also been investigated and the result is shown in Fig. 5.4. pH of reaction solution was adjusted by small amount of HCl 0.5 M and NaOH 0.5 M solutions. The presence of small amount of Cl^- and Na^+ was also confirmed not

to affect the O_2 evolution. The increase of O_2 evolution with the increase in pH indicates that hole-initiated processes are rate-determining steps in photodecomposition of H_2O. In more detail, negative charged TiO_2 surface in alkaline solution is favorable for building up holes, which determines oxygen evolution rate.

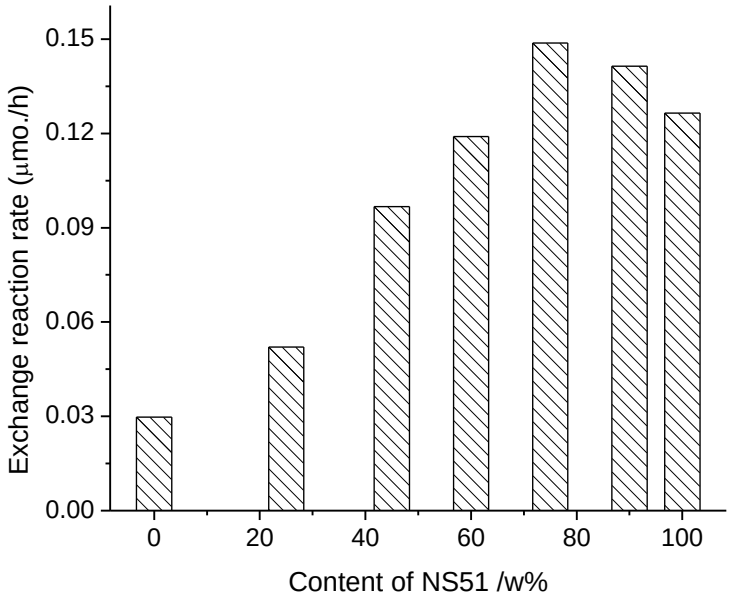

Fig. 5.5. Evolution rate of oxygen versus content of NS-51 in mixture of NS-51 and ST-01. No steal mask was used.

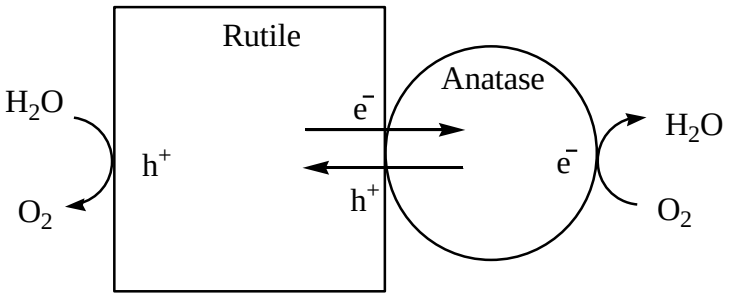

Scheme 5.3. Schematic illustration the synergy effect between rutile and anatase particles

When a mixture of anatase (ST-01) and rutile (NS-51) was used as photocatalyst, a synergism effect was observed as shown in Fig. 5.5. The synergism has been found in photooxidation of naphthalene [17], in which, photogenerated holes are supposed to move

from anatase to rutile phases and photogenerated electrons move in the opposite direction (Scheme 5.3). This opposite migrations of electrons and holes leads to the decrease in recombination of them. Therefore, there exists an optimal ratio between anatase and rutile that shows highest photo-activity and higher than individual anatase or rutile. This optimal ratio depends on the reaction condition, starting powders and the contact between particles. This value for NS-51 and ST-01 in photooxidation of water indicated in Fig. 5.5 is around 70-75% NS-51.

5.4 Conclusions

By tracing oxygen-18 isotope in both photo-induced Fenton reactions and photocatalytic reactions, we confirmed that the water photooxidation occurs on TiO_2 surface under UV photoirradiation and O_2 evolution is the result of accumulation of trapped holes. Rutile has higher activity in four-hole oxidation of water than anatase. The addition of platinum particles and increase in pH of reaction solution increase the accumulation of trapped holes to form surface intermediate species with O-O bonding and evolution of oxygen. The increase of quantum yield with light intensity in range of 10-70 $mW/cm^{-2}s$ suggests that the formation of O-O bonding species on TiO_2 surface is crucial step in evolution of oxygen. The existence of optimal ratio between anatase and rutile showing highest photo-activity confirmed the synergy effect between anatase and rutile in photocatalytic reaction.

References

[1] A. Fujishima, X. Zhang and D. A. Tryk, *Surf. Sci. Rep.* 63, **2008**, 515-582.

[2] A. M. Fox and T. M. Dulay, Chem. Rev. 93, **1993**, 341-357.

[3] R. M. Hoffmann, S. T. Martin, W. Choi and W. D. Bahnemann, *Chem. Rev.* 95, **1995**, 69-96.

[4] G. Palmisano, V. Augugliaro, M. Pagliaro and L. Palmisano, *Chem. Commun.* **2007**, 3425-3437.

[5] Y. Shiraishi and T. Hirai, *J. Photochem. Photobiol. C* 9, **2008**, 157-170.

[6] M. Ni, M.K.H. Leung, D.Y.C. Leung and K. Sumathy, *Renewable Sustainable Energy Rev.* 11, **2007**, 401-425.

[7] T. Hirakawa, K. Yawata and Y. Nosaka, *Appl. Catal., A* 325, **2007**, 105–111.

[8] T. Daimon, T. Hirakawa, M. Kitazawa, J. Suetake, and Y. Nosaka, *Appl. Catal., A* 340, **2008**, 169–175.

[9] H. Goto, Y. Hanada, T. Ohno and M. Matsumura, *J. Catal.* 225, 2004, 223–229.

[10] V. Maurino, C. Minero, G. Mariella and E. Pelizzetti, *Chem.Commun.,* **2005**, 2627–2629.

[11] O. I. Micic, Y. Zhang, K. R. Cromack, A. D. Trifunac and M. C. Thurnauer, *J. Phys. Chem.* 97, **1993**, 1211-1283.

[12] P. *J.* Salvador, *Phys. Chem. C* 111, **2007**, 17038-17043.

[13] M. Anbar, *J. Am. Chem. Soc.* 83 (9), **1961**, 2031-2035.

[14] M. R. Tarasevich and G. I. Zakharkin, *React. Kinet. Catal. Lett.* 6 (1), **1977**, 77-82.

[15] R. Abe, K. Sayama and H.Sugihara, *J. Phys. Chem. B* 109, **2005**, 16052-16061.

[16] T. Ohno, K. Tokieda, S. Higashida and M. Matsumura, *Appl. Catal., A* 244, **2003**, 383-391.

Chapter 6: CONCLUTIONS AND RESEARCH RECOMMENDATIONS FOR FUTURE STUDIES

Conclusions

Photooxidations of water and benzene on TiO_2 powders were successfully investigated by using both chemical and physical methods. Especially, many important insights of mechanism of the reactions were obtained from the isotope-tracing methods.

The deactivation of TiO_2 during photooxidation of aromatic compounds was investigated systematically. Intermediate products from benzene in TiO_2-photoctalyzed reactions both in solution phase and on TiO_2 surface was completely analyzed. The products formed in solution are phenol, p-hydroquinone, p-benzoquinone, muconaldehyde and some aliphatic acids. On the surface of TiO_2, besides these compounds, are catechol and a polymeric substance. The deactivation of TiO_2 during photocatalytic reaction is mainly coursed by adsorbed intermediate products, especially adsorbed phenolic and polymeric products. Adsorbed phenolic compounds chemically poison TiO_2 powders, whereas, polymeric substance physically block TiO_2 surface.

Both oxygen and water molecules were confirmed as oxygen sources in photooxidation of benzene on TiO_2 particles. Each contribution of them depends on TiO_2 structure, surface modification and reaction conditions. Contribution of O_2 in formation of phenol is higher in case of rutile, increases with partial pressure of O_2 and decreases with addition of Pt particles. The higher photocatalytic activity of anatase powders is attributed to the better use of water as oxygen source.

Benzene-ring cleavage in photocatalytic reaction was confirmed by the first time detection of muconaldehyde as an initial product from benzene. Ring-opening pathway and hydroxylation pathway going through formation of phenol that is another initial product from benzene are two parallel paths in photooxidation of benzene. Although, muconaldehyde is produced slower, it is decomposed much faster than phenol. As a result, phenol gradually accumulates and muconaldehyde is decomposed soon after its formation during photooxidation of benzene. Therefore, the ring-opening pathway produces more CO_2 in initial photodecomposition of benzene.

The formation of phenol and muconaldehyde as the two important initial intermediate products from benzene was discussed in detail. Phenol can be produced in two possible pathways. The first one is oxygen-transfer pathway using water as oxygen source. The other is electron-transfer pathway going through a coupling step between benzene cation and oxygen molecule. Unfortunately, the ^{18}O-tracing method is not applicable to investigate the formation of muconaldehyde because of fast O-exchange between carbonyl products and water. However, there are two possible mechanisms compatible with experimental results for muconaldehyde formation. They are an ozonization-like process and a mechanism going through dioxetane species.

We confirmed that both the photooxidation of water and the reduction of oxygen can simultaneously occur on TiO_2 surface under UV photoirradiation. Rutile has higher activity than anatase in formation of O_2. The increase in quantum yield in low light intensity region (from 10 to 70 mW/cm^2 s) indicates that the O_2 evolution requires a certain degree of accumulation of trapped holes on TiO_2 surface. The addition of platinum particles and increase in pH of reaction solution enhance the evolution of oxygen. The synergism between anatase and rutile was also observed in photooxidation of water.

The photocatalytic activity of rutile and anatase was also discussed. The oxidation processes in overall photocatalytic reaction on rutile and anatase are similar. But, the degrees of each process are different. The experimental results indicated that the differences in structural properties rather than band edges positions account for the differences in photocatalytic activity of rutile and anatase powders. Below table shows the main differences and possible corresponding reasons between the two commonly used types of TiO_2.

Comparisons	***Possible explanations***
In general, anatase is better than rutile in decomposition of organics	Activity of oxidizing species (most of them are holes and trapped holes) on anatase is stronger than on rutile. This difference is mostly due to the

	differences in structure rather than in band edge positions. Because valance band edges of rutile and anatase are coincide.
Rutile is better than anatase in formation of O_2 in photooxidation of water	Maybe, because trapped holes on rutile are less oxidative, they last longer and have more chance to gather to each other than those on anatase. In addition, the rutile structure may be favorable for the accumulation of trapped holes. Therefore, the evolution of O_2 can compete with the oxidation of benzene when rutile powder is mixed with Pt particles.
Anatase is better than rutile in decomposition of muconaldehyde	Due to strong activity of oxidizing species on anatase
Rutile is better than anatase in **selectivity** in decomposition of phenol	Maybe because structural properties of rutile facilitates the oxidation of phenol
Contribution of water in formation of phenol is higher in case of anatase	Strong oxidizing species on anatase (mostly holes and trapped holes) can make use of water better
Contribution of O_2 in formation of phenol is higher in case of rutile	The contribution of water through week oxidizing species is less, therefore, the relative contribution of O_2 is larger in the case of rutile

Research recommendations for future studies

Although this study provides many important insights of photocatalytic reaction and is a big step of researches on photooxidation of benzene, it could not end with a concrete detailed mechanism. Most of results obtained here are still indirect evidences to clarify primary steps on surface of TiO_2 during photocatalytic reactions. Therefore, further works on this subject should be done:

- To further investigate the formation of oxidizing species and their involvement in primary step on TiO_2 surface during photocatalytic reactions.
- To prove and clarify the relationship between structural properties and photocatalytic activity of photocatalysts.
- To fabricate or design a photocatalytic system for selective conversion applicable to organic synthesis.
- To overcome the deactivation of TiO_2 in environmental applications.

List of publications

Published papers

1. ***Lowering of Photocatalytic Activity of TiO_2 Particles during Oxidative Decomposition of Benzene in Aerated Liquid***

   Thuan Duc Bui, Akira Kimura, Shigeru Ikeda and Michio Matsumura

   Appl. Catal., B 94, **2010**, 186–191.

2. ***Determination of Oxygen Sources for Oxidation of Benzene on TiO_2 Photocatalysts in Aqueous Solutions Containing Molecular Oxygen***

   Thuan Duc Bui, Akira Kimura, Shigeru Ikeda and Michio Matsumura

   J. Am. Chem. Soc. 132, **2010**, 8453–8458.

Conferences

Oral presentations

3. ***Study on Aqueous Photooxidation of Benzene over TiO_2 by Labeled Oxygen Tracing Method***

   Thuan Duc Bui, Akira Kimura, Shigeru Ikeda and Michio Matsumura

   Spring Meeting of The Electrochemical Society, Toyama, 31st March **2010**.

4. ***Is Phenol is the Only Initial Product from Benzene in the TiO_2 Photocatalyzed Reaction?***

   D. T. Bui, A. Kimura, S. Higashida and M. Matsumura

   Autumn Meeting of the Electrochemical Society, Tokyo, 19th September **2007.**

Poster presentation

5. ***Lowering of Photocatalytic Activity of TiO_2 Particles during Oxidative Decomposition of Benzene***

Thuan Duc Bui, Akira Kimura, Shigeru Ikeda and Michio Matsumura

The 14th International Conference on TiO_2 Photocatalysis: Fundamentals and Applications (TIO2-14), Niagara Falls, New York, October 5-8, **2009.**

Submitted oral presentation

6. ***Production of Muconaldehyde from Benzene by Ring-Opening Reaction over UV-Irradiated TiO_2***

Thuan Duc Bui, Akira Kimura, Suguru Higashida, Shigeru Ikeda, and Michio Matsumura.

Pacifichem 2010 conference, Honolulu, Hawaii, USA, Dec. **2010.**

Acknowledgements

This thesis is completed in a sandwich program for PhD course under an agreement on cooperative education programs between College of Technology, Vietnam National University of Hanoi; Institute of Materials Science, Vietnamese Academy of Science and Technology; and Graduate School of Engineering Science, Osaka University. I would like to thank all the parties for their effort to give me a chance to study in the best conditions. I also very grateful to Vietnam International Education Development, Ministry of Education and Training, Vietnam, and Graduate School of Engineering Science, Osaka University, Japan for financial support and Faculty of Chemistry, Hanoi National University of Education, where I work, for the best helping me to complete the course.

Most of works in this thesis have been carried out in Research Center for Solar Energy Chemistry, Osaka University in my three years in Japan, from Oct. 2006 to Sept. 2007 and from Oct. 2008 to Sept. 2010. I am heartily thankful to my Japanese supervisors, Professor Michio Matsumura and Associate Professor Shigeru Ikeda, for their encouragement, guidance and support since my first days, which have enabled me to develop an understanding of photocatalysis.

I also would like to show my gratitude to Vietnamese supervisors, Professor Nguyen Xuan Phuc in Institute of Materials Science, Vietnamese Academy of Science and Technology, and Professor Nguyen Hanh in Faculty of Chemical Technology, Hanoi University of Technology for their enthusiastic guidance and help in my one year in Vietnam, from Oct. 2007 to Sept. 2008.

This thesis would not have been possible without the help of all other members in Research Center for Solar Energy Chemistry, especially Mr. Akira Kimura, with whom I have had many meaningful and interesting discussions and talks in both academic and daily life

subjects, and Dr. Takashi Harada who has been willing to assist me whenever I needed. It is also a pleasure to thank Professor Suguru Higashida in Industrial Systems Engineering, Osaka Prefectural College of Technology for his help and discussions.

I am indebted to my parents, Mr. Bui Duc Luu and Mrs. Hoang Thi Ha, my elder brother's family, Mr. Bui Duc Thuan, Mrs. Nguyen Thi Thoan, nephews Bui Duc Dung, Bui Duc Anh and niece Bui Minh Anh, and my beloved fiancée, Miss. Nguyen Thi Huyen for their endless love and considerateness.

Lastly, I offer my regards and blessings to all of my friends, who have supported me in any respect and shared with me friendship, experiences and enjoyment, including Mrs. Yoshihiro Kuronita (Japanese teacher), Mr. Takahiro Oosasa (Japanese tutor), Mr. Vu Hai, Mr. Nguyen Tan Da, Mr. Vu Van Dung, Ms. Vu Thi Huong, Ms. Tran Kim Thu, Mr. Trinh Khanh Duy, Mr. Ng Yun Hau, Mr. Lee Chia Lung, Ms. Lee Sun Min, Mr. Weize Wang and many others.

BUI DUC THUAN

OSAKA, JUNE 2010